CHEMICAL REACTION DYNAMICS: MANY-BODY CHAOS AND REGULARITY

TAMIKI KOMATSUZAKI

Department of Earth and Planetary Sciences, Faculty of Science, Kobe University, Kobe 657-8501 Japan

R. STEPHEN BERRY

Department of Chemistry and The James Franck Institute, The University of Chicago, Chicago, IL 60637

CONTENTS

Advances in Chemical Physics, *Volume 123*, Edited by I. Prigogine and Stuart A. Rice.
ISBN 0-471-21453-1

I. INTRODUCTION

Chemists have long envisioned reactions as passages from an initial, reactant state, locally stable, through an unstable transition state, to a final, stable product state. Described in terms of a multidimensional surface of internal energy as a function of the locations of the atomic nuclei, this model has the reacting system go from one local minimum across a saddle in the landscape to another local minimum. The questions, How fast does a system actually traverse the saddles? and What kinds of trajectories carry the system through?, have been among the most intriguing subjects in chemical reaction theories over the past several decades [1–15]. The introduction of the concept of "transition state" by Eyring and Wigner in 1930s [3–5] had great successes in the understanding of the kinetics of chemical reactions: It led to the definition of a hypersurface (generally in phase space) through which a reacting system should pass only once on the way from reactants to products. It has also provided us with a magnifying glass to understand the kinetics by decomposing the evolution of the reactions into, first, how a reacting system reaches into the transition state from the reactant state by getting a certain amount of thermal or light energy, and, second, how the system leaves the transition state after its arrival there, for example, its passage velocity and pattern of crossings.

A widespread assumption in a common class of chemical reaction theories [3–11] is the existence of such a hypersurface in phase space dividing the space into reactant and product regions that a chemical species crosses it only once on its path to reaction. However, many formulations of chemical reaction rate theories have had to allow this probability, the "transmission coefficient κ," to be less than unity. Toward resolving the recrossing problem that spoils this "no-return" hypothesis, researchers have so far tried to interpret the reaction rates by using either variational transition state theory (TST) [9–11] which optimizes a *configurational* dividing surface by minimizing the recrossings, or the (generalized) Langevin formalism developed by Kramers [14] and Grote and Hynes [15], which regards the recrossings as arising from "(molecular) friction" by the "bath" degrees of freedom, which retards any of the reactive trajectories. Neither of these approaches, however, could have clarified the actual mechanics of the systems' passage through a transition state.

Several findings, both theoretical [16–29] and experimental [30, 31], during the last decades have shed light on the mechanics of passage through the reaction bottlenecks, and on the concept of transition state, especially in systems with only a few degrees of freedom (dof). The striking experimental studies by Lovejoy et al. [30] "see" this transition state via the photofragment excitation spectra for unimolecular dissociation of highly vibrationally

excited ketene. These spectra revealed that the rate of this reaction is controlled by the flux through *quantized thresholds* within a certain energy range above the barrier. The observability of the quantized thresholds in the transition state was first discussed by Chatfield et al. [32]. Marcus [33] pointed out that this indicates that the transverse vibrational quantum numbers might indeed be approximate constants of motion, presumably in the saddle region.

In the same period, Berry and his co-workers explored the nonuniformity of dynamical properties of Hamiltonian systems of several N-atom clusters, with N from 3 to 13; in particular, they explored how regular and chaotic behavior may vary locally with the topography of the potential energy surfaces (PESs) [16–23]. They revealed, by analyses of local Liapunov functions and Kolmogorov entropies, that when systems have just enough energy to pass through the transition state, the systems' trajectories become collimated and regularized through the transition state, developing approximate *local* invariants of motion different from those in the potential well. This occurs even though the dynamics in the potential well is fully chaotic under these conditions. It was also shown that at higher energies above the threshold, emerging mode–mode mixing wipes out these approximate invariants of motions even in the transition state.

Davis and Gray [24] first showed that in Hamiltonian systems with two dof, the transition state defined as the separatrix in the phase space is always free from barrier recrossings, so the transmission coefficient for such systems is unity. They also showed the existence of the dynamical bottlenecks to intramolecular energy transfer in the region of potential well, that is, cantori (in a two-dof system), which form partial barriers between irregular regions of phase space [24–26]. Zhao and Rice [26] developed a convenient approximation for the rate expression for the intermolecular energy transfer. However, their inference depends crucially on the Poincaré section having only two dimensions, and no general theory exists yet for systems of higher dimensionality [27, 34–36].

By focusing on the transition state periodic orbits in the vicinity of the unstable saddle points, Pechukas et al. [37] first showed in the late 1970s, for two-dimensional (2D) Hamiltonian systems such as the collinear $H + H_2$ reaction, that, within a suitable energy range just above the saddle, the reaction bottleneck over which no recrossings occur with a minimal flux of the system, can be uniquely identified as one periodic orbit dividing surface (PODS), a dividing surface $S(q_1 = 0)$. (Here q_1 is the hyperbolic normal coordinate about the saddle point.) Moreover, as the energy increases, pairs of the PODSs appearing on each reactant and product side migrate outward, toward reactant and product state, and the outermost PODS become identified as the reaction bottleneck. De Leon [28] devel-

oped a so-called reactive island theory; the reactive islands are the phase-space areas surrounded by the periodic orbits in the transition state, and reactions are interpreted as occurring along cylindrical invariant manifolds through the islands. Fair et al. [29] also found in their two- and three-dof models of the dissociation reaction of hydrazoic acid that a similar cylinder-like structure emerges in the phase space as it leaves the transition state. However, these are crucially based on the findings and the existence of (pure) periodic orbits for all the dof, at least in the transition states. Hence, some questions remain unresolved, for example, "How can one extract these periodic orbits from many-body dof phase space?" and "How can the periodic orbits persist at high energies above the saddle point, where chaos may wipe out any of them?

Recently, we developed a new method to look more deeply into these local regularities about the transition state of N-particle Hamiltonian systems [38–44]. The crux of the method is the application of Lie canonical perturbation theory (LCPT) [45–53], combined with microcanonical molecular dynamics (MD) simulation of a region around a saddle point. This theory constructs the nonlinear transformation to a hyperbolic coordinate system, which "rotates away" the recrossings and nonregular behavior, especially of the motion along the reaction coordinate. We showed by using intramolecular proton-transfer reaction of malonaldehyde [38, 39] and isomerization reactions in a simple cluster of six argon atoms [40–44] that, even to energies so high that the transition state becomes manifestly chaotic, at least one action associated with the reaction coordinate remains an approximate invariant of motion throughout the transition state. Moreover, it is possible to choose a multidimensional phase-space dividing surface through which the transmission coefficient for the classical reaction path is unity [40]. We "visualized" the dividing hypersurface in the phase space by constructing the projections onto subspaces of a very few coordinates and momenta, revealing how the "shape" of the reaction bottleneck depends on energy of the system and the passage velocity through the transition state, and how the complexity of the recrossings emerges over the saddle in the configurational space [41, 42]. (The dividing hypersurface migrates, depending on the passage velocity, just as PODS do.) We showed that this also makes it possible to visualize the stable and unstable invariant manifolds leading to and from the hyperbolic point of the transition state, like those of the one-dimensional (1D), integrable pendulum, and how this regularity turns to chaos with increasing total energy of the system. This, in turn, illuminates a new type of phase-space bottleneck in a transition state that emerges as the total energy, which keeps a reacting system increasingly trapped in that state, irrespective of any coordinate system one might see the dynamical events [43, 44].

This chapter is a review of our recent theoretical developments [38–44], in which we address two fundamental questions:

1. How can we extract a dividing hypersurface as free as possible from recrossings between the reactant and product states? And what is the physical foundation of why the reacting system can climb through the saddles?

2. How do the topographical features of a potential surface transform the dynamics of saddle crossings as the energy of the reacting system increases from threshold to much higher values? As a corollary, what role do saddles, including those of rank >1, play in the system's transition from regular to chaotic dynamics?

The outline of this chapter is as follows. In Section II, we briefly review canonical perturbation theory and an efficient technique, so-called algebraic quantization, for applying this method to a regional Hamiltonian about any stationary point. In Section III, we show the approximate local invariant of motion buried in the complexity of the original Hamiltonian $H(\mathbf{p}, \mathbf{q})$, without invoking any explicit assumption of its integrability. We use, as an illustrative vehicle, the isomerization of an Ar_6 cluster and show that the invariants associated with a reaction coordinate in the phase space — whose reactive trajectories are all "no-return" trajectories — densely distribute in the sea of chaotic dof in the regions of (first-rank) saddles. We also show how the invariants locate in the phase space and how they depend on the total energy of the system and other physical quantities, and discuss its implication for reaction dynamics, especially for many dof systems. In Section IV, we examine a universal consequence that holds in the regions of any first-rank saddle, that is, a hierarchical regularity in the transition states. In Section V, we give some concluding remarks and future prospects. In the appendices, we present the detailed description of Lie transform-based canonical perturbation theory with algebraic quantization, LCPT–AQ, and apply it there to a simple 2D system.

II. CANONICAL PERTURBATION THEORY

To begin, let us see what all the several forms of Canonical Perturbation Theories (CPT) provide. All the CPTs [45–53], including normal form theories [54, 55], require that an M-dimensional Hamiltonian $H(\mathbf{p}, \mathbf{q})$ in question be expandable as a series in powers of "ε," where the zeroth-order Hamiltonian H_0 is integrable as a function of the action variables $\mathbf{J}$ only

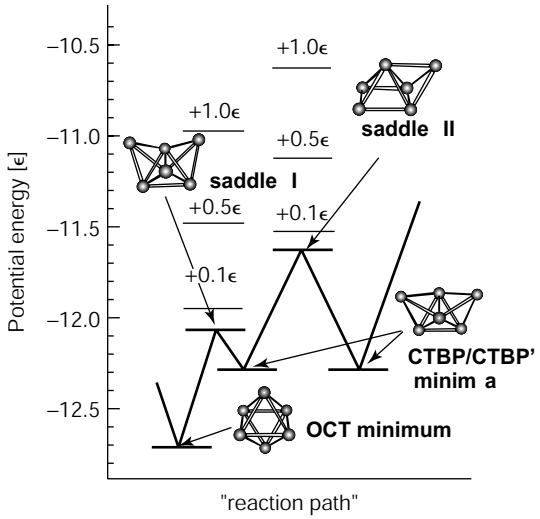

Figure 2.1. Potential energy profile of an Ar_6 atom cluster: ϵ is the unit of energy ($=121$ K).

and does not depend on the conjugate angle variables $\boldsymbol{\Theta}$,

$$H(\mathbf{p}, \mathbf{q}) = \sum_{n=0} \varepsilon^n H_n(\mathbf{p}, \mathbf{q}) = H_0(\mathbf{J}) + \sum_{n=1} \varepsilon^n H_n(\mathbf{J}, \boldsymbol{\Theta}) \tag{2.1}$$

where $\mathbf{p}$ and $\mathbf{q}$ represent momenta and the conjugate coordinates of the system, respectively.

Furthermore, the canonical transformation W of the coordinate system minimizes the angular dependencies of the new Hamiltonian $\bar{H}$, thereby making the new action variables $\bar{\mathbf{J}}$ as nearly constant as possible. If $\bar{H}$ can be obtained altogether independent of the angle $\bar{\boldsymbol{\Theta}}$ (at least, at the order of the perturbative calculation performed), then

$$H(\mathbf{p}, \mathbf{q}) \xrightarrow{W} \bar{H}(\bar{\mathbf{p}}, \bar{\mathbf{q}}) = \bar{H}(\bar{\mathbf{J}}) = \sum_{n=0} \varepsilon^n \bar{H}_n(\bar{\mathbf{J}}) \tag{2.2}$$

so the new action and angle variables for mode k are expressed as

$$\frac{d\bar{J}_k}{dt} = \dot{\bar{J}}_k = -\frac{\partial \bar{H}(\bar{\mathbf{J}})}{\partial \bar{\Theta}_k} = 0 \tag{2.3}$$

$$\bar{J}_k = \text{constant} \tag{2.4}$$

and

$$\dot{\bar{\Theta}}_k = \frac{\partial \bar{H}(\bar{\mathbf{J}})}{\partial \bar{J}_k} \equiv \bar{\omega}_k(\bar{\mathbf{J}}) = \text{constant} \tag{2.5}$$

$$\bar{\Theta}_k = \bar{\omega}_k(\bar{\mathbf{J}})t + \beta_k \tag{2.6}$$

where β_k is the arbitrary initial phase factor of mode k, and $\bar{\mathbf{p}}(=\bar{p}(\mathbf{p},\mathbf{q}))$ and $\bar{\mathbf{q}}(=\bar{\mathbf{q}}(\mathbf{p},\mathbf{q}))$ are canonically transformed new momenta and the conjugate coordinates, respectively.

If the zeroth-order Hamiltonian $H_0(\mathbf{p},\mathbf{q})$ is a system of harmonic oscillators,

$$H_0(\mathbf{p},\mathbf{q}) = \sum_{k=1}^{M} \frac{1}{2}(p_k^2 + \omega_k^2 q_k^2) = \sum_{k=1}^{M} \omega_k J_k \tag{2.7}$$

where ω_k is the fundamental frequency of mode k, these yield the equations of motion for $\bar{q}_k$ and $\bar{p}_k$, to obey the $\bar{H}$:

$$\frac{d^2\bar{q}_k(\mathbf{p},\mathbf{q})}{dt^2} + \bar{\omega}_k^2 \bar{q}_k(\mathbf{p},\mathbf{q}) = 0 \tag{2.8}$$

and

$$\bar{p}_k(\mathbf{p},\mathbf{q}) = \frac{\omega_k}{\bar{\omega}_k} \frac{d\bar{q}_k(\mathbf{p},\mathbf{q})}{dt} \tag{2.9}$$

where $\bar{\omega}_k(=\bar{\omega}_k(\bar{\mathbf{J}}) = \bar{\omega}_k(\bar{\mathbf{p}},\bar{\mathbf{q}}))$ is independent of time t because $\bar{\mathbf{J}}$ are constant (see its derivation in Appendix A). The general form of the solution can be represented as

$$\bar{q}_k(\mathbf{p},\mathbf{q}) = \alpha e^{i\bar{\omega}_k(\bar{\mathbf{J}})t} + \beta e^{-i\bar{\omega}_k(\bar{\mathbf{J}})t} \tag{2.10}$$

$$\bar{p}_k(\mathbf{p},\mathbf{q}) = \alpha\omega_k e^{i\bar{\omega}_k(\bar{\mathbf{J}})t} - \beta\omega_k e^{-i\bar{\omega}_k(\bar{\mathbf{J}})t} \tag{2.11}$$

Here, α and β are arbitrary constants depending on the initial value of $\bar{q}_k$ and $\bar{p}_k$.

The action, canonical momenta in action-angle coordinate system, is of fundamental importance for understanding of regularity in dynamics, that is, the constancy or invariancy of the action implies how separable the mode is. The advantage of any of the several forms of CPT is the reduction of dimensionality needed to describe the Hamiltonian. For example, Eqs. (2.8)

and (2.9) tell us that even though the motions look quite complicated in the old coordinate system, they could be followed as simple decoupled periodic orbits in the phase space. For realistic many-body nonlinear systems, Eqs. (2.8) and (2.9) might not be retained through the dynamical evolution of the system because the (near-)commensurable conditions may densely distribute in typical regions throughout the phase space; that is, any integer linear combination of frequencies that vanishes identically at some order, ε^n;

$$\sum_{k=1}^{M} n_k \omega_k \leqslant \mathcal{O}(\varepsilon^n) \tag{2.12}$$

(n_k is arbitrary integer), makes the corresponding new Hamiltonian diverge and destroys invariants of motion. If the system satisfies any such (near-) commensurable condition, the new Hamiltonian might have to include the corresponding angle variables to avoid divergence [48–50, 55]. Otherwise the CPT calculation would have to be performed to infinite order in near-commensurable cases.

Until now, most studies based on the CPTs have focused on transforming the new Hamiltonian itself to as simple a form as possible, to avoid divergence, and to obtain this form through specific CPT calculations of low finite order. In other terms, CPT imputes the responsibility of determining the integrability of the Hamiltonian to the inclusion of some specific angle variables and/or the convergence of the perturbation calculation. Another, potentially powerful usage of CPT, especially for many-body chemical reaction systems, should be its application as a detector to monitor occurrence of local invariance, by use of the new action $\bar{J}_k(\mathbf{p}, \mathbf{q})$ and the new frequency $\bar{\omega}_k(\mathbf{p}, \mathbf{q})$ along classical trajectories obeying equations of motion of the *original* Hamiltonian $H(\mathbf{p}, \mathbf{q})$. That is, it is quite likely that the more dof in the system, the more the global invariants through the whole phase space become spoiled; nevertheless the invariants of motion might survive within a *certain locality*, that is, for a certain finite duration, a region of phase space or in a certain limited subset of dof. The standard resonance Hamiltonian [55] constructed to avoid the near-commensurability might also prevent the possibility of detecting such a limited, approximate invariant of motion retained in a certain locality. Note that the strength of local invariants could not be detected in use of (traditional) Liapunov analysis because *local* Liapunov exponents, characterized as the finite time averages of the rate of exponential growth of an infinitesimal deviation, are affected both by the well-known horseshoe mechanism and by the degrees of noncompactness or local hyperbolicity of potential energy topographies, for example, any Liapunov exponent becomes a positive definite for an integr-

able Hamiltonian system composed of negatively curved harmonic oscillators.

A. Lie Canonical Perturbation Theory

The traditional Poincaré–Von Zeipel approach [53] of CPT is based on mixed-variable generating functions F:

$$\bar{\mathbf{q}} = \frac{\partial F(\bar{\mathbf{p}}, \mathbf{q})}{\partial \bar{\mathbf{p}}} \qquad \mathbf{p} = \frac{\partial F(\bar{\mathbf{p}}, \mathbf{q})}{\partial \mathbf{q}} \tag{2.13}$$

which requires functional inversion to obtain explicit formulas for $(\mathbf{p}, \mathbf{q})$ in terms of $(\bar{\mathbf{p}}, \bar{\mathbf{q}})$ and vice versa, at each order of the perturbative calculation. This imposes a major impediment to implementing higher order perturbations and to treating systems with many-degrees of freedom.

With the mixed-variable generating functions, after Birkoff [54], Gustavson [55] developed an elegant technique to extract the new Hamiltonian to avoid divergence by assuming that the new Hamiltonian is expandable in normal form; if complete inversion of the variables is not required, the procedure to calculate the new Hamiltonian can be rather straightforward.

LCPT [46, 47, 51, 52, 56] first developed by a Japanese astrophysicist, Hori [51, 52], is superior to all the most traditional methods, in that no cumbersome functions of mixed variables appear and all the terms in the series are repeating Poisson brackets. The crux is the use of Lie transforms, which is regarded as a "virtual" time evolution of phase-space variables $\mathbf{z}(=(\mathbf{p}, \mathbf{q}))$ along the "time" ε driven by a "Hamiltonian" W; that is,

$$\frac{d\mathbf{z}}{d\varepsilon} = \{\mathbf{z}, W(\mathbf{z})\} \equiv -L_W \mathbf{z} \tag{2.14}$$

Here, $\{\,\}$ denotes the Poisson bracket. The formal solution can be represented as

$$\mathbf{z}(\varepsilon) = \exp\left[-\int^{\varepsilon} L_{W(\varepsilon')}\, d\varepsilon'\right]\mathbf{z}(0) \tag{2.15}$$

As shown in Appendix B, it can easily be proved for any transforms described by the functional form of Eq. (2.15), that if $\mathbf{z}(0)$ are canonical, $\mathbf{z}(\varepsilon)$ are also canonical (and vice versa), as the time evolution of any Hamiltonian system is regarded as a canonical transformation from canonical variables at an initial time to those at another time, maintaining the structure of Hamilton's equations.

For any function f evaluated at "a point" $\mathbf{z}(0)$, the evolution operator T, defined as below, yields a new function g represented as a function of $\mathbf{z}(0)$ and ε, whose functional *value* is equal to $f(\mathbf{z}(\varepsilon))$:

$$f(\mathbf{z}(\varepsilon)) = Tf(\mathbf{z}(0)) = \exp\left[-\int^{\varepsilon} L_{W(\mathbf{z}(0);\varepsilon')}\, d\varepsilon'\right] f(\mathbf{z}(0)) = g(\mathbf{z}(0);\varepsilon) \quad (2.16)$$

The Lie transforms of an autonomous Hamiltonian H to a new Hamiltonian $\bar{H}$ can be brought about by

$$\bar{H}(\mathbf{z}(\varepsilon)) = T^{-1}H(\mathbf{z}(\varepsilon)) = H(\mathbf{z}(0)) \quad (2.17)$$

by determining W (also assumed to be expandable in powers of ε as H and $\bar{H}$ are) so as to make the new Hamiltonian as free from the new angle variables $\bar{\Theta}$ as possible, at each order in ε. Here, the *inverse* evolution operator T^{-1} brings the system dwelling at a "time" backward to a past in ε from *that* "time" along the dynamical evolution $\mathbf{z}$, yielding $H(\mathbf{z}(0))$ (see Appendix C in detail). We shall hereafter designate the initial values of $\mathbf{z}$, $\mathbf{z}(0)$, by $(\mathbf{p}, \mathbf{q})$, and those at "time" ε by $(\bar{\mathbf{p}}, \bar{\mathbf{q}})$. Then, one can see that Eq. (2.17) corresponds to a well-known relation between the old and new Hamiltonians hold under any canonical transformation for autonomous systems:

$$\bar{H}(\bar{\mathbf{p}}, \bar{\mathbf{q}}) = H(\mathbf{p}, \mathbf{q}) \quad (2.18)$$

The great advantage of LCPT in comparison with the Birkoff–Gustavson's normal form [54, 55] is that, after W is once established through each order, the new transformed physical quantities, for example, new action $\bar{J}_k$, frequency $\bar{\omega}_k$, momentum $\bar{p}_k$, and coordinate $\bar{q}_k$ of mode k, can be expressed straightforwardly as functions of the original momenta and coordinates $(\mathbf{p}, \mathbf{q})$ by using the evolution operator T

$$\bar{J}_k(\mathbf{p}, \mathbf{q}) = TJ_k(\mathbf{p}, \mathbf{q}) = T\left(\frac{p_k^2 + \omega_k^2 q_k^2}{2\omega_k}\right) \quad (2.19)$$

$$\bar{\omega}_k(\mathbf{p}, \mathbf{q}) = T\frac{\partial \bar{H}(\mathbf{J})}{\partial J_k} \quad (2.20)$$

$$\bar{p}_k(\mathbf{p}, \mathbf{q}) = Tp_k \quad (2.21)$$

$$\bar{q}_k(\mathbf{p}, \mathbf{q}) = Tq_k \quad (2.22)$$

For convenience, we denote hereafter the transformed quantities f in

terms of original $(\mathbf{p}, \mathbf{q})$ (and ε) by $\bar{f}(\mathbf{p}, \mathbf{q})$, for example, $\bar{J}_k(\mathbf{p}, \mathbf{q})$ when $f = J_k$, and we use the notation $J_k(\mathbf{p}, \mathbf{q})$ to represent the action of H_0;

$$J_k(\mathbf{p}, \mathbf{q}) = \frac{p_k^2 + \omega_k^2 q_k^2}{2\omega_k} = \frac{1}{2\pi} \oint_{E = H_0(\mathbf{p}, \mathbf{q})} p_k \, dq_k \tag{2.23}$$

Note that the *original* coordinate system $(\mathbf{p}, \mathbf{q})$ are, in other terms, regarded as the canonical variables to represent harmonic motions of H_0, but $(\bar{\mathbf{p}}(\mathbf{p}, \mathbf{q}), \bar{\mathbf{q}}(\mathbf{p}, \mathbf{q}))$ correspond to the canonical variables, which represent periodic/hyperbolic regular motions in the phase space for the nonlinear $H(\mathbf{p}, \mathbf{q})$ *if* $\bar{H}(\bar{\mathbf{p}}, \bar{\mathbf{q}})$ *actually exists.*

For example, $\bar{p}_k^{i\text{th}}(\mathbf{p}, \mathbf{q})$ and $\bar{q}_k^{i\text{th}}(\mathbf{p}, \mathbf{q})$ have the following forms, respectively,

$$\bar{p}_k^{i\text{th}}(\mathbf{p}, \mathbf{q}) = \sum_{n=0}^{i} \varepsilon^n \sum_j c_{nj} \mathbf{p}^{2\mathbf{s}_{nj}+\mathbf{1}} \mathbf{q}^{\mathbf{t}_{nj}} \tag{2.24}$$

$$\bar{q}_k^{i\text{th}}(\mathbf{p}, \mathbf{q}) = \sum_{n=0}^{i} \varepsilon^n \sum_j c'_{nj} \mathbf{p}^{2\mathbf{s}'_{nj}} \mathbf{q}^{\mathbf{t}'_{nj}} \tag{2.25}$$

where, for example,

$$\mathbf{p}^{2\mathbf{s}_{nj}+\mathbf{1}} \equiv \prod_{l=1}^{M} p_l^{s_{njl}} \left(\sum_{l=1}^{M} s_{njl} = |2\mathbf{s}_{nj} + \mathbf{1}| \right) \tag{2.26}$$

and

$$\mathbf{q}^{\mathbf{t}_{nj}} \equiv \prod_{l=1}^{M} q_l^{t_{njl}} \left(\sum_{l=1}^{M} t_{njl} = |\mathbf{t}_{nj}| \right) \tag{2.27}$$

Each coefficient depends on the original Hamiltonian and the order of CPT: for example, c_{nj} and c'_{nj} denote the (real) coefficients of the jth term at the nth order in $\bar{p}_k^{i\text{th}}(\mathbf{p}, \mathbf{q})$ and $\bar{q}_k^{i\text{th}}(\mathbf{p}, \mathbf{q})$, respectively; $\mathbf{s}_{nj}$ and $\mathbf{t}_{nj}$ are arbitrary positive integer vectors where $|\mathbf{s}_{nj}|, |\mathbf{t}_{nj}| \geqslant 0$ [s_{njl} and t_{njl}, arbitrary positive integers ($\geqslant 0$)] associated with the jth term at the nth order in $\bar{p}_k^{i\text{th}}(\mathbf{p}, \mathbf{q})$. The new $\bar{p}_k^{i\text{th}}(\mathbf{p}, \mathbf{q})$ and $\bar{q}_k^{i\text{th}}(\mathbf{p}, \mathbf{q})$ maintain time reversibility. We showed in the online supplement [40] the expressions through second order for $\bar{p}_1(\mathbf{p}, \mathbf{q})$ and $\bar{q}_1(\mathbf{p}, \mathbf{q})$ at saddle I, defined below, of Ar_6. The contributions of the original p_1 and q_1 in $\bar{p}_1^{i\text{th}}(\mathbf{p}, \mathbf{q})$ and $\bar{q}_1^{i\text{th}}(\mathbf{p}, \mathbf{q})$ are not necessarily large and almost all modes contribute to $\bar{p}_1^{i\text{th}}(\mathbf{p}, \mathbf{q})$ and $\bar{q}_1^{i\text{th}}(\mathbf{p}, \mathbf{q})$ for $i \geqslant 1$.

Despite its versatility, CPT has rarely been applied to many dof realistic molecular systems. The main reason is twofold: First is the cumbersome task

of the *analytical* derivative and integral calculations that appear successively in all kinds of CPT procedures. Second is the near-impossibility of obtaining even moderately simple *analytical* expressions to describe the accurate (e.g., ab initio) PESs in full. Two prescriptions for these obstacles have been developed, that is, the construction of an approximate Hamiltonian focusing on not global, but rather regional feature of dynamics in the vicinity of an arbitrary stationary point in question [38, 39], and a so-called "algebraic quantization" [38, 48–50], which replaces the cumbersome analytical differentiations and integrations carried out by computing directly with symbolic operations based on simple Poisson bracket rules.

B. Regional Hamiltonian

We first expand the full $3N$-dof potential energy surface about a chosen stationary point, that is, minimum, saddle, or higher rank saddle. By taking the zeroth-order Hamiltonian as a harmonic oscillator system, which might include some negatively curved modes, that is, reactive modes, we establish the higher order perturbation terms to consist of nonlinear couplings expressed in arbitrary combinations of coordinates.

$$H = H_0 + \sum_{n=1}^{\infty} \varepsilon^n H_n \tag{2.28}$$

where

$$H_0 = \frac{1}{2}\sum_j (p_j^2 + \omega_j^2 q_j^2) \tag{2.29}$$

$$\sum_{n=1}^{\infty} \varepsilon^n H_n = \varepsilon \sum_{j,k,l} C_{jkl} q_j q_k q_l + \varepsilon^2 \sum_{j,k,l,m} C_{jklm} q_j q_k q_l q_m + \cdots \tag{2.30}$$

Here, q_j and p_j are the jth normal coordinate and its conjugate momentum, respectively; ω_j and C_{jkl}, $C_{jklm}, \ldots$ are, respectively, the frequency of the jth mode, the coupling coefficient among q_j, q_k, and q_l and that among q_j, q_k, q_l, and q_m, and so forth. The frequency associated with an unstable reactive mode F and those of the other stable modes B are pure-imaginary and real, respectively. At any stationary point there are six zero-frequency modes corresponding to the total translational and infinitesimal rotational motions, and the normal coordinates of the infinitesimal rotational motions appear in the perturbation terms $H_n(\mathbf{q})$ $(n > 0)$. The contribution of the total translational motion is simply separated.

We make no more mention of this. If one deals with a system whose total angular momentum is zero, one could eliminate the contributions of the

total rotational motions from $H_n(\mathbf{q})$ ($n > 0$) by operating with a suitable projection operator [57]; at the stationary point it corresponds to putting to zero each normal coordinate and corresponding conjugate momentum representing the infinitesimal total rotational motion [58]. If the total angular momentum is not zero, the coupling elements among the rotational and vibrational modes must be taken into account. For the sake of simplicity, we focus on a ($3N$-6)-dof Hamiltonian system with total linear and angular momenta of zero, so that the kinetic and potential energies are purely vibrational [59]. For such a zeroth-order Hamiltonian $\omega_k \neq 0$ for all $k(=1, 2, \ldots, 3N-6)$, the associated action-angle variables of the stable modes B ($\omega_B \in \Re$:*real*) and the unstable mode F ($\omega_F \in \Im$:*imaginary*) are expressed as

$$J_B = \frac{1}{2\pi}\oint p_B\, dq_B = \frac{1}{2}\left(\frac{p_B^2}{\omega_B} + \omega_B q_B^2\right) \tag{2.31}$$

$$\Theta_B = \tan^{-1}\left(\frac{\omega_B q_B}{p_B}\right) \tag{2.32}$$

and

$$J_F = \frac{1}{2\pi} Im \int_{\text{barrier}} p_F\, dq_F \tag{2.33}$$

$$= \frac{i}{2}\left(\frac{p_F^2}{|\omega_F|} - |\omega_F| q_F^2\right) \tag{2.34}$$

$$\Theta_F = -i \tanh^{-1}\left(\frac{|\omega_F| q_F}{p_F}\right) \qquad \omega_F \equiv -|\omega_F| i \tag{2.35}$$

Here, the action associated with the reactive mode F has first been postulated in semiclassical transition state theory by Miller [12, 13, 60], and it is easily verified

$$\{\Theta_j, J_k\} = \delta_{jk} \qquad \{\Theta_j, \Theta_k\} = \{J_j, J_k\} = 0 \tag{2.36}$$

that any set of variables $\mathbf{J}$ and $\boldsymbol{\Theta}$ is canonical, including those associated with the unbound mode F.

C. Algebraic Quantization

The CPT calculation requires decomposing the functions appearing at each order in ε, called $\xi(\mathbf{p}, \mathbf{q})$ for brevity, usually represented by a sum of an

arbitrary combination of arbitrary power series in $\mathbf{p}$ and $\mathbf{q}$,

$$\xi(\mathbf{p}, \mathbf{q}) = \sum_j c_j \mathbf{p}^{\mathbf{s}_j} \mathbf{q}^{\mathbf{t}_j} \tag{2.37}$$

into

$$\langle \xi \rangle = \frac{1}{2\pi} \oint \xi(\mathbf{p}, \mathbf{q})\, d\boldsymbol{\Theta} \qquad \text{and} \qquad \{\xi\} = \xi - \langle \xi \rangle \tag{2.38}$$

where

$$\mathbf{p}^{\mathbf{s}_j} \equiv \prod_{l=1}^{M} p_l^{s_{jl}} \left(\sum_{l=1}^{M} s_{jl} = |\mathbf{s}_j| \right) \tag{2.39}$$

$$\mathbf{q}^{\mathbf{t}_j} \equiv \prod_{l=1}^{M} q_l^{t_{jl}} \left(\sum_{l=1}^{M} t_{jl} = |\mathbf{t}_j| \right) \tag{2.40}$$

Here c_j, the coefficient of the jth term of ξ, is not only real but also imaginary for the CPT calculations, if they include imaginary frequency mode(s); $\mathbf{s}_j$ and $\mathbf{t}_j$ are arbitrary positive integer vectors where $|\mathbf{s}_j|$, $|\mathbf{t}_j| \geqslant 0$ (their components s_{jl} and t_{jl}, arbitrary positive integers ($\geqslant 0$)) associated with $\mathbf{p}$ and $\mathbf{q}$ (p_l and q_l) of the jth term.

For a wide class of Hamiltonians described in Section II.B, a quite efficient technique, called algebraic quantization (AQ), was developed [38, 48–50]. This method first formally transforms $\xi(\mathbf{p}, \mathbf{q})$ to $\xi(\mathbf{a}^*, \mathbf{a})$ in terms of $(\mathbf{a}^*, \mathbf{a})$, which may correspond to customary creation and annihilation operators in quantum field theory, that is,

$$\xi(\mathbf{p}, \mathbf{q}) \to \xi(\mathbf{a}^*, \mathbf{a}) = \sum_s d_s \mathbf{a}^{*\mathbf{v}_s} \mathbf{a}^{\mathbf{u}_s} \tag{2.41}$$

where

$$\mathbf{a}^{*\mathbf{v}_s} \equiv \prod_{l=1}^{M} (a_l^*)^{v_{sl}} \left(\sum_{l=1}^{M} v_{sl} = |\mathbf{v}_s| \right) \tag{2.42}$$

$$\mathbf{a}^{\mathbf{u}_s} \equiv \prod_{l=1}^{M} a_l^{u_{sl}} \left(\sum_{l=1}^{M} u_{sl} = |\mathbf{u}_s| \right) \tag{2.43}$$

and

$$a_k^* = \frac{1}{\sqrt{2}}(p_k + i\omega_k q_k) \qquad a_k = \frac{1}{\sqrt{2}}(p_k - i\omega_k q_k) \tag{2.44}$$

Here, d_s, and $\mathbf{v}_s$ and $\mathbf{u}_s$, where $|\mathbf{v}_s|$, $|\mathbf{u}_s| \geqslant 0$ (their components v_{sl} and u_{sl}) depend on c_j, and $\mathbf{s}_j$ and $\mathbf{t}_j$ (s_{jl} and t_{jl}) in Eq. (2.37). By solving the following equation of motion,

$$\frac{da_k^*}{d\tau} = \{a_k^*, H_0\} \qquad \frac{da_k}{d\tau} = \{a_k, H_0\} \tag{2.45}$$

a_k^* and a_k can be expressed in terms of action J_k, frequency ω_k, and time τ obeying Hamiltonian H_0:

$$a_k^*(\tau) = \sqrt{\omega_k J_k}\, e^{i\Theta_k} = \sqrt{\omega_k J_k}\, e^{i(\omega_k \tau + \beta_k)} \tag{2.46}$$

$$a_k(\tau) = \sqrt{\omega_k J_k}\, e^{-i\Theta_k} = \sqrt{\omega_k J_k}\, e^{-i(\omega_k \tau + \beta_k)} \tag{2.47}$$

Then, one can rewrite Eq. (2.41) thanks to these equations as

$$\xi(\tau) = \sum_s \text{constant} \times d_s \exp[i(\mathbf{v}_s - \mathbf{u}_s) \cdot \boldsymbol{\omega}\tau] \tag{2.48}$$

which enables us to identify $\{\xi\}$ and $\langle\xi\rangle$ by simply checking the strength of the quantity associated with sth term,

$$|(\mathbf{v}_s - \mathbf{u}_s) \cdot \boldsymbol{\omega}| = \left| \sum_{l=1} (v_{sl} - u_{sl})\omega_l \right| \tag{2.49}$$

that is, all the terms in the summation of Eq. (2.48), which are regarded as free from and depending on time τ, are those of $\langle\xi\rangle$ and $\{\xi\}$. Furthermore, the cumbersome analytical calculations of the convolutions by Poisson bracket are also replaced by symbolic operations with no special mathematical manipulators, thanks to the simple Poisson bracket rules,

$$\{a_j^*, a_k^*\} = \{a_j, a_k\} = 0 \qquad \{a_j^*, a_k\} = i\omega_k \delta_{jk} \tag{2.50}$$

where δ is Kronecker delta. (See an illustrative example in Appendix D.)

III. REGULARITY IN CHAOTIC TRANSITIONS

We have applied this method to saddle crossing dynamics in intramolecular proton-transfer reaction of malonaldehyde [38, 39] and isomerization reaction of Ar_6 [40–44]. The former is a reacting system, involving a typical chemical bond breaking-and-forming; the latter is the smallest inert gas cluster in which no saddle dynamics more regular than the dynamics within

the local wells was revealed by the local K entropy analysis by Hinde and Berry [21].

In this chapter, we will show our recent analyses of Ar_6 isomerization, as an illustrative vehicle, with no peculiar or specific mode(s), that offers well representable, generalizable situations. The potential energy of Ar_6 is represented by the sum of pairwise Lennard–Jones potentials,

$$V(\mathbf{r}) = 4\epsilon \sum_{i>j} \left[\left(\frac{\sigma}{r_{ij}} \right)^{12} - \left(\frac{\sigma}{r_{ij}} \right)^{6} \right] \tag{2.51}$$

Here, we assigned laboratory scales of energy and length appropriate for argon, that is, $\epsilon = 121$ K and $\sigma = 3.4$ Å with the atomic mass $m = 39.948$ amu, and the total linear and angular momenta are set to zero [40]. This cluster has two kinds of potential energy minima (see Figure 2.1). The global minimum corresponds to an octahedral arrangement of the atoms (OCT), with energy $E = -12.712\epsilon$, and the other, higher minimum, to a trigonal bipyramid structure of five atoms, capped on one face by the sixth atom (CTBP), with energy $E = -12.303\epsilon$. There are two distinct kinds of first-rank saddles. One, saddle I, at energy $E = -12.079\epsilon$ joins the OCT and the CTBP minima. The other higher saddle, saddle II, at energy $E = -11.630\epsilon$, joins two permutationally distinct CTBP structures. Saddle II is slightly flatter than the lower saddle (Table II.1). We analyzed the invariants of motion during the course of isomerization reaction at total energies $E = 0.1$, 0.5, and 1.0ϵ above each saddle point energy at each saddle, for example, 16(45), 79(223), and 158(446)% of the barrier height of OCT $\rightarrow$ CTBP (OCT $\leftarrow$ CTBP). The computational recipe for constructing the $3N$-6(=12)-dof regional Hamiltonian was described elsewhere [40]. The three- and four-body coupling terms for both the saddles were determined by introducing an appropriate cut-off value; the total numbers of terms were 106 three-, and 365 four-body couplings for saddle I, and 189 and 674 for saddle II.

Here, we analyzed the Lie-transformed physical quantities, for example, $\bar{J}_k(\mathbf{p}, \mathbf{q})$, $\bar{\omega}_k(\mathbf{p}, \mathbf{q})$, $\bar{p}_k(\mathbf{p}, \mathbf{q})$, $\bar{q}_k(\mathbf{p}, \mathbf{q})$, up to second order, through which no (exact) commensurable conditions were encountered.

Throughout this chapter the parabolic barrier, the reaction coordinate in the original $(\mathbf{p}, \mathbf{q})$ space [and in the new $(\bar{\mathbf{p}}, \bar{\mathbf{q}})$ space] is denoted as q_1 ($\bar{q}_1$) and the other nonreactive coordinates, as $q_2, q_3, \ldots, q_{12}$ ($\bar{q}_2, \bar{q}_3, \ldots, \bar{q}_{12}$) in order of increasing frequency, $\omega_2 \leqslant \omega_3 \leqslant, \ldots, \leqslant \omega_{12}$ ($\bar{\omega}_2 \leqslant \bar{\omega}_3 \leqslant, \ldots, \leqslant \bar{\omega}_{12}$). The units of energy, distance, momentum, action, frequency, temperature, mass and time are, respectively, ϵ, $m^{1/2}\sigma$, $m^{1/2}\sigma \text{ps}^{-1}$, kps, ps^{-1}, K, argon atomic mass and ps, unless otherwise noted.

TABLE II.1
The Fundamental Frequencies ω_k for Saddles I and II (cm^{-1})[a]

Mode	Saddle I	Saddle II
1	$-49.29i(-1.477i)$	$-35.04i(-1.050i)$
2	96.06 (2.880)	89.01 (2.668)
3	113.04 (3.389)	98.54 (2.954)
4	122.91 (3.684)	124.37 (3.729)
5	149.40 (4.478)	138.24 (4.144)
6	149.71 (4.488)	153.00 (4.587)
7	173.06 (5.188)	171.13 (5.130)
8	197.81 (5.930)	178.34 (5.346)
9	200.03 (5.996)	198.44 (5.949)
10	206.19 (6.181)	206.63 (6.195)
11	235.10 (7.047)	229.78 (6.889)
12	238.47 (7.148)	241.04 (7.226)

[a]The values in the parentheses are in the unit of reciprocal picoseconds (ps^{-1}).

For analyses of the infrequent saddle crossings, we employed a modified Keck–Anderson method [40] to generate the microcanonical ensemble of well-saddle-well trajectories. We generated 10,000 well-saddle-well trajectories for both the saddles, which were found to be enough to yield statistical convergence in calculating the transmission coefficients in terms of many-body phase-space dividing hypersurfaces $S(\bar{q}_1^{i\text{th}}(\mathbf{p}, \mathbf{q}) = 0)$ $(i = 0, 1, 2)$ at $E = 0.1, 0.5, 1.0\epsilon$ above both the saddles. For the trajectory calculations, we used a fourth-order Runge–Kutta method with adaptive step-size control [61], and the total energies in their MD calculations were conserved within $\pm 1 \times 10^{-6}\epsilon$.

A. Invariancy of Actions in Transition States

To begin, we look into the new action variables $\bar{J}_k(\mathbf{p}, \mathbf{q})$ along the saddle crossing trajectories over saddle I, linking the global minimum OCT and the higher minimum CTBP, obeying equations of motion of the original Hamiltonian $H(\mathbf{p}, \mathbf{q})$. The trajectory of an isolated bound oscillator retraces the same points during each oscillation and the associated action is a constant of the motion. The extent to which the new kth action $\bar{J}_k(\mathbf{p}, \mathbf{q})$ mimics this behavior indicates how separable the new kth mode, described by $\bar{p}_k$ and $\bar{q}_k$, is. Figure 2.2 shows a representative trajectory projected onto the (q_1, q_{12}) plane for each total energy, 0.05, and 0.5ϵ. Here the trajectory at 0.05ϵ is shown specifically because intuition tells us it should be less

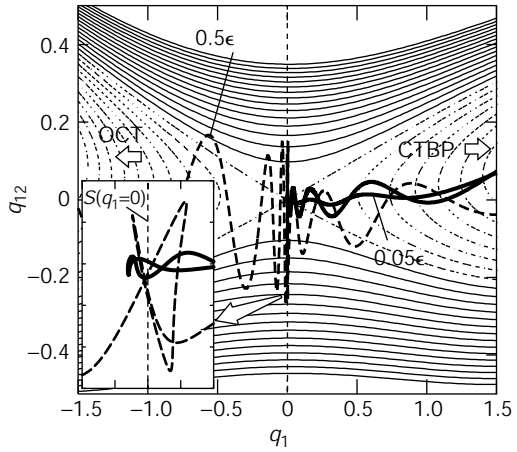

Figure 2.2. A representative saddle-recrossing trajectory at $E = 0.05$, and 0.5ϵ over the dividing surface $S(q_1 = 0)$, projected onto the (q_1, q_{12}) plane and the PES contour plot in this plane. The window in this figure is scaled to $-0.01 \leqslant q_1 \leqslant 0.01$ and $-0.3 \leqslant q_{12} \leqslant 0.2$. The trajectories from the left to the right side correspond to crossing from the OCT to the CTBP minimum. While the sampled trajectory at 0.05ϵ (bold solid line) is nonreactive, that is, coming from the CTBP and returning to the same CTBP, that at $E = 0.5\epsilon$ (dashed line) is reactive. The PES contour is plotted with an energy step 0.03ϵ, whose solid and dashed lines represent positive and negative values, respectively.

chaotic than those at $0.1 - 1.0\epsilon$, because at such an energy, in the vicinity of the saddle point, the system has insufficient kinetic energy to reach regions where nonlinearity and mode–mode mixing are significant.

Figure 2.3 shows the zeroth-, first-, and second-order new actions along the trajectory at 0.05ϵ. At even $E = 0.05\epsilon$, only slightly above the saddle point energy, almost of all the zeroth-order actions $\bar{\mathbf{J}}^{0\text{th}}(\mathbf{p}, \mathbf{q})$ do not maintain constancy of motion at all. This result implies that the system's trajectory reflects even very small nonlinearities on the PES and deviates from a simple normal mode picture. As we extend the order of LCPT, some but not all LCPT actions $\bar{J}_k$ tend to be conserved in the saddle region.

Figure 2.3. The time dependencies of $\bar{J}_k(\mathbf{p}, \mathbf{q})$ for the saddle-crossing trajectory at 0.05ϵ in Figure 2.2: (*a*) zeroth-, (*b*) first-, and (*c*) second-order actions. The units of action for mode 1 must be multiplied by a factor of an imaginary number i throughout the following figures. In $1.5 < t < 7.5$ ps, the system trajectories remain in a region $\sim -0.01 < q_1 < 0.2$ $[m^{1/2}\sigma]$. The solid, dashed, diamond, circle, square, doted, long-dashed, triangle, x, +, dot–dashed, and bold-solid lines throughout this chapter will denote modes 1, 2, 3, 4, 5, 6, 7, 8, 9, 10, 11, and 12, respectively.

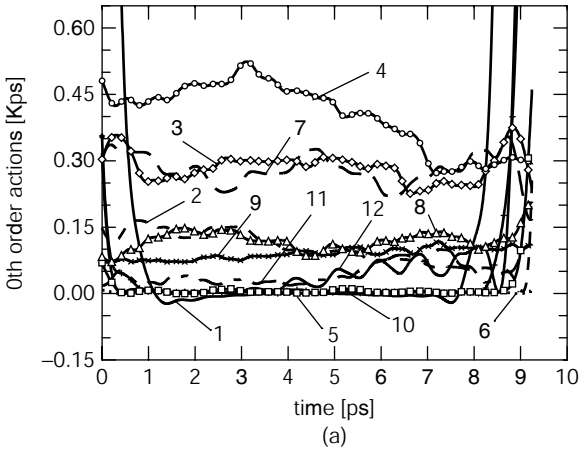
0th order actions [Kps]
0.60
0.45
0.30
0.15
0.00
–0.15
0 1 2 3 4 5 6 7 8 9 10
time [ps]
4
3
7
2
9
11
12
8
1
5
10
6
(a)

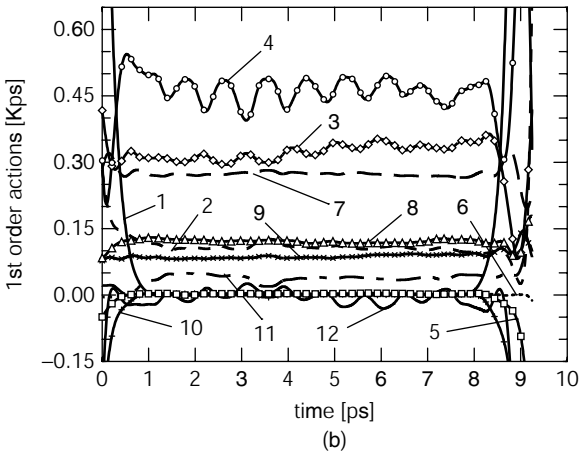
1st order actions [Kps]
0.60
0.45
0.30
0.15
0.00
–0.15
0 1 2 3 4 5 6 7 8 9 10
time [ps]
4
3
1
2
9
7
8
6
10
11
12
5
(b)

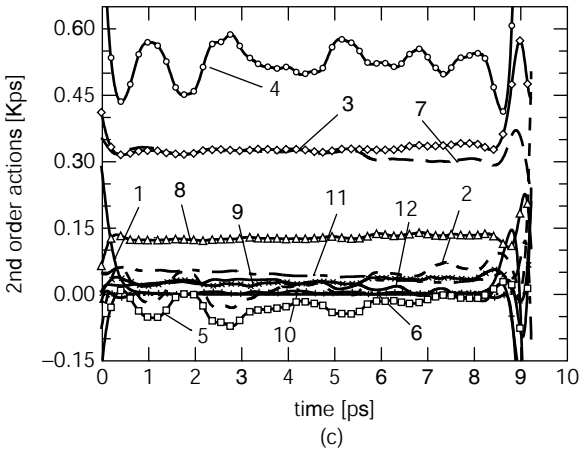
2nd order actions [Kps]
0.60
0.45
0.30
0.15
0.00
–0.15
0 1 2 3 4 5 6 7 8 9 10
time [ps]
4
3
7
1
8
9
11
12
2
5
10
6
(c)

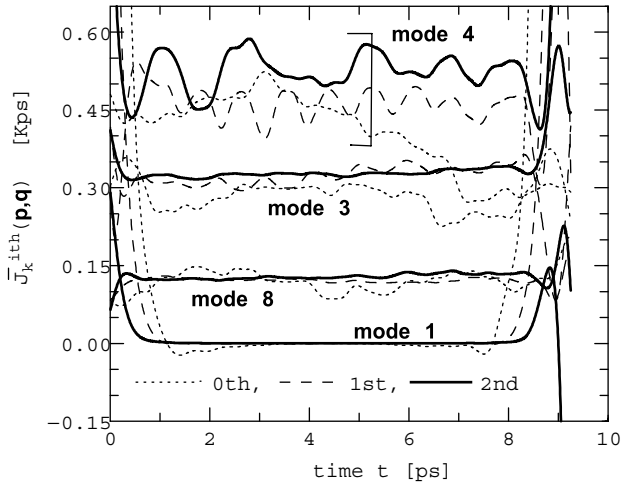

Figure 2.4. $\bar{J}_k^{ith}(\mathbf{p}(t), \mathbf{q}(t))$ ($i = 0, 1$, and 2) at $E = 0.05\epsilon$ in Figure 2.3: thin, dot, and bold lines, respectively, denote the zeroth-, first-, and second-order LCPT action.

Figure 2.4 shows each order $\bar{J}_k^{ith}(\mathbf{p}, \mathbf{q})$ for $k = 1, 3, 4$, and 8 on the same figure axes. Even at such an energy, only slightly above the saddle point energy; just 8% of the activation energy 0.633ϵ from the OCT minimum, almost none of the zeroth-order actions $\bar{\mathbf{J}}^{0th}(\mathbf{p}, \mathbf{q})$ maintain any constancy of motion at all; that is, even there, most modes violate a simple normal mode picture. The higher the order to which the LCPT is carried, the more *some* of the actions $\bar{J}_k$ tend to be well conserved, and to persist as nearly conserved quantities for longer times. The initial drop and/or rise observed in $\bar{J}_k(\mathbf{p}, \mathbf{q})$ at short times (e.g., 0–0.5 ps in Fig. 2.4) to the flat region implies that initially, the system is just entering a "regular region" near the saddle point, outside of which the system is subject to considerable nonlinearities of the PES. That is, in the saddle region, some modes are well decoupled and follow periodic orbits in phase space; examples are those of Eqs. (2.8) and (2.9), while the others are coupled at least within coupled mode-subsets in the $(\bar{\mathbf{p}}^{2nd}, \bar{\mathbf{q}}^{2nd})$ coordinate system.

How does the crossing dynamics change as the energy of the system increases? Intuition suggests that at higher total energies, the nonlinearities of the PES cannot be considered as a "sufficiently weak perturbation", and the number of approximate local invariants of motion becomes smaller and smaller, going to zero at sufficiently high energy, that is, causing the transition from quasiregular to chaotic dynamics. This is actually a universal picture assumed in almost of all chemical reaction theories, in the vicinity

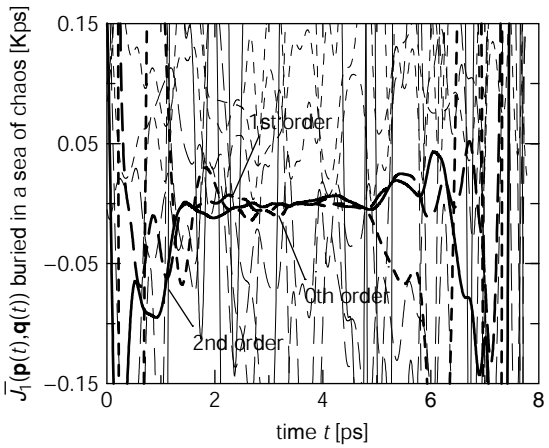

Figure 2.5. An example of $\bar{J}_k^{\text{ith}}(\mathbf{p}(t), \mathbf{q}(t))$ $(i = 0, 1, 2)$ along a representative trajectory recrossed over $S(q_1 = 0)$ at saddle I $(E = 0.5\epsilon)$: all the lines denote all the actions except bold ones $\bar{J}_1^{\text{ith}}$.

of potential energy minima, which validates the assumption of local vibrational equilibrium in the reactant well. In Figure 2.5, we show that at $E = 0.5\epsilon$, 79% above of the activation energy from the OCT minimum, while none of the action variables for the nonreactive modes, $\bar{q}_k$ $(2 \leqslant k \leqslant 3N - 6)$, are conserved even through $\mathcal{O}(\varepsilon^2)$, the reactive mode $\bar{q}_1$ stands out among all the rest: Its action is more conserved as the order of LCPT increases. (We rigorously demonstrated [43, 44] that these findings, that the phase-space reaction coordinate $\bar{q}_1(\mathbf{p}, \mathbf{q})$ persists its action even in the sea of chaos, is quite generic, irrespective of these sampled trajectories.)

However, how do these trajectories, observed as recrossing over the configurational dividing surface $S(q_1 = 0)$, look in the new $(\bar{\mathbf{p}}, \bar{\mathbf{q}})$ space?

B. "See" Trajectories Recrossing the Configurational Dividing Surface in Phase Space

Let us see these two trajectories, recrossing the conventional, configurational dividing surface $S(q_1 = 0)$, by projecting these onto the zeroth-, first-, and second-order new coordinate planes of $\bar{q}_j(\mathbf{p}, \mathbf{q})$ and $\bar{q}_k(\mathbf{p}, \mathbf{q})$. Remember that the zeroth-order coordinate system $(\bar{q}_j^{\text{0th}}, \bar{q}_k^{\text{0th}})$ is the original normal coordinate system (q_j, q_k). Figure 2.6 shows the projections onto a 2D subspace chosen from the nonreactive coordinates, $(\bar{q}_3^{\text{ith}}(\mathbf{p}, \mathbf{q}), \bar{q}_8^{\text{ith}}(\mathbf{p}, \mathbf{q}))$, at both the energies.

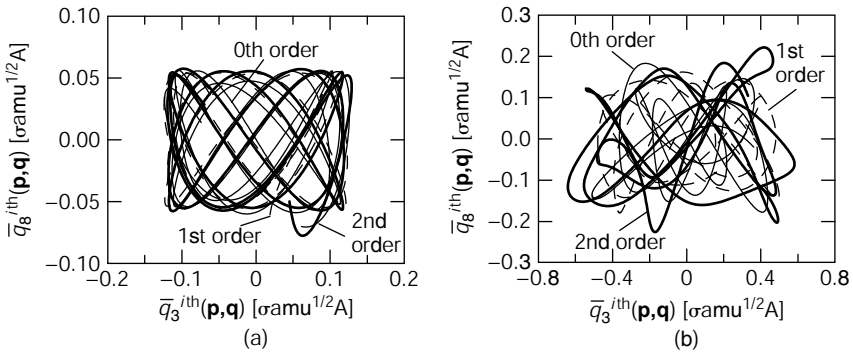

Figure 2.6. The viewpoint from $(\bar{q}_3^{i\text{th}}(\mathbf{p},\mathbf{q}), \bar{q}_8^{i\text{th}}(\mathbf{p},\mathbf{q}))$ (saddle I). (*a*) $E = 0.05\epsilon$, (*b*) $E = 0.5\epsilon$.

At the lower energy, 0.05ϵ [see Fig. 2.6(*a*)], in all the orders one can see the approximate Lissajous figures, which implies that in the subspace of these two nonreactive dof, the motions are composed of two approximately decoupled, simple harmonic oscillations. As the total energy increases to 10 times higher, $\sim 0.5\epsilon$, as one may anticipate from Figure 2.5, that no approximate invariants of motion survive in the nonreactive subspace, and the nonreactive modes change from regular to fully chaotic dynamics [see Fig. 2.6(*b*)].

An even more striking consequence of the LCPT transformation appears in the behavior of the reactive degrees of freedom. Figure 2.7 shows the projections of the recrossing trajectories onto the $(\bar{q}_1^{i\text{th}}(\mathbf{p},\mathbf{q}), \bar{q}_4^{i\text{th}}(\mathbf{p},\mathbf{q}))$. The abscissas in the figure correspond to a reaction coordinate, that is, $\bar{\omega}_1 \in \mathfrak{F}$, and the ordinates, to the nonreactive coordinates, that is, $\bar{\omega}_4 \in \mathfrak{R}$, in each order's coordinate system. To do this, we first examine the nonreactive *re*crossing trajectory at 0.05ϵ in Figure 2.2, which has returned to the original state after recrossing over the naive dividing surface $S(q_1 = 0)$. As shown in Figure 2.7, this trajectory never cross any dividing surface $S(\bar{q}_1^{1\text{st}}(\mathbf{p},\mathbf{q}) = 0)$ and $S(\bar{q}_1^{2\text{nd}}(\mathbf{p},\mathbf{q}) = 0)$ from the CTBP minimum where the trajectory originates. The trajectory is simply not that of a reaction. We can deduce one important feature from this: If the local invariants of motion persist along the higher order reactive coordinate, for example, $\bar{q}_1^{2\text{nd}}(\mathbf{p},\mathbf{q})$, all nonreactive recrossing trajectories observed over any configurational dividing surface, for example, $S(q_1 = 0)$, is transformed to trajectories that do not cross the dividing hypersurface $S(\bar{q}_1^{2\text{nd}}(\mathbf{p},\mathbf{q}) = 0)$ in the phase space. The reason is that decoupling the motion along the reactive LCPT coordinate removes all forces that would return the system back across the dividing

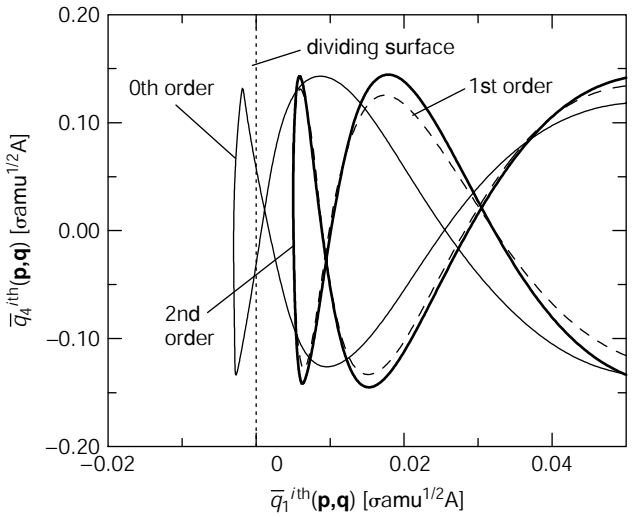

Figure 2.7. The projections onto $(\bar{q}_1^{i\text{th}}(\mathbf{p},\mathbf{q}), \bar{q}_4^{i\text{th}}(\mathbf{p},\mathbf{q}))$ at $E = 0.05\epsilon$ over saddle I.

hypersurface. Such nonreactive trajectories are those with insufficient incident momentum in the reactive coordinate $\bar{p}_1(\mathbf{p}(0), \mathbf{q}(0))$ to climb over the saddle. In other words, all the trajectories should react, whose incident momentum $\bar{p}_1(\mathbf{p}(0), \mathbf{q}(0))$ is larger than a certain threshold to carry the system through it.

Next, turn to the behavior of the reactive recrossing trajectory at 0.5ϵ, at which the transition state is almost chaotic (see Fig. 2.5). Here, as seen in Figure 2.8, the recrossings that occur over the naive dividing surface $S(q_1 = 0)$ in zeroth order are eliminated; they occur as no-return crossing motions over the second-order dividing surface $S(\bar{q}_1^{2\text{nd}}(\mathbf{p},\mathbf{q}) = 0)$. Furthermore, the system's trajectories along the second-order reactive coordinate $\bar{q}_1^{2\text{nd}}(\mathbf{p},\mathbf{q})$ are not forced to return to the dividing surface $S(\bar{q}_1^{2\text{nd}}(\mathbf{p},\mathbf{q}) = 0)$ over the (saddle) region, $-0.04 < \bar{q}_1^{2\text{nd}}(\mathbf{p},\mathbf{q}) < 0.04$. On the other hand, the zeroth- and first-order reactive coordinates are not decoupled from the other modes in the regions either near or more distant from the dividing surface. For example, the cyclic motion around $0.025 < \bar{q}_1^{1\text{st}}(\mathbf{p},\mathbf{q}) < 0.030$ implies the existence of some couplings between $\bar{q}_1^{1\text{st}}(\mathbf{p},\mathbf{q})$ and $\bar{q}_4^{1\text{st}}(\mathbf{p},\mathbf{q})$. Up to such moderately high energies, "apparent" recrossing reactive trajectories, observed in a low-order phase-space coordinate system $(\bar{\mathbf{p}}, \bar{\mathbf{q}})$ or the configurational space, can be rotated away to the ballistic, single crossing motions in the higher orders.

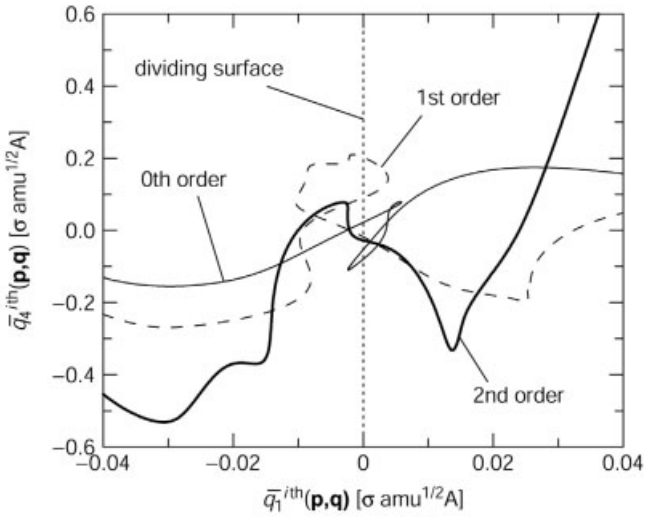

Figure 2.8. The projections onto $(\bar{q}_1^{i\text{th}}(\mathbf{p},\mathbf{q}), \bar{q}_4^{i\text{th}}(\mathbf{p},\mathbf{q}))$ at $E = 0.5\epsilon$ over saddle I.

C. "Unify" Transition State Theory and Kramers–Grote–Hynes Theory

In all the cases that saddle crossings have approximate local invariants of motion associated with the "reactive mode F" in a short time interval but long enough to determine the final state of the crossings, $S(\bar{q}_F(\mathbf{p},\mathbf{q}) = 0)$ can be identified as a "no-return" dividing hypersurface, free from the long-standing ambiguity in reaction rate theories, the recrossing problem. Recall that it is because there is no means or force returning the system to $S(\bar{q}_F(\mathbf{p},\mathbf{q}) = 0)$ even though the system may recross any of the configurational surfaces. The reformulated microcanonical (classical) transition state theory (TST) rate constant $\bar{k}^{\text{TST}}(E)$ is obtained [38] as an average of the one-way fluxes $j_+(=\dot{\bar{q}}_F(\mathbf{p},\mathbf{q})h(\dot{\bar{q}}_F(\mathbf{p},\mathbf{q})))$ across $S(\bar{q}_F(\mathbf{p},\mathbf{q}) = 0)$ over microcanonical ensembles constructed over a range of energies E.

$$\begin{aligned}\bar{k}^{\text{TST}}(E) &= \langle j_+ \rangle_E = \langle \dot{\bar{q}}_F(\mathbf{p},\mathbf{q})\delta[\bar{q}_F(\mathbf{p},\mathbf{q})]h[\dot{\bar{q}}_F(\mathbf{p},\mathbf{q})]\rangle_E \\ &= \int_1 dq_1\, dp_1 \cdots \int_N dq_N\, dp_N \\ &\quad \times \delta[E - H(\mathbf{p},\mathbf{q})]\dot{\bar{q}}_F(\mathbf{p},\mathbf{q})\delta[\bar{q}_F(\mathbf{p},\mathbf{q})]h[\dot{\bar{q}}_F(\mathbf{p},\mathbf{q})] \qquad (2.52)\end{aligned}$$

where $h(x)$ and $\delta(x)$, respectively, denote the Heaviside function and Dirac's delta function of x.

The deviation of $\bar{k}^{\mathrm{TST}}(E)$ from the experimental rate coefficient $k^{\mathrm{exp}}(E)$ is defined as a new transmission coefficient κ_c:

$$\kappa_c = \frac{k^{\mathrm{exp}}(E)}{\bar{k}^{\mathrm{TST}}(E)} \tag{2.53}$$

If the vibrational energy relaxation is fast enough to let us assume quasi-equilibration in the well, and the tunneling effect is negligible, one may use κ_c to estimate the extent of the *true* recrossing effect independent of the viewpoint or coordinate along which one observe its reaction events. This would be a means to measure the extent to which the action associated with the reactive mode cease to be approximate invariants; their nonconstancy reflects the degree of closeness to *fully developed* chaos in which no invariant of motion exists.

In order to focus on how the recrossings over a given dividing surface contribute to κ_c, we estimated the quantities $\kappa_c^{i\mathrm{th}}(t)$

$$\kappa_c^{i\mathrm{th}}(t) \equiv \kappa_c(t; S(\bar{q}_F^{i\mathrm{th}}(\mathbf{p}, \mathbf{q}) = 0)) = \frac{\langle j(t=0) h[\bar{q}_F^{i\mathrm{th}}(\mathbf{p}, \mathbf{q})] \rangle_E}{\langle j_+(t=0) \rangle_E} \tag{2.54}$$

using the 10,000 well-saddle-well classical trajectories across both the saddles at these three distinct energies above the threshold of Ar_6. Here $j(t=0)$ and $j_+(t=0)$, respectively, denote the initial total, and initial positive fluxes crossing the ith-order phase-space dividing surface $S(\bar{q}_F^{i\mathrm{th}}(\mathbf{p}, \mathbf{q}) = 0)$, and the origin of time t was set when the system trajectory first crosses the given dividing surface.

The $\kappa_c^{i\mathrm{th}}(t)$ in the regions of saddle I and saddle II are shown at $E = 0.1$, 0.5, and 1.0ϵ in Figure 2.9. The zeroth-order transmission coefficient $\kappa_c^{0\mathrm{th}}(t)$, using the conventional configurational dividing surface $S(q_1 = 0)$, deviates significantly from unity (except at a very short times) and these deviations increase with increasing total energy. The plateau in $\kappa_c^{i\mathrm{th}}(t)$ apparent in the figures implies that the recrossing trajectories eventually go into their final state and never again cross the given dividing surface within some interval long compared with the transit time. The plateau value of the $\kappa_c^{0\mathrm{th}}(t)$ may be identified as the conventional transmission coefficient κ. All these κ's smaller for saddle I than for saddle II show that the traditional reaction coordinate q_1 is more coupled to the other nonreactive dof in the region of saddle I than it is near saddle II [20–22]. We showed, however, that in terms of the phase-space dividing hypersurface $S(\bar{q}_1^{i\mathrm{th}}(\mathbf{p}, \mathbf{q}) = 0)$, for low and moderately high energies, ~ 0.1–0.5ϵ, for both the saddles, the higher is the order of the perturbative calculation, the closer the $\kappa_c^{i\mathrm{th}}$ is to unity. Even at

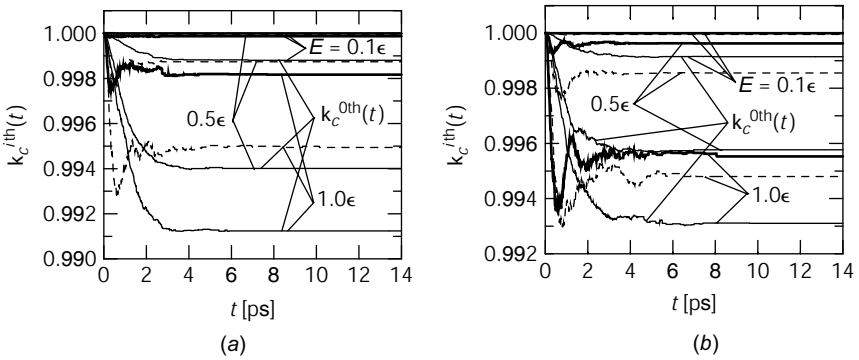

Figure 2.9. The new transmission coefficient $\kappa_c^{i\text{th}}(t)$ ($i = 0, 1, 2$) ($E = 0.1$, 0.5, and 1.0ε); (*a*) saddle I; (*b*) saddle II. The solid, dot, and bold lines denote the zeroth-, first-, and second-order $\kappa_c^{i\text{th}}(t)$, respectively. The converged values at saddle I are 0.9988(0), 0.99996(1), 1.00000(2) ($E = 0.1\varepsilon$); 0.9940(0), 0.9987(1), 0.9999(2) ($E = 0.5\varepsilon$); 0.9912(0), 0.9949(1), 0.9982(2) ($E = 1.0\varepsilon$), and those at saddle II 0.9991(0), 0.99995(1), 1.000000(2) ($E = 0.1\varepsilon$); 0.9958(0), 0.9986(1), 0.9996(2) ($E = 0.5\varepsilon$); 0.9931(0), 0.9948(1), 0.9955(2) ($E = 1.0\varepsilon$). The number in parentheses denotes the order of LCPT.

energies $\sim 0.5\varepsilon$, the plateau values of $\kappa_c^{2\text{nd}}(t)$ are almost unity, for example, 0.9999 (for saddle I) and 0.9996 (for saddle II). As the total energy becomes much higher, $\sim 1.0\varepsilon$, even $\kappa_c^{2\text{nd}}$ becomes deviate significantly from unity as the conventional $\kappa_c^{0\text{th}}$ does. This "deviation from unity at the order $\mathcal{O}(\varepsilon^2)$" represents the degrees of

1. The difficulty of exposing the approximate invariants of motion associated with $\bar{q}_1$ with only a finite orders, $\sim \mathcal{O}(\varepsilon^2)$, to decouple the reactive $\bar{q}_1$ from the others.
2. Encroaching into a sufficiently high-energy region where the *length* of the path where the reactive mode is separable diminishes (i.e., even though it would be possible to carry CPT through an infinite order, it is anticipated, especially for nonlinear many-body systems, that there exist a certain energy region so high that the convergence radius of CPT becomes negligibly small).

The fact that the deviation is smaller for saddle I than that for saddle II implies that the crossing dynamics over saddle I should exhibit better approximate invariants of motion with $\bar{q}_1$ than that over saddle II at $\mathcal{O}(\varepsilon^2)$. Note that less chaotic saddle-crossing dynamics need not imply a better approximate invariant of motion associated with $\bar{q}_1$ at any specific order of the perturbative calculation. Furthermore, the strength of chaos in the regions of saddles, as characterized by the local Kolmogorov entropy, the

sum of all the positive local Liapunov exponents $\boldsymbol{\lambda}^{\mathrm{sad}}$, is only weakly affected by a single (small) positive exponent λ_1^{sad} associated with the somewhat-regularized $\bar{q}_1(\mathbf{p}, \mathbf{q})$ motion. This "burial" of a few locally regular modes in a sea of chaotic modes is apparent in the results of Hinde and Berry [21].

All these results indicate that, even in the region where the system is almost chaotic, an approximate analytical expression for (first-rank) saddle-crossing dynamics may nonetheless exist along a negatively curved mode in the phase space coordinate system $(\bar{\mathbf{p}}, \bar{\mathbf{q}})$;

$$\bar{q}_1(\mathbf{p}(t), \mathbf{q}(t)) \simeq \alpha e^{|\bar{\omega}_1|t} + \beta e^{-|\bar{\omega}_1|t} \tag{2.55}$$

$$\alpha = \frac{1}{2}\left(\bar{q}_1(t_0) + \frac{\bar{p}_1(t_0)}{|\omega_1|}\right) \tag{2.56}$$

$$\beta = \frac{1}{2}\left(\bar{q}_1(t_0) - \frac{\bar{p}_1(t_0)}{|\omega_1|}\right) \tag{2.57}$$

Here, t_0 is arbitrary time in t in the vicinity of saddles. These expressions imply that, even though almost all degrees of freedom of the system are chaotic, the final state (and initial state) may have been determined a priori. For example, if the trajectories that have initiated from $S(q_1 = 0)$ at time t_0 have $\alpha > 0$, the final state has already been determined at "the time t_0 when the system has just left the $S(q_1 = 0)$" to be a stable state directed by $\bar{q}_1 > 0$. Similarly, from only the phase-space information at $t = t_0$ (the sign of β), one can grasp whether the system on $S(q_1 = 0)$ at time t_0 has climbed from either stable state, that is, reactant or product, without calculating any time-reversed trajectory [62].

To address the recrossing problem, which spoils the "no-return" hypothesis, one has tried to interpret the reaction rates either by variational TST [9–11] or by (generalized) Langevin formalism by Kramers [14] and Grote and Hynes [15]. van der Zwan and Hynes [63] proved that, for a class of Hamiltonians representing (first-rank) saddles by parabolic barrier–harmonic oscillator systems linearly coupled with one another (i.e., an integrable system!), the TST rate constant is equivalent to that of the Grote–Hynes formulation with the parabolic mode as the reactive dof, if the reaction coordinate is chosen as an unstable normal coordinate composed of the total system (= reacting system + bath), under the condition that the vibrational relaxation is fast enough to attain "quasiequilibration" in the reactant well.

Our findings suggest that their equivalence is much more generic and applicable to a wider range of Hamiltonian classes, even when the system is almost chaotic. This stimulates us to reconsider a fundamental question of what constitutes the "thermal bath" for reacting systems. One may antici-

pate that reactions take place along a *ballistic* path composed of the *total* system in the sea of chaos, at least, in the region of saddles. The "thermal bath" for reactions, simply defined thus far as all the rest of the atoms or molecules except the reacting system, does not necessarily retard the reactive trajectories; rather, such a bath may control and assist the reactants to climb and go through the saddles.

Most reactions take place not on *smooth* but *rugged* PESs, for which the (generalized) Langevin formalism was originally developed. Nevertheless, a picture similar to that of a simple reacting system may emerge even on a rugged PES. In cases in which a "coarse-grained" landscape connecting one basin with another can be well approximated as parabolic at the zeroth order, we may elucidate how the coarse-grained action persists along the (coarse-grained) reactive degree of freedom during the dynamical evolution obeying the original Hamiltonian $H(\mathbf{p}, \mathbf{q})$. A technique or a scheme [64] to extract such a coarse-grained regularity or cooperativity from "random thermal" motions is quite demanding, especially to establish the equivalence or differences of descriptions by different representations or coordinate systems.

D. "Visualize" a Reaction Bottleneck in Many-Body Phase Space

The dividing surface in this representation is analogous to the conventional dividing surface in the sense that it is the point set for which the reaction coordinate has the constant value it has at the saddle-point singularity. However the nonlinear, full-phase-space character of the transformation makes the new crossing surface a complicated, abstract object. We proposed [41, 42] a visualization scheme of $S(\bar{q}_1(\mathbf{p}, \mathbf{q}) = 0)$ by projections into spaces of a few dimensions, for example, the (q_j, q_k) plane:

$$\begin{aligned}\bar{S}(q_j, q_k; E) &= \langle \delta[\bar{q}_1(\mathbf{p}', \mathbf{q}')]\delta(q_j' - q_j)\delta(q_k' - q_k)\rangle_E \\ &= \int_1 dq_1' \, dp_1' \cdots \int_N dq_N' \, dp_N' \\ &\quad \times \delta[E - H(\mathbf{p}', \mathbf{q}')]\delta[\bar{q}_1(\mathbf{p}', \mathbf{q}')]\delta(q_j' - q_j)\delta(q_k' - q_k) \quad (2.58)\end{aligned}$$

For example, the projection onto the configurational reaction coordinate q_1 is an important device to reveal how $S(\bar{q}_1(\mathbf{p}, \mathbf{q}) = 0)$ differs from the conventional dividing surface $S(q_1 = 0)$. Remember that in an energy range close to the threshold energy in which the normal mode picture is approximately valid, the phase-space $S(\bar{q}_1 = 0)$ collapses onto the traditional configuration-space surface where $q_1 = 0$. Similarly, the projection onto p_1

TABLE II.2
Pattern Classification (N_{+-}, N_{-+}, σ) of Nonreactive, Recrossing Trajectories Over the Configurational Dividing Surface $S(q_1 = 0)$ at Saddle I

$E =$	0.1ϵ ($= -11.979\epsilon$)	0.5ϵ ($= -11.579\epsilon$)	1.0ϵ ($= -11.079\epsilon$)
(1, 1, −)	161	329	369
(2, 2, −)	7	23	22
(3, 3, −)	0	1	3
(4, 4, −)	0	0	0
(1, 1, +)	26	67	86
(2, 2, +)	1	6	12
(3, 3, +)	0	0	0
(4, 4, +)	0	1	0

is an important device to reveal how the passage velocity through the saddles affects the $S(\bar{q}_1(\mathbf{p}, \mathbf{q}) = 0)$.

One should be careful about the implication of $S(q_1 = 0)$ in the phase space. Accessible values of $\mathbf{p}$ and $\mathbf{q}$ are restricted by total energy E. Thus, in stating that $S(\bar{q}_1(\mathbf{p}, \mathbf{q}) = 0)$ partially collapses onto $S(q_1 = 0)$, the relevant regions of $S(q_1 = 0)$ are not all of this surface determined by only q_1 irrespective of the other variables, but only parts of a hypersurface where $q_1 = 0$, generally determined by $\mathbf{p}$ and $\mathbf{q}$.

Next, we ask, What could one learn from these projections of the complicated, energy and momenta-dependent abstract object, $S(\bar{q}_1(\mathbf{p}, \mathbf{q}) = 0)$?

First, we look into the complicated nonreactive, recrossing behavior of trajectories over the conventional dividing surface $S(q_1 = 0)$ at saddle I. Table II.2 shows the numbers of nonreactive crossings in 10,000 well-saddle-well trajectories over $S(q_1 = 0)$ as the energy increases from $E = 0.1$ to 1.0ϵ. Here, (N_{+-}, N_{-+}, σ) represents the number of times each crosses the dividing surface in a specific direction: if a crossing trajectory, whose sign of the flux at the first crossing is σ, crosses a given dividing surface N_{+-} times from positive to negative, and N_{-+} times from negative to positive along the reactive coordinate, the trajectory is classified into the (N_{+-}, N_{-+}, σ)-type crossing, for example, for saddle I a trajectory that crosses the dividing surface two times and the first crossing is from the OCT to the CTBP minimum is (1, 1, +).

The table tells us the trajectories climbing from the CTBP minimum are more likely to return after crossing $S(q_1 = 0)$, than the trajectories from the OCT global minimum, for example, $329(1, 1, -) \gg 67(1, 1, +)$ at 0.5ϵ (the corresponding figures are essentially the same for the symmetrical saddle II within the statistical error [41]).

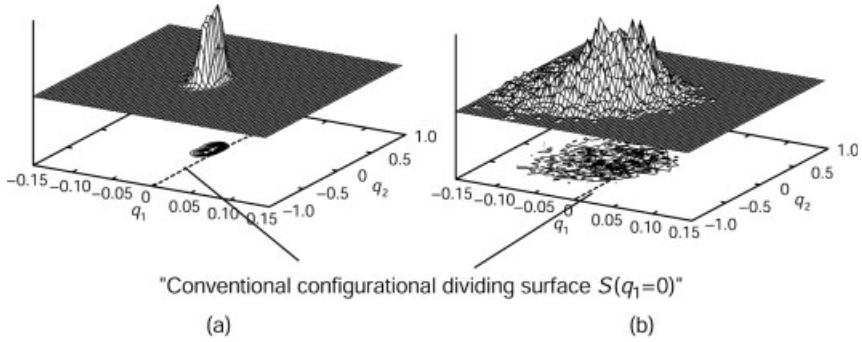

Figure 2.10. $\bar{S}^{2\text{nd}}(q_1, q_2; E)$ at saddle I, (*a*) $E = 0.1\epsilon$; (*b*) $E = 0.5\epsilon$.

So far, there has been no means to address why, as the system passes through the transition state, there is such a distinct dependence of probability on the direction of climbing. The visualization scheme of the phase-space dividing surface lets us probe deeper into such questions. Figures 2.10 and 2.11 show projections of the *i*th order dividing surface $S(\bar{q}_1^{i\text{th}}(\mathbf{p}, \mathbf{q}) = 0)$ onto the two-dimensional (q_1, q_2) subspace at $E = 0.1$ and 0.5ϵ for saddle I and saddle II, respectively. As the total energy increases, the projections of the phase-space dividing surfaces, $S(\bar{q}_1^{i\text{th}}(\mathbf{p}, \mathbf{q}) = 0)$ $(i = 1, 2)$, broaden and extend to regions more removed from the conventional dividing surface $S(q_1 = 0)$. Note for saddle I that these $S(\bar{q}_1(\mathbf{p}, \mathbf{q}) = 0)$ are more heavily distributed on the minus side (to the OCT minimum) than on the plus side (to the CTBP minimum) in the q_1 axis. This asymmetrical feature of the $S(\bar{q}_1(\mathbf{p}, \mathbf{q}) = 0)$ explains the higher frequencies found for $(n, n, -)$ than for $(n, n, +)$ type

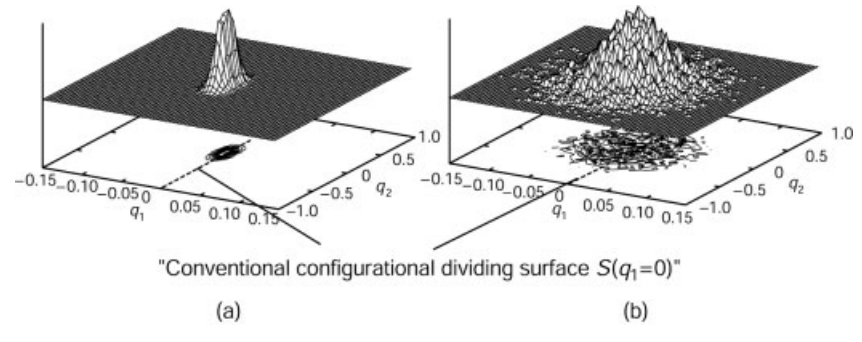

Figure 2.11. $\bar{S}^{2\text{nd}}(q_1, q_2; E)$ at saddle II, (*a*) $E = 0.1\epsilon$; (*b*) $E = 0.5\epsilon$.

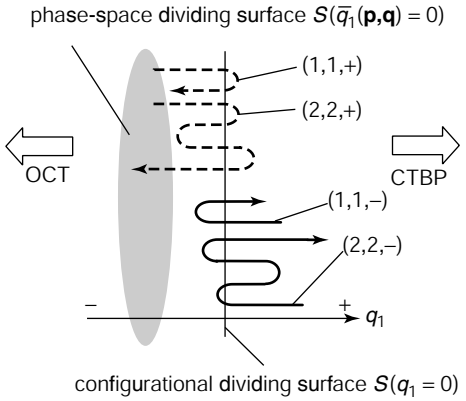

Figure 2.12. The schematic pictures of the $(1, 1, +)$, $(1, 1, -)$, $(2, 2, +)$, and $(2, 2, -)$ crossing patterns.

crossings over $S(q_1 = 0)$ of saddle I (see also Fig. 2.12):

- $- \rightarrow +$: If the system once crossed the *naive* dividing surface $S(q_1 = 0)$ from minus to plus, the system rarely returns to $S(q_1 = 0)$ because of the small driving force to make the system go back to $S(q_1 = 0)$ after it has passed the greater part of the distribution constituting the real $S(\bar{q}_1 = 0)$.
- $+ \rightarrow -$: Even if the system crossed $S(q_1 = 0)$ from plus to minus, the system has not necessarily passed the surface $S(\bar{q}_1 = 0)$. The system will recross $S(q_1 = 0)$ if the system does not possess sufficient incident (reactive) momentum $\bar{p}_1$ to pass through the $S(\bar{q}_1 = 0)$.

In other terms, almost nonreactive recrossings initiated from the CTBP state occur because the *real* dividing surface mainly distributes outwards to the OCT side from the $S(q_1 = 0)$, while the less frequent nonreactive recrossings from the other OCT state occur when the system finds an edge of the reaction bottleneck, that is, a tiny part of the dividing hypersurface in the phase space.

We also found [41] that besides total energy, the velocity across the transition state plays a major role in many-dof systems to migrate the reaction bottleneck outward from the naive dividing surface $S(q_1 = 0)$. A similar picture has been observed by Pechukas and co-workers [37] in 2D Hamiltonian systems, that is, as energy increases, pairs of the periodic orbit dividing surfaces (PODSs) appearing on each reactant and product side migrate outwards, toward reactant and product state, and the outermost

PODS can be identified as the reaction bottleneck. However, their crucial idea is based on the findings of *pure* periodic orbits in the saddle region. In many-body systems with more than three dof, the saddle-crossing dynamics often exhibits chaos due to resonance among nonreactive stable modes, extinguishing any periodic orbit in that region. As far as we know, this is the first example to picture reaction bottlenecks for such many-dof systems.

E. "Extract" Invariant Stable and Unstable Manifolds in Transition States

To identify those parts of space (either configurational, or phase space) in which invariants of motion "actually" survive or break during the course of dynamical evolution, obeying the exact Hamiltonian, we proposed [43, 44] "local invariancy analysis", in terms of a new concept of "duration of regularity (τ)", for each mode of the system, at each ith order of perturbation; these are the residence times each mode remains close to its near-constant values of the variables, as determined by a chosen bound on the fluctuation $\Delta\bar{J}$ or $\Delta\bar{\omega}$; for example, $\Delta\bar{J}$ for mode k, is

$$|\bar{J}_k^{i\text{th}}(\mathbf{p}(t+\tau), \mathbf{q}(t+\tau)) - \bar{J}_k^{i\text{th}}(\mathbf{p}(t), \mathbf{q}(t))| \leqslant \Delta\bar{J} \tag{2.59}$$

By transforming a time series of the variables, denoted hereinafter as $x(t)$, to a sequence of stationary points, $\ldots \min[i] - \max[i+1] - \min[i+2] - \cdots$ along $x(t)$ with the corresponding times $t[i]$, and choosing all the possible combinations of $\max[i]$ and $\min[j]$, one can calculate each residence time τ for which $x(t)$ traverses each fluctuation window Δx defined as $\max[i] - \min[j]$. For a bundle of $x(t)$, we can calculate how frequently $x(t)$ traverses the region of a certain fluctuation window Δx for a certain τ, that is, residence probability, say, $P_2(\Delta x; \tau)$, and also several distinct forms of joint probabilities, $P_{h+1}(\xi_1, \xi_2, \ldots, \xi_h; \tau)$ where ξ_i is either Δx, x, $\Delta x'$, or x' of any other variable $x'(t)$, x' and x are the short-term averages of $x'(t)$ and $x(t)$ for a certain period τ, say, from t' to $t' + \tau$, for example,

$$x' \equiv \frac{1}{\tau}\int_{t'}^{t'+\tau} x'(t)dt \tag{2.60}$$

This enables us to extract and visualize the stable and unstable invariant manifolds along the reaction coordinate in the phase space, to and from the hyperbolic point of the transition state of a many-body nonlinear system. $P_4(\Delta\bar{J}_1^{2\text{nd}}, \bar{p}_1, \bar{q}_1; \tau)$ and $P_4(\Delta\bar{J}_1^{2\text{nd}}, p_1, q_1; \tau)$ shown in Figure 2.13 can tell us how the system distributes in the two-dimensional $(\bar{p}_1(\mathbf{p}, \mathbf{q}), \bar{q}_1(\mathbf{p}, \mathbf{q}))$ and (p_1, q_1) spaces while it retains its local, approximate invariant of action $\bar{J}_1^{2\text{nd}}(\mathbf{p}, \mathbf{q})$ for a certain locality, $\sim\Delta\bar{J} = 0.05$ and $\tau \geqslant 0.5$, in the vicinity of

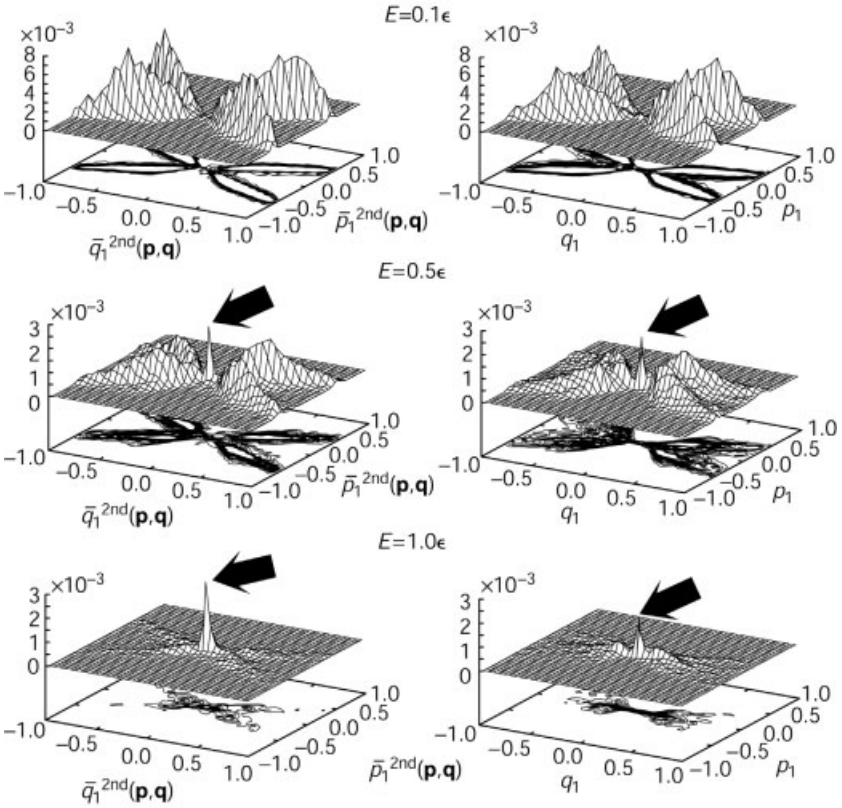

Figure 2.13. Probability distributions of approximate invariants of action $\bar{J}_1^{2nd}(\mathbf{p},\mathbf{q})$ on $(\bar{p}_1^{2nd}(\mathbf{p},\mathbf{q}), \bar{q}_1^{2nd}(\mathbf{p},\mathbf{q}))$ and (p_1, q_1) at $E = 0.1$, 0.5, and 1.0ϵ in the region of saddle I: $\Delta\bar{J} = 0.05$ and $\tau \geqslant 0.5$.

saddle I at the three distinct energies. The figures clearly capture the existence of a local near invariant of motion in the reactive coordinate $\bar{q}_1(\mathbf{p},\mathbf{q})$ even at moderately high energy, $\sim E = 0.5\epsilon$ (such invariant regions in the nonreactive dof totally disappear at $E \geqslant 0.5\varepsilon$). The clear "X" shapes of the 2D contour maps on $(\bar{p}_1^{2nd}(\mathbf{p},\mathbf{q}), \bar{q}_1^{2nd}(\mathbf{p},\mathbf{q}))$ at all the three energies indicate that, without any explicit assumption of the separation of time scales associated with individual modes, as expected from Eqs. (2.8) and (2.9), one can extract and visualize the stable and unstable invariant manifolds, at least in the region of the first-rank saddle, along the 1D reaction coordinate $\bar{q}_1(\mathbf{p},\mathbf{q})$ in many-body nonlinear systems, just like that of a 1D, integrable pendulum.

These figures should be contrasted with the corresponding diffuse contour maps in the conventional (p_1, q_1) plane, especially, at $E \geqslant 0.5\epsilon$. The more striking and significant consequence is this; the rather "long-lived" approximate invariant $\bar{J}_1(\mathbf{p}, \mathbf{q})$, around the origin, $\bar{p}_1(\mathbf{p}, \mathbf{q}) \cong \bar{q}_1(\mathbf{p}, \mathbf{q}) \cong 0$, emerges with an increase of energy, even surviving at 1.0ϵ, despite the consequent high passage velocity through the saddle (indicated by the arrows in the figures). Such a long-persistent invariant around that point could not be observed in the quasiregular region, up to 0.1ϵ. As shown in Eqs. (2.8) and (2.9), if approximate invariants of action $\bar{J}_1$ and frequency $\bar{\omega}_1$ survive, the entire phase-space flow $(\bar{p}_1\ \bar{q}_1)$ should be just like those of a 1D integrable pendulum, and hence no sharp spike should appear in the region where such invariants exist.

The sharp spike around the origin $\bar{p}_1 \cong \bar{q}_1 \cong 0$ in the probability distribution of approximate constant of action $\bar{J}_1(\mathbf{p}, \mathbf{q})$ implies that slow passages through the reaction bottleneck tend to spoil the approximate invariant of frequency, and the system's reactive dof $(\bar{p}_1, \bar{q}_1)$ couples with the other nonreactive dof throughout the small region $\bar{p}_1 \cong \bar{q}_1 \cong 0$. The rather long residence in the region of constant $\bar{J}_1$ implies that the system is transiently trapped in the nonreactive space during the course of the reaction due to the mode–mode couplings that emerge with increasing total energy. In such an intermediate regime between these two energy regions, any simplistic picture, ballistic or diffusive, of the system's passage through transition states may be spoiled.

We also pointed out that with a residence time τ much shorter than that in Figure 2.13 (with the same fluctuation bound), for example, $\tau \leqslant 0.2$, a similar sharp spike exists at $E = 0.1\epsilon$ around the origin, $\bar{p}_1^{2\text{nd}}(\mathbf{p}, \mathbf{q}) \cong \bar{q}_1^{2\text{nd}}(\mathbf{p}, \mathbf{q}) \cong 0$. This finding implies that the original Hamiltonian cannot completely be transformed to an exact, integrable Hamiltonian at second order in the LCPT calculation in the real situation at $E = 0.1\epsilon$. However, as inferred [40] from the analysis of the transmission coefficients κ_c using the phase-space dividing hypersurface $S(\bar{q}_1^{2\text{nd}}(\mathbf{p}, \mathbf{q}) = 0)$, the system could be regarded as "fully" separable at 0.1ϵ in the transition state because the transmission coefficient κ_c's value was evaluated to be 1.00000, which suggests that the different rates of energy exchange between the nonreactive dof and the reactive dof make the nonreactive *near-integrable* subset of modes contribute far less, and with less influence on the kinetics, than those modes in the *chaotic* subset. Recall that the Rice–Ramsperger–Kassel–Marcus (RRKM) theory [6–8] postulates that the greater the number of dof that couple with the reactive mode, the slower is the process of a specific mode gathering the energy required to react. If some nonreactive modes remain very regular, we might expect them to contribute nothing at all toward trapping the trajectory.

F. A Brief Comment on Semiclassical Theories

At the end of this section, we want to make some comments on the applicability of LCPT to semiclassical theories. In this discussion, we neglected tunneling through the potential barriers for the sake of simplicity, but rather have focused on the (classical) physical foundations of transitions buried in the complexity of reactions. However, CPT, including normal form theories, also provides us with a versatile means to address multidimensional tunneling problems [65–67]. In the scope of the semiclassical WKB approach, Keshavamurthy and Miller [65] first developed a semiclassical theory to extract the 1D phase-space path along which the tunneling action is conserved locally, obeying the original nonintegrable Hamiltonian. By using the following two-mode nonlinear reacting system:

$$H(\mathbf{p},\mathbf{q}) = \frac{1}{2m}(p_1^2 + p_2^2) + \frac{1}{2}aq_1^2 - \frac{1}{3}bq_1^3 + \frac{1}{2}m\omega^2\left(q_2 - \frac{cq_1}{m\omega^2}\right)^2 \quad (2.61)$$

where the parameters a and b were chosen to correspond to a barrier height of 7.4 kcal/mol, the mass m of a hydrogen atom, the harmonic frequency ω to be 300 cm^{-1}, and c a coupling constant (typical values for hydrogen-atom transfer reactions), they showed that all the actions are well conserved irrespective of the coupling strength c. Moreover, the value of the new Hamiltonian truncated at the second-order E_{pert} is as close as possible to the exact total energy, in the *local* saddle region. The unimolecular decay rate evaluated by the tunneling time, chosen to be that when $\bar{J}_F$ is locally conserved (stationary) in time, coincides well with the exact quantum rate, even in a case in which strong coupling spoils any (apparent) mode-specificity of the reaction.

We infer here that this is always true irrespective of the kind of system, if the number of degrees-of-freedom N is two. It is because there is no source to yield "resonance" by a single imaginary- and a single real-frequency mode. If N is >2, it is no longer integrable in the saddles except at just above the threshold energy because of resonance arising from nonreactive–nonreactive modes' nonlinear couplings. As discussed in Section IV, there should be at least three distinct energy ranges in terms of regularity of transitions. In other terms, we can classify energy ranges according to the extent of the system to possess "good" approximate, local quantum numbers. In the *semichaotic* region, E_{pert} totally differs from the exact total energy, and the conventional semiclassical TST breaks down completely. Nevertheless, the tunneling action along the *phase-space* path is quite likely conserved during the events. One may thus anticipate that their semiclassical approach [65] is quite applicable through a wide range of total energies

above the saddle point, in which the system is manifestly chaotic (even more than they might have expected!).

IV. HIERARCHICAL REGULARITY IN TRANSITION STATES

As seen in Sections I–III, there are at least three distinct energy regions above the saddle point energy that can be classified in terms of the regularity of saddle-crossing dynamics. We articulated the distinctions among them as follows:

Quasiregular Region: All or almost all the degrees of freedom of the system *locally* maintain approximate constants of motion in the transition state. The saddle crossing dynamics from well to well is fully deterministic, obeying M-analytical solutions [see Eqs. (2.8) and (2.9)] for systems of M degrees of freedom. The dynamical correlation between incoming and outgoing trajectories from and to the transition state is quite strong, and the dimensionality of saddle crossings is essentially one, corresponding to the reactive mode $\bar{q}_F$ in the $(\bar{\mathbf{p}}, \bar{\mathbf{q}})$ space. Barrier recrossing motions observed over a naive dividing

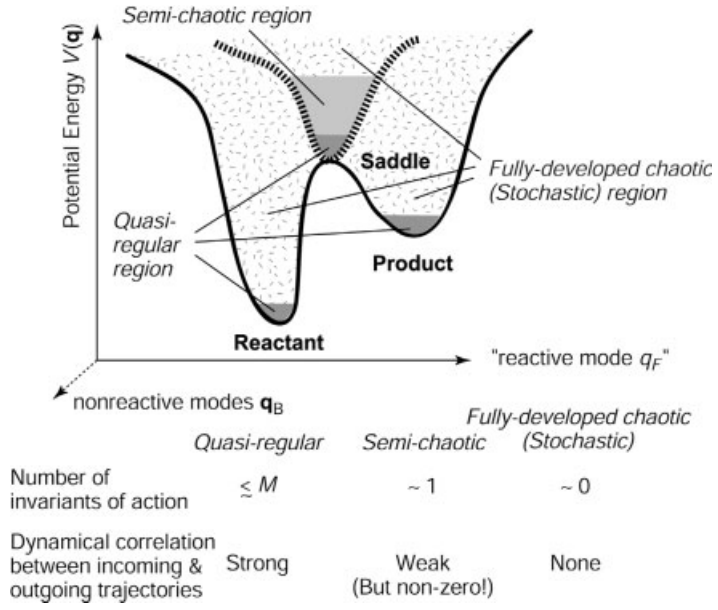

Figure 2.14. Schematic picture of hierarchical regularity in transition states.

surface defined in the configurational space are *all* rotated away to no-return single crossing motions across a phase-space dividing surface $S(\bar{q}_F(\mathbf{p}, \mathbf{q}) = 0)$. If the vibrational energy relaxes fast enough to let us assume quasiequilibration in the wells, the initial conditions $(\bar{\mathbf{p}}(0), \bar{\mathbf{q}}(0))$ of the system as it enters the transition state from either of the stable states can be simply sampled from microcanonical ensembles. One may then evaluate the (classical) exact rate constant, free from the recrossing problem. The staircase energy dependence observed by Lovejoy et al. [30, 31] for highly vibrationally excited ketene indicates that the transverse vibrational modes might indeed be approximately invariants of motion [33]. We classify such a range of energy, in which the rate coefficient shows staircase structure, as corresponding to this quasiregular region. Note that the incommensurable situations likely happen for systems having peculiar or specific mode(s), that is, modes *effectively* separable in time. We found in the proton-transfer reaction of malonaldehyde [38, 39], involving the proton movement, the O—O stretching, the out-of-plane wagging, and C═O stretching motions, that dynamics over the saddle is well regularized through all the dof, even at a moderately high total energy of the system, for example, 1.0 kcal/mol above the activation barrier whose height is 5.0 kcal/mol.

Intermediate, *Semichaotic Region:* Due to significant (near-)resonance emerging at these intermediate energies, *almost* all the approximate invariants of motion disappear, consequently inducing a topological change in dynamics from quasiregular-to-chaotic saddle crossings. However, at least one approximate invariant of motion survives during the saddle crossings, associated with the reactive coordinate $\bar{q}_F(\mathbf{p}, \mathbf{q})$. This is due to the fact that an arbitrary combination of modes cannot satisfy the resonance conditions of Eq. (2.12) if one mode has an imaginary frequency, the reactive mode in this case, is included in the combination. The other frequencies associated with nonreactive modes fall on the real axis, orthogonal to the imaginary axis in the complex $\boldsymbol{\omega}$ plane. That is,

$$\left| \sum_{k=1}^{M} {}^{\dagger} n_k \omega_k \right| \geqslant |\omega_F| > O(\varepsilon^n) \tag{2.62}$$

for arbitrary integers n_k with $n_F \neq 0$, where $\Sigma^{\dagger}$ denotes the combination including the reactive mode. This finding was first pointed out by Hernandez and Miller in their semiclassical TST studies [60]. In this region, the dynamical correlation between incoming and outgoing

trajectories to and from the transition state becomes weak (but nonzero!), and the saddle crossings' dimensionality is $\simeq M-1$, excluding the 1D of $\bar{q}_F$, in this region. If the associated imaginary frequency $\bar{\omega}_F(\mathbf{p},\mathbf{q})$ is approximately constant during a saddle crossing as the action $\bar{J}_F(\mathbf{p},\mathbf{q})$ is, the reaction coordinate $\bar{q}_F$ decouples from a subspace composed of the other nonreactive dof, in which the system dynamics is manifestly chaotic. The $\bar{q}_F$ dynamics is then represented analytically during saddle crossings, and a dividing surface $S(\bar{q}_F(\mathbf{p},\mathbf{q})=0)$ can still be extracted free from the recrossing problem, even for saddle crossings chaotic in the nonreactive modes.

We may expect that various kinds of resonance zones occur in the transition state, densely distributed, associated with very complicated patterns of level crossings in phase space, in a so-called "Arnold web" [53]. The transport among the states in such a web in many-dof systems raises many interesting and unresolved questions [24, 68, 69]. By using their local frequency analysis, Martens et al. [68] showed in a three-dof model for intramolecular energy flow in the OCS molecule that, although the motion is chaotic, some local frequencies are often fairly constant over times corresponding to many vibrational periods when the system moves along resonance zones, and long time-correlations are often observed near the junctions of resonance zones. As shown in Figures 7 [40] and 6 and 7 [44], one can see that in addition to the reactive mode frequency $\bar{\omega}_1^{2\text{nd}}(\mathbf{p},\mathbf{q})$, some other frequencies are also fairly constant through the saddle region, although the corresponding actions do not maintain constancy at all. We may expect that the LCPT frequency analysis will provide us with a versatile tool to analyze the resonance mechanism in chaotic motions.

Stochastic (*= Fully Developed Chaotic*) *Region:* The system becomes subject to considerable nonlinearities of the PES at much higher energies, and the convergence radius becomes negligibly small for the LCPT near the fixed (saddle) point for the invariant of motion associated with the reactive coordinate $\bar{q}_F$. In this energy region, no approximate invariant of motion can be expected to exist, even in the passage over the saddle between wells.

The saddle-crossing dynamics is entirely stochastic, with dimensionality essentially equal to the number of degrees of freedom of the system. It may not be possible to extract a dividing surface free from barrier recrossings. Going from semichaotic into fully developed chaotic regions, a new type of phase-space bottleneck emerges, that makes a reacting system increasingly trapped in the transition state as

the total energy of the system increases. This emergence of a new bottleneck challenges the simple pictures one has supposed for a reacting system crossing a transition state, that is, both the ballistic (or separable) and diffusive transitions, and sheds light on the nature of trapping of a reacting system in the transition state; one should distinguish "apparent" and "true" trappings. In the former, although the system looks transiently trapped around a saddle, its reaction proceeds, independently, along the *nearly separable* reactive degree of freedom in *phase* space, but in the latter, the system not only looks trapped but also resists proceeding along any reactive degree of freedom one might choose, due to the nonvanishing mode-couplings appearing between semichaotic and fully developed chaotic energy regimes. To describe reaction dynamics in this region, it will probably be more convenient to go back to the conventional reaction path approach in the configuration space **q**. In such a case, the variational TST approach, to choose the dividing surface to minimize the reactive flux, becomes one reasonable means to address the problem [9–11].

V. CONCLUDING REMARKS AND FUTURE PROSPECTS

So far, one has conventionally taken a reaction coordinate in the *configurational* space, for example, a distance between atoms to form or break their bond, a reactive normal coordinate, or (configurational) steepest descent path [70, 71]. Our results have shown the persistence of the approximate invariants of motion associated with the reaction coordinate $\bar{q}_1(\mathbf{p}, \mathbf{q})$, at least, in the region of the (first-rank) saddle even in a "sea" of high-dimensional chaos, and strongly support the use of the concept of a single, nearly-separable reactive degree of freedom in the system's *phase space*, a dof that is as free as possible from coupling to all the rest of the dof. This result immediately tells us that the observed deviations from unity of the *conventional* transmission coefficient κ should be due to the choice of the reaction coordinate q_1 of the system along which one might want to see the reaction event, whenever the κ arises from the recrossing problem.

The remaining ambiguity in reaction rate theories is the assumption of local vibrational equilibrium. Recall that reactions involving (a) chemical bond formation and/or cleavage may have, as a typical activation energy, a few tens of kilocalories per mole while an average thermal energy associated with a single dof is ~ 0.6 kcal/mol at room temperature. Therefore, we may anticipate that such chemical reactions are regarded as very rare events, and any (strongly chaotic) many-dimensional reacting system moves through all the accessible phase space in the reactant domain before finding the transition state.

However, in some unimolecular reactions of a few degrees of freedom, [24–26], there is a dynamical bottleneck to intramolecular energy transfer even in the reactant well. That is, cantori appear to form partial barriers between irregular regions of phase space. As yet, there is no general answer or analytical tool to determine whether such a dynamical bottleneck even exists for larger nonlinear reacting systems, say, >10 dof.

Along this direction, although we only argued how the invariant of frequency arises, varying the ratios of frequencies $\bar{\omega}_k$ among the modes [68, 72, 73] should shed light on what kinds of energy flows take place among the modes of $\bar{q}_k(\mathbf{p}, \mathbf{q})$ space, elucidated about potential minima. Obviously, the more the dof, the more possible combinations emerge to make the system very complicated. Another possible diagnostic method to look into this in many-body systems would be to execute the backward trajectory calculation, starting on the phase-space dividing hypersurface $S(\bar{q}_1(\mathbf{p}, \mathbf{q}) = 0)$, sampled from the microcanonical ensemble. If the system exhibits an invariant of motion for a certain time in the reactant phase space, that is, if the system is trapped in a certain limited region for some period, this should imply how the local equilibrium is suppressed in the reaction. The backward calculations initiated with large momenta $\bar{p}_1(\mathbf{p}, \mathbf{q})$ on that dividing hypersurface, that is, the bundle of the fast transitions from the reactant to product if one inverts the time, would reveal how any mode-specific nature of a reaction relates to the local topography of the phase space in the reactant state.

People have usually supposed that the elusive transition state is localized somewhere in the vicinity of a first-rank saddle linking reactant and product states, and that the evolution of the reactions can be decomposed into the two distinct parts, that is, how the system passes into the transition state from the reactant state, and then how it leaves there after its arrival. These have enabled us to argue the physical (classical) foundation of the deviation from the theories [as represented by a conventional $\kappa(<1)$], in terms of how violated "local equilibrium", and "no-return" assumptions may be. However, if, for example, the energy barrier of the reacting systems become comparable with the average thermal energy of a single dof, such a common scenario implicitly assumed so far should no longer be valid. If a dividing hypersurface were still to exist even in such cases, it might not be localized near the saddles but somehow delocalized throughout the whole accessible phase space as the separatrix theories [24–26] indicate for a few-dof systems. One may anticipate that the stable and unstable invariant manifolds we could extract in the region of the saddles even in a sea of *many-body* chaos can be connected through the rest of the phase space, and this provides us with an essential clue to generalize separatrix theories to *multidimensional* systems. Recently, Wiggins et al. [74] just started their research along this scenario.

Biological reactions take place on complex energy landscapes, involving

sequential crossings over multiple saddles, which, however, result in specific *robust* functions in living organisms. The question arising now is this: Can we understand why such robust functions or efficiencies exist in biological systems? We start from a viewpoint that each reaction crossing over each saddle takes place in dynamically independent fashion, that is, the local equilibration is considered to be attained quickly in each basin before the system goes to the next saddle, so the system loses all *dynamical* memories. As yet, of course, there is no answer as to whether dynamical connectivity or non-Markovian nature along the sequential multiple saddle crossing dynamics plays a significant role in maintaining robust functions.

One of the relevant interesting papers on protein foldings is that by García et al [75]. They showed how non-Brownian strange kinetics emerge in multi-basin dynamics trajectories generated by all-atom MD simulations of cytochrome *c* in aqueous solution at a wide range of temperature. They used a so-called molecule optimal dynamic coordinates (MODC) derived by a linear transformation of the Cartesian coordinates of the protein system, which best represent the configurational protein fluctuations (in a least square sense). They found that some slow MODC manifestly exhibits non-Brownian dynamics, that is, protein motions are more suppressed and cover less configurational space than a normal Brownian process on a short time scale, but they become more enhanced as a faster, well-concerted motion on a long time scale between a temperature at which the protein is in the native state and a temperature above melting (see also [76–79]).

The Lie techniques may provide us with the physical footings or analytical means to elucidate dynamical correlations among successive saddle crossings by enabling us to scrutinize "connectivity" of manifolds from and to the sequential saddle points and "extent of volume" of the region of a junction of manifolds in terms of the backward system trajectories initiated from $S(\bar{q}_1(\mathbf{p}, \mathbf{q}) = 0)$ at one saddle point and the forward from the other $S(\bar{q}_1(\mathbf{p}, \mathbf{q}) = 0)$ at the previous saddle point, through which the system has passed before reaching the first [80].

At high energies above the lowest, presumably (but not necessarily) first-rank saddle, the system trajectories may pass over higher rank saddles of the PES. These provides us with a new, untouched, exciting problem, that is, what is the role of resonance in the imaginary ω-plane for the bifurcation? (This even arises in the degenerate bending modes for a linear transition state of a triatomic molecule.) This is one of the most exciting questions, especially for relaxation dynamics on a rugged PES, if the system finds higher rank saddles, which may be densely distributed in the regions of high potential energies, and would pass through such complicated regions at least as frequently as through the lowest, first-rank transition states. This will require going back to the fundamental question of what the transition state is, that is, whether a dividing hypersurface could still exist or be definable,

in terms of separating the space of the system into regions identifiable with individual stable states.

Acknowledgments

We would like to acknowledge Professor Mikito Toda and Professor Stuart A. Rice for their continuous, stimulating discussions. We also thank Professor William Miller for his helpful comments and for sending us relevant articles [65]. T. K. also thanks Y. and Y. S. Komatsuzaki for their continuous encouragements. We thank the Aspen Center for Physics for its hospitality during the completion of this work. This research was supported by the National Science Foundation, the Japan Society for the Promotion of Science, and Grant-in-Aid for Research on Priority Areas (A) "Molecular Physical Chemistry" and (C) "Genome Information Science" of the Ministry of Education, Science, Sports and Culture of Japan.

APPENDIX

A. The Proof of Eqs. (2.8) and (2.9)

The equation of motion of new coordinates $\bar{\mathbf{q}}$ and momenta $\bar{\mathbf{p}}$ can straightforwardly be solved, with the new Hamiltonian $\bar{H}$ independent of the new angle variable $\bar{\boldsymbol{\Theta}}$.

$$\frac{d\bar{p}_k}{dt} = -\frac{\partial \bar{H}(\bar{\mathbf{J}})}{\partial \bar{q}_k} = -\frac{\partial \bar{H}(\bar{\mathbf{J}})}{\partial \bar{J}_k}\frac{\partial \bar{J}_k}{\partial \bar{q}_k} \tag{A.1}$$

$$= -\bar{\omega}_k(\bar{\mathbf{J}})\omega_k \bar{q}_k \tag{A.2}$$

$$\frac{d\bar{q}_k}{dt} = \frac{\partial \bar{H}(\bar{\mathbf{J}})}{\partial \bar{p}_k} = \frac{\partial \bar{H}(\bar{\mathbf{J}})}{\partial \bar{J}_k}\frac{\partial \bar{J}_k}{\partial \bar{p}_k} \tag{A.3}$$

$$= \frac{\bar{\omega}_k(\bar{\mathbf{J}})}{\omega_k}\bar{p}_k \tag{A.4}$$

By differentiating Eq. (A.4) in time t and combining Eq. (A.2), one can obtain

$$\frac{d^2\bar{q}_k}{dt^2} = \frac{\bar{\omega}_k(\bar{\mathbf{J}})}{\omega_k}\frac{d\bar{p}_k}{dt} = -\bar{\omega}_k^2(\bar{\mathbf{J}})\bar{q}_k \tag{A.5}$$

Here, the last equal signs of Eqs. (A.2) and (A.4) follow from Eq. (2.5) and

$$\bar{J}_k = \frac{1}{2\pi}\oint \bar{p}_k\, d\bar{q}_k = \frac{\bar{p}_k^2 + \omega_k^2\bar{q}_k^2}{2\omega_k} \tag{A.6}$$

One can easily see Eq. (A.6) as follows: as described in Appendix C, the new Hamiltonian $\bar{H}_0$ at zeroth-order corresponds to replacing the canonical variables, for example, $(\mathbf{p}, \mathbf{q})$, $(\mathbf{J}, \boldsymbol{\Theta}), \ldots,$ in the counterpart of old Hamil-

tonian H_0 by the corresponding, new canonical variables, $(\bar{\mathbf{p}}, \bar{\mathbf{q}})$, $(\bar{\mathbf{J}}, \bar{\mathbf{\Theta}}), \ldots$

$$\bar{H}_0(\bar{\mathbf{p}}, \bar{\mathbf{q}}) = H_0(\bar{\mathbf{p}}, \bar{\mathbf{q}}) \tag{A.7}$$

$$= \sum_k \frac{1}{2}(\bar{p}_k^2 + \omega_k^2 \bar{q}_k^2) \tag{A.8}$$

$$= \sum_k \omega_k \bar{J}_k \tag{A.9}$$

[one can also verify the second equal sign in Eq. (A.6) by inserting Eqs. (2.10) and (2.11) into Eq. (A.6)].

B. Lie Transforms

Let us suppose the following Hamilton's equations of motion:

$$\frac{d\bar{p}_i}{d\varepsilon} = -\frac{\partial W}{\partial \bar{q}_i} \tag{A.10}$$

$$\frac{d\bar{q}_i}{d\varepsilon} = \frac{\partial W}{\partial \bar{p}_i} \tag{A.11}$$

where ε and W are "time" and "Hamiltonian", a function of canonical coordinates $\bar{\mathbf{q}}$ and its conjugate canonical momenta $\bar{\mathbf{p}}$. These can be represented collectively in the notation $z_i = (\bar{p}_i, \bar{q}_i)$:

$$\frac{dz_i}{d\varepsilon} = \{z_i, W(\mathbf{z})\} \equiv -L_W z_i \tag{A.12}$$

Here $\{\,\}$ denotes Poisson bracket:

$$\{u, v\} \equiv \sum_i \left(\frac{\partial u}{\partial \bar{q}_i} \frac{\partial v}{\partial \bar{p}_i} - \frac{\partial v}{\partial \bar{q}_i} \frac{\partial u}{\partial \bar{p}_i} \right) \tag{A.13}$$

which has the following properties, for arbitrary differentiable functions u, v, and w,

$$\{u, v\} = -\{v, u\} \tag{A.14}$$

$$\{u, v + w\} = \{u, v\} + \{u, w\} \tag{A.15}$$

$$\{u, vw\} = \{u, v\}w + v\{u, w\} \tag{A.16}$$

and

$$\{u, \{v, w\}\} + \{v, \{w, u\}\} + \{w, \{u, v\}\} = 0 \tag{A.17}$$

Recall that for a set of any canonical variables, for example $(\bar{\mathbf{p}}, \bar{\mathbf{q}})$,

$$\{\bar{q}_i, \bar{p}_j\} = \delta_{ij} \qquad \{\bar{q}_i, \bar{q}_j\} = \{\bar{p}_i, \bar{p}_j\} = 0 \tag{A.18}$$

(δ_{ij} is Kronecker delta) and, in turn, a set of variables that satisfy Eq. (A.18) is canonical.

An operator, $L_W(\equiv \{W, \ \})$, called the *Lie derivative generated by W*, obeys the following properties easily derived from Eqs. (A.15)–(A.17):

$$L_W(\alpha u + \beta v) = \alpha L_W u + \beta L_W v \tag{A.19}$$

$$L_W uv = uL_W v + vL_W u \tag{A.20}$$

$$L_W\{u, v\} = \{u, L_W v\} + \{L_W u, v\} \tag{A.21}$$

$$L_V L_W = L_{\{V,W\}} + L_W L_V \tag{A.22}$$

where α, β, and V are any numbers and any differentiable function. The n times repeated operations of L_W to Eqs. (A.19)–(A.21) give

$$L_W^n(\alpha u + \beta v) = \alpha L_W^n u + \beta L_W^n v \tag{A.23}$$

$$L_W^n uv = \sum_{m=0}^{n} {}_nC_m (L_W^m u)(L_W^{n-m} v) \tag{A.24}$$

$$L_W^n\{u, v\} = \sum_{m=0}^{n} {}_nC_m \{L_W^m u, L_W^{n-m} v\} \tag{A.25}$$

and, hence,

$$e^{-\varepsilon L_W} uv = (e^{-\varepsilon L_W} u)(\varepsilon^{-\varepsilon L_W} v) \tag{A.26}$$

$$e^{-\varepsilon L_W}\{u, v\} = \{e^{-\varepsilon L_W} u, e^{-\varepsilon L_W} v\} \tag{A.27}$$

1. *Autonomous Cases*

The formal solution of Eq. (A.12) can be represented as

$$\mathbf{z}(\varepsilon) = e^{-\varepsilon L_W}\mathbf{z}(0) \equiv T\mathbf{z}(0) \tag{A.28}$$

for autonomous systems having no explicit dependence on "time" ε of

"Hamiltonian" W. Here, we introduce the *evolution* operator T for brevity.

It can be easily proved for any transforms described by this that if $\mathbf{z}(0)$ are canonical, $\mathbf{z}(\varepsilon)$ are also canonical (and vice versa) as follows: Let us designate the phase-space variables $\mathbf{z}$ at the "time" being zero as $(\mathbf{p}, \mathbf{q})$ and those at the "time" ε as $(\bar{\mathbf{p}}, \bar{\mathbf{q}})$. Then,

$$\bar{p}_i = Tp_i = e^{-\varepsilon L_{W(\mathbf{p},\mathbf{q})}} p_i = \bar{p}_i(\mathbf{p}, \mathbf{q}; \varepsilon) \tag{A.29}$$

$$\bar{q}_i = Tq_i = e^{-\varepsilon L_{W(\mathbf{p},\mathbf{q})}} q_i = \bar{q}_i(\mathbf{p}, \mathbf{q}; \varepsilon) \tag{A.30}$$

and

$$\{\bar{q}_i, \bar{p}_j\} = \{Tq_i, Tp_j\} = T\{q_i, p_j\} \tag{A.31}$$

$$\{\bar{q}_i, \bar{q}_j\} = \{Tq_i, Tq_j\} = T\{q_i, q_j\} \tag{A.32}$$

$$\{\bar{p}_i, \bar{p}_j\} = \{Tp_i, Tp_j\} = T\{p_i, p_j\} \tag{A.33}$$

where the second equal signs of these three equations are thanks to Eq. (A.27). Therefore, if $(\mathbf{p}, \mathbf{q})$ is canonical [i.e., Eq. (A.18) is satisfied for $(\mathbf{p}, \mathbf{q})$], $(\bar{\mathbf{p}}, \bar{\mathbf{q}})$ is also canonical because

$$\{\bar{q}_i, \bar{p}_j\} = T\delta_{ij} = e^{-\varepsilon L_W}\delta_{ij} = \delta_{ij} \tag{A.34}$$

$$\{\bar{q}_i, \bar{q}_j\} = \{\bar{p}_i, \bar{p}_j\} = T \cdot 0 = 0 \tag{A.35}$$

Note that the successive operations of $L_{W(\mathbf{p},\mathbf{q})}$ to p_i or q_i usually produce, complicated, nonlinear functions expressed explicitly in terms of $(\mathbf{p}, \mathbf{q})$. In Eqs. (A.29) and (A.30), $\bar{p}_i$ and $\bar{q}_i$ are represented as functions of the "time" ε and the initial condition $(\mathbf{p}, \mathbf{q})$ along the dynamical evolution obeying the "Hamiltonian" W, that is, $\bar{p}_i(\mathbf{p}, \mathbf{q}; 0) = p_i$, $\bar{q}_i(\mathbf{p}, \mathbf{q}; 0) = q_i$.

By assuming the inverse transformation from ε to 0 in the "time", that is,

$$\mathbf{z}(0) = T^{-1}\mathbf{z}(\varepsilon) \tag{A.36}$$

in other terms,

$$p_i = T^{-1}\bar{p}_i = e^{\varepsilon L_{W(\bar{\mathbf{p}},\bar{\mathbf{q}})}} \bar{p}_i = p_i(\bar{\mathbf{p}}, \bar{\mathbf{q}}; \varepsilon) \tag{A.37}$$

$$q_i = T^{-1}\bar{q}_i = e^{\varepsilon L_{W(\bar{\mathbf{p}},\bar{\mathbf{q}})}} \bar{q}_i = q_i(\bar{\mathbf{p}}, \bar{\mathbf{q}}; \varepsilon) \tag{A.38}$$

where $TT^{-1} = T^{-1}T = 1$, it can also be proved straightforwardly by the premultiplication of Eqs. (A.31)–(A.32) by *inverse* evolution operator T^{-1} that, if $(\bar{\mathbf{p}}, \bar{\mathbf{q}})$ is canonical, $(\mathbf{p}, \mathbf{q})$ is also canonical.

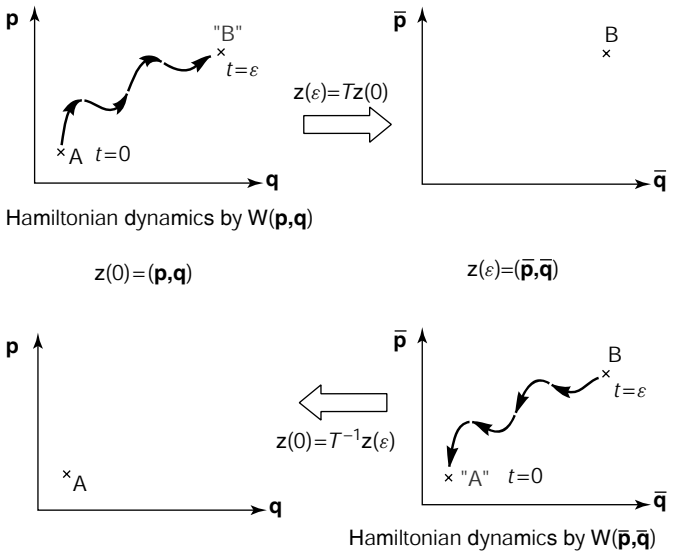

Figure 2.15. The schematic picture of the Lie transforms: If W is free from the "virtual" time t explicitly, the *functional* structure of W is preserved through the "time" evolution.

Figure 2.15 shows pictorially what the Lie transforms and its inversion perform: $T\mathbf{z}(0)$ transforms, for example, a point **A** in the $(\mathbf{p}, \mathbf{q})$ coordinate system to a point **B** in the other $(\bar{\mathbf{p}}, \bar{\mathbf{q}})$ system, which corresponds to a "virtual" time evolution of the phase-space variable (p_i, q_i) from "time" 0 to ε driven by a "Hamiltonian" $W(\mathbf{p}, \mathbf{q})$. In turn, $T^{-1}\mathbf{z}(\varepsilon)$ transforms the point **B** in $(\bar{\mathbf{p}}, \bar{\mathbf{q}})$ to the point **A** in $(\mathbf{p}, \mathbf{q})$, the reversed-time evolution of $(\bar{p}_i, \bar{q}_i)$ from ε to 0 driven by a "Hamiltonian" $W(\bar{\mathbf{p}}, \bar{\mathbf{q}})$, just replaced the "symbol" p_i and q_i in $W(\mathbf{p}, \mathbf{q})$ by $\bar{p}_i$ and $\bar{q}_i$, whose functional *form* is unchanged.

How Does a Lie Transform Operate on Functions? Given an arbitrary differentiable function $f(\mathbf{p}, \mathbf{q})$, let us consider the Lie transforms of the function, $Tf(\mathbf{p}, \mathbf{q})$.

$$Tf(\mathbf{p}, \mathbf{q}) = e^{-\varepsilon L_W} f(\mathbf{p}, \mathbf{q}) = \sum_{n=0} \frac{\varepsilon^n}{n!} (-L_W)^n f(\mathbf{p}, \mathbf{q}) \equiv g(\mathbf{p}, \mathbf{q}; \varepsilon) \qquad \text{(A.39)}$$

where the recursive operations of the Lie derivatives by $W(\mathbf{p}, \mathbf{q})$ on the function f yield a new function, denoted hereafter g, represented as a nonlinear function of $\mathbf{p}$ and $\mathbf{q}$, and ε. The resultant, transformed new

function $g(\mathbf{p}, \mathbf{q}; \varepsilon)$ can be interpreted as follows:

$$L_W f = \{W, f\} = \sum_i \left(\frac{\partial W}{\partial \bar{q}_i} \frac{\partial f}{\partial \bar{p}_i} - \frac{\partial W}{\partial \bar{p}_i} \frac{\partial f}{\partial \bar{q}_i} \right) \tag{A.40}$$

$$= -\sum_i \left(\frac{d\bar{p}_i}{d\varepsilon} \frac{\partial f}{\partial \bar{p}_i} + \frac{d\bar{q}_i}{d\varepsilon} \frac{\partial f}{\partial \bar{q}_i} \right) \tag{A.41}$$

$$= -\frac{df}{d\varepsilon} \tag{A.42}$$

and, for example, the operation twice of the Lie derivatives on f, $L_W^2 f$, implies

$$L_W^2 f = L_W(L_W f) = L_W \left(-\frac{df}{d\varepsilon} \right) = \frac{d^2 f}{d\varepsilon^2} \tag{A.43}$$

and thus by recurrence over n,

$$(-L_W)^n f = \frac{d^n f}{d\varepsilon^n} \tag{A.44}$$

Therefore, the new function $g(\mathbf{z}(0); \varepsilon)$ is represented as

$$g(\mathbf{z}(0); \varepsilon) = Tf(\mathbf{z}(0)) = \sum_{n=0} \frac{\varepsilon^n}{n!} (-L_{W(\mathbf{z}(0))})^n f(\mathbf{z}(0)) = \sum_{n=0} \frac{\varepsilon^n}{n!} \frac{d^n f}{d\varepsilon^n} \bigg|_{\varepsilon=0} \tag{A.45}$$

The last term corresponds to a Taylor series in "time" ε (about the origin) of the function f, which does not depend explicitly on ε but implicitly through $\mathbf{z}$. Thus, we can lead

$$g(\mathbf{z}(0); \varepsilon) = f(\mathbf{z}(\varepsilon)) = f(T\mathbf{z}(0)) \tag{A.46}$$

One can see that the new function $g(\mathbf{z}(0); \varepsilon)$ represents the functional *value* f at *the point* $\mathbf{z}(\varepsilon)$ as a function of the *initial point* $\mathbf{z}(0)$ and the "*time*" ε, where the phase space variables $\mathbf{z}$ evolve in the "time" obeying "Hamiltonian" W.

One can interpret schematically what the Lie transforms and its inversion perform on *function* f in Figure 2.16: $Tf(\mathbf{p}, \mathbf{q})$ (as indicated by an arrow in the top of the figure) transforms f evaluated at a point $\mathbf{A}$, $(\mathbf{p}_A, \mathbf{q}_A)$ in the $(\mathbf{p}, \mathbf{q})$ system to a new function, say, $g(\mathbf{p}, \mathbf{q}; \varepsilon)$, represented at the *same* point $\mathbf{A}$, whose functional *value* is equivalent to $f(\bar{\mathbf{p}}_B, \bar{\mathbf{q}}_B)$ evaluated at a point $\mathbf{B}$

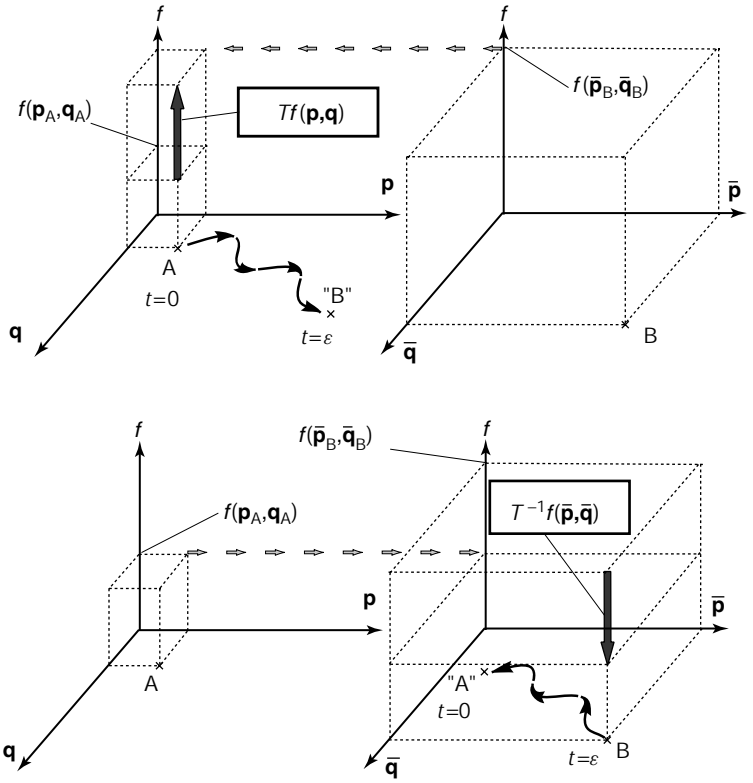

Figure 2.16. The schematic picture of the Lie transforms on a function f.

in the $(\bar{\mathbf{p}}, \bar{\mathbf{q}})$ system, which corresponds to a "virtual" time evolution driven by $W(\mathbf{p}, \mathbf{q})$, $(T\mathbf{p}_\mathbf{A}, T\mathbf{q}_\mathbf{A})$. In turn, $T^{-1}f(\bar{\mathbf{p}}, \bar{\mathbf{q}})$ (as indicated by an another arrow in the bottom of the figure) transforms f evaluated at the point **B** in $(\bar{\mathbf{p}}, \bar{\mathbf{q}})$ to a new function, say, $g'(\bar{\mathbf{p}}, \bar{\mathbf{q}}; \varepsilon)$, at the *same* point **B**, whose functional *value* is equivalent to $f(\mathbf{p}_\mathbf{A}, \mathbf{q}_\mathbf{A})$ evaluated at the point **A** in the $(\mathbf{p}, \mathbf{q})$ system.

Finally, the Lie transforms on functions f generated by "Hamiltonian" W is represented as

$$Tf(\mathbf{z}(0)) = f(\mathbf{z}(\varepsilon)) = f(T\mathbf{z}(0)) = g(\mathbf{z}(0); \varepsilon) \tag{A.47}$$

or

$$Tf(\mathbf{p}, \mathbf{q}) = f(\bar{\mathbf{p}}, \bar{\mathbf{q}}) = f(T\mathbf{p}, T\mathbf{q}) = g(\mathbf{p}, \mathbf{q}; \varepsilon) \tag{A.48}$$

It implies that for an arbitrary differentiable function f evaluated at $(\mathbf{p}, \mathbf{q})$, the Lie transforms provides us with a new function $g(\mathbf{p}, \mathbf{q}; \varepsilon)$, representing the functional *value* of f at $(\bar{\mathbf{p}}, \bar{\mathbf{q}})$, whose all components $\bar{p}_i$ and $\bar{q}_i$ obey $\bar{p}_i = Tp_i$ and $\bar{q}_i = Tq_i$.

For example, if f is the "Hamiltonian" W,

$$W(\bar{\mathbf{p}}, \bar{\mathbf{q}}) = W(e^{-\varepsilon L_W}\mathbf{p}, e^{-\varepsilon L_W}\mathbf{q}) \tag{A.49}$$

$$= e^{-\varepsilon L_W} W(\mathbf{p}, \mathbf{q}) \tag{A.50}$$

$$= W(\mathbf{p}, \mathbf{q}) \tag{A.51}$$

because $L_W^n W = 0$ except $n = 0$. That is, the Lie transforms generated by W, which does not depend on ε explicitly, preserves the functional form of W itself along the dynamical evolution in "time" ε.

Differentiating the equation $Tf(\mathbf{p}, \mathbf{q}) = f(\bar{\mathbf{p}}, \bar{\mathbf{q}})$ with respect to ε,

$$\begin{aligned}
\frac{dT(\varepsilon)}{d\varepsilon} f(\mathbf{p}, \mathbf{q}) &= \sum_i \left(\frac{\partial f(\bar{\mathbf{p}}, \bar{\mathbf{q}})}{\partial \bar{q}_i} \frac{d\bar{q}_i}{d\varepsilon} + \frac{\partial f(\bar{\mathbf{p}}, \bar{\mathbf{q}})}{\partial \bar{p}_i} \frac{d\bar{p}_i}{d\varepsilon} \right) \\
&= \sum_i \left(\frac{\partial f(\bar{\mathbf{p}}, \bar{\mathbf{q}})}{\partial \bar{q}_i} \frac{\partial W}{\partial \bar{p}_i} - \frac{\partial f(\bar{\mathbf{p}}, \bar{\mathbf{q}})}{\partial \bar{p}_i} \frac{\partial W}{\partial \bar{q}_i} \right) \\
&= \{ f(\bar{\mathbf{p}}, \bar{\mathbf{q}}),\ W(\bar{\mathbf{p}}, \bar{\mathbf{q}}) \} \\
&= \{ T(\varepsilon) f(\mathbf{p}, \mathbf{q}),\ T(\varepsilon) W(\mathbf{p}, \mathbf{q}) \} \\
&= T(\varepsilon) \{ f(\mathbf{p}, \mathbf{q}),\ W(\mathbf{p}, \mathbf{q}) \} \\
&= -T(\varepsilon) L_W f(\mathbf{p}, \mathbf{q})
\end{aligned}$$

which holds for all $f(\mathbf{p}, \mathbf{q})$. Thus, one can have

$$\frac{dT}{d\varepsilon} = -TL_W \tag{A.52}$$

Similarly, differentiating the equation $TT^{-1} = 1$ with respect to ε yields

$$\frac{dT^{-1}}{d\varepsilon} = L_W T^{-1} \tag{A.53}$$

because

$$0 = \frac{dT(\varepsilon)T^{-1}(\varepsilon)}{d\varepsilon} = \frac{dT}{d\varepsilon}T^{-1} + T\frac{dT^{-1}}{d\varepsilon}$$
$$= -TL_W T^{-1} + T\frac{dT^{-1}}{d\varepsilon}$$

one can have Eq. (A.53) by premultiplying the final equation by T^{-1}.

2. Nonautonomous Cases

The Lie transforms for which the "Hamiltonian" W explicitly depends on "time" ε preserve the formal properties of the autonomous $W(\bar{\mathbf{p}}, \bar{\mathbf{q}})$. Hamilton's equations of motion do not change form for nonautonomous systems:

$$\frac{d\bar{p}_i}{d\varepsilon} = \{\bar{p}_i, W\} = -\frac{\partial W(\bar{\mathbf{p}}, \bar{\mathbf{q}}, \varepsilon)}{\partial \bar{q}_i}$$
$$\frac{d\bar{q}_i}{d\varepsilon} = \{\bar{q}_i, W\} = \frac{\partial W(\bar{\mathbf{p}}, \bar{\mathbf{q}}, \varepsilon)}{\partial \bar{p}_i}$$

and collectively,

$$\frac{dz_i}{d\varepsilon} = \{z_i, W(\mathbf{z}, \varepsilon)\} = -L_W z_i$$

The second derivatives of $\bar{p}_i$ over "time" ε becomes,

$$\frac{d^2\bar{p}_i}{d\varepsilon^2} = \frac{d}{d\varepsilon}\{\bar{p}_i, W\}$$
$$= \sum_j \left(\frac{\partial}{\partial \bar{q}_j}\{\bar{p}_i, W\}\frac{d\bar{q}_j}{d\varepsilon} + \frac{\partial}{\partial \bar{p}_j}\{\bar{p}_i, W\}\frac{d\bar{p}_j}{d\varepsilon} \right) + \frac{\partial}{\partial \varepsilon}\{\bar{p}_i, W\}$$
$$= \sum_j \left(\frac{\partial}{\partial \bar{q}_j}\{\bar{p}_i, W\}\frac{\partial W}{\partial \bar{p}_j} - \frac{\partial}{\partial \bar{p}_j}\{\bar{p}_i, W\}\frac{\partial W}{\partial \bar{q}_j} \right) + \left\{ \bar{p}_i, \frac{\partial W}{\partial \varepsilon} \right\}$$
$$= \{\{\bar{p}_i, W\}, W\} + \left\{ \bar{p}_i, \frac{\partial W}{\partial \varepsilon} \right\} \tag{A.54}$$

and similarly,

$$\frac{d^2\bar{q}_i}{d\varepsilon^2} = \{\{\bar{q}_i, W\}, W\} + \left\{\bar{q}_i, \frac{\partial W}{\partial \varepsilon}\right\} \tag{A.55}$$

One can combine these two expressions collectively in terms of z_i:

$$\frac{d^2 z_i}{d\varepsilon^2} = \frac{d}{d\varepsilon}\{z_i, W\} = \{\{z_i, W\}, W\} + \left\{z_i, \frac{\partial W}{\partial \varepsilon}\right\} \tag{A.56}$$

$$= \frac{d}{d\varepsilon}(\Delta_{-W}) z_i = \Delta_{-W}^2 z_i \tag{A.57}$$

where a newly introduced operator Δ_W is defined by

$$\Delta_W \equiv \{W, \ \} + \frac{\partial}{\partial \varepsilon} = L_W + \frac{\partial}{\partial \varepsilon} \tag{A.58}$$

and easily verify that the nth derivatives of z_i in "time" ε is given, in terms of Δ_{-W}, by

$$\frac{d^n z_i}{d\varepsilon^n} = (\Delta_{-W})^n z_i \tag{A.59}$$

Thus, the expansion of the solution $\mathbf{z}(\varepsilon)$ in power series of ε around the origin result in the expressions using Δ_{-W}:

$$z_i(\varepsilon) = \sum_{n=0}^{\infty} \frac{\varepsilon^n}{n!} \frac{d^n z_i}{d\varepsilon^n}\bigg|_{\varepsilon=0} = \sum_{n=0}^{\infty} \frac{\varepsilon^n}{n!} (\Delta_{-W})^n z_i|_{\varepsilon=0} \tag{A.60}$$

$$= \exp\left[-\int^{\varepsilon} L_{W(\varepsilon')}\, d\varepsilon'\right] z_i(0) = T z_i(0) \tag{A.61}$$

$$\bar{p}_i = T p_i = \exp\left[-\int^{\varepsilon} L_{W(\mathbf{p},\mathbf{q};\varepsilon')}\, d\varepsilon'\right] p_i = \bar{p}_i(\mathbf{p}, \mathbf{q}; \varepsilon) \tag{A.29a}$$

$$\bar{q}_i = T q_i = \exp\left[-\int^{\varepsilon} L_{W(\mathbf{p},\mathbf{q};\varepsilon')}\, d\varepsilon'\right] q_i = \bar{q}_i(\mathbf{p}, \mathbf{q}; \varepsilon) \tag{A.30a}$$

just the same as the Lie transforms generated by an autonomous $W(\mathbf{p}, \mathbf{q})$. It can easily be verified that Δ_W satisfy similar properties of L_W that just replace L_W by Δ_W in Eqs. (A.19)–(A.25). The only exception is that, instead

of Eq. (A.22), Δ_W holds

$$\Delta_V \Delta_W = \Delta_W \Delta_V + L_{\{V, W\}} + L_{\frac{\partial W}{\partial \varepsilon} - \frac{\partial V}{\partial \varepsilon}} \tag{A.62}$$

Hence, one sees immediately that,

$$Tuv = (Tu)(Tv) \tag{A.26a}$$

$$T\{u, v\} = \{Tu, Tv\} \tag{A.27a}$$

and that Eqs. (A.29a) and (A.30a) yield a completely canonical mapping like those by an autonomous $W(\bar{\mathbf{p}}, \bar{\mathbf{q}})$.

In general, for an arbitrary differentiable function $f(\bar{\mathbf{p}}, \bar{\mathbf{q}})$, the nth derivatives of f are given by

$$\frac{d^n}{d\varepsilon^n} f = (\Delta_{-W})^n f$$

because

$$\begin{aligned}
\frac{df}{d\varepsilon} &= \sum_j \left(\frac{\partial f}{\partial \bar{q}_j} \frac{d\bar{q}_j}{d\varepsilon} + \frac{\partial f}{\partial \bar{p}_j} \frac{d\bar{p}_j}{d\varepsilon} \right) \\
&= \sum_j \left(\frac{\partial f}{\partial \bar{q}_j} \frac{\partial W}{\partial \bar{p}_j} - \frac{\partial f}{\partial \bar{p}_j} \frac{\partial W}{\partial \bar{q}_j} \right) = \{f, W\} = \Delta_{-W} f \\
\frac{d^2 f}{d\varepsilon^2} &= \frac{d}{d\varepsilon} (\Delta_{-W} f) = \{\Delta_{-W} f, W\} + \frac{\partial (\Delta_{-W} f)}{\partial \varepsilon} \\
&= \Delta_{-W}^2 f
\end{aligned}$$

and so forth.

Consequently,

$$\begin{aligned}
f(\bar{\mathbf{p}}, \bar{\mathbf{q}}) &= \sum_{n=0}^{\infty} \frac{\varepsilon^n}{n!} \left. \frac{d^n f}{d\varepsilon^n} \right|_{\varepsilon = 0} \\
&= \sum_{n=0}^{\infty} \frac{\varepsilon^n}{n!} (\Delta_{-W})^n f \big|_{\varepsilon = 0} \\
&= \exp \left[- \int^{\varepsilon} L_{W(\mathbf{p}, \mathbf{q}; \varepsilon')} \, d\varepsilon' \right] f(\mathbf{p}, \mathbf{q}) = Tf(\mathbf{p}, \mathbf{q}) \\
&= g(\mathbf{p}, \mathbf{q}; \varepsilon)
\end{aligned} \tag{A.45a}$$

As argued in autonomous cases, $g(\mathbf{p}, \mathbf{q}; \varepsilon)$ implies that while the functional *value* of $Tf(\mathbf{p}, \mathbf{q})$ is exactly equal to $f(\bar{\mathbf{p}}, \bar{\mathbf{q}})$, the transformed, usually complicated, nonlinear function becomes represented as a function of $\mathbf{p}$ and $\mathbf{q}$, and ε, whose functional *form* differs from the original f.

Finally, the Lie transforms on functions f generated by a non-autonomous "Hamiltonian" W can be represented as

$$Tf(\mathbf{z}(0)) = f(\mathbf{z}(\varepsilon)) = f(T\mathbf{z}(0)) = g(\mathbf{z}(0); \varepsilon) \tag{A.47a}$$

or

$$Tf(\mathbf{p}, \mathbf{q}) = f(\bar{\mathbf{p}}, \bar{\mathbf{q}}) = f(T\mathbf{p}, T\mathbf{q}) = g(\mathbf{p}, \mathbf{q}; \varepsilon) \tag{A.48a}$$

Here, one can see that we have the same formulations, Eqs. (A.47) and (A.48), derived for autonomous W. One can easily see that Eqs. (A.52) and (A.53), and the schematic interpretations of the Lie transforms, Figures 2.15 and 2.16 also hold for nonautonomous Lie transforms $W(\bar{\mathbf{p}}, \bar{\mathbf{q}}, \varepsilon)$, except the "Hamiltonian" W changes its form depending on the "time" ε along the "time" evolution.

C. Perturbation Theory Based on Lie Transforms

It is well known that for any canonical transforms $(\mathbf{p}, \mathbf{q}) \to (\bar{\mathbf{p}}, \bar{\mathbf{q}})$ of an autonomous system, the new Hamiltonian, denoted hereinafter $\bar{H}$, is related to the old Hamiltonian H by

$$\bar{H}(\bar{\mathbf{p}}, \bar{\mathbf{q}}) = H(\mathbf{p}, \mathbf{q}) \tag{A.63}$$

Now let us suppose that the canonical transformation is brought about by "Lie transforms", and hence, in the $\mathbf{z}$ representation, this becomes

$$\bar{H}(\mathbf{z}(\varepsilon)) = H(\mathbf{z}(0)) \tag{A.64}$$

that is, one can see that the *new* Hamiltonian $\bar{H}$ evaluated at the *new point* $\mathbf{z}(\varepsilon)$ along the dynamical evolution obeying W is equal to the *old* Hamiltonian H at the *old point* $\mathbf{z}(0)$.

By comparing this to the equation

$$f(\mathbf{z}(\varepsilon)) = g(\mathbf{z}(0)) \tag{A.65}$$

[e.g., Eq. (A.47)] and applying $f = T^{-1}g$, one has

$$\bar{H}(\mathbf{z}(\varepsilon)) = T^{-1}H(\mathbf{z}(\varepsilon)) = H(\mathbf{z}(0)) \tag{A.66}$$

or,

$$\bar{H}(\bar{\mathbf{p}}, \bar{\mathbf{q}}) = T^{-1}H(\bar{\mathbf{p}}, \bar{\mathbf{q}}) = H(\mathbf{p}, \mathbf{q}) \tag{A.67}$$

Here, the *inverse* evolution operator T^{-1} brings the system dwelling at a "time" backward to a past in ε from *that* "time" along the dynamical evolution $\mathbf{z}$; yielding $H(\mathbf{z}(0))$, that is, $H(\mathbf{p}, \mathbf{q})$.

In cases that H, $\bar{H}$, and W (hence, also L_W, T, T^{-1}) are expandable as power series in ε, one can obtain a recursive, perturbation series to yield a desired new Hamiltonian.

$$H = \sum_{n=0} \varepsilon^n H_n \tag{A.68}$$

$$\bar{H} = \sum_{n=0} \varepsilon^n \bar{H}_n \tag{A.69}$$

$$W = \sum_{n=0} \varepsilon^n W_{n+1} \tag{A.70}$$

$$L_W = \sum_{n=0} \varepsilon^n L_{n+1} \tag{A.71}$$

$$T = \sum_{n=0} \varepsilon^n T_n \tag{A.72}$$

$$T^{-1} = \sum_{n=0} \varepsilon^n T_n^{-1} \tag{A.73}$$

where

$$L_n = \{W_n, \ \} \tag{A.74}$$

First, we derive a versatile perturbation series among the relations between T_n and T_n^{-1} and L_n. Inserting Eqs. (A.71) and (A.72) into Eq. (A.52), and Eqs. (A.71) and (A.73) into Eq. (A.53), and equating like powers of ε, one can obtain a recursive relation for T_n and T_n^{-1} ($n > 0$):

$$T_n = -\frac{1}{n} \sum_{m=0}^{n-1} T_m L_{n-m} \tag{A.75}$$

$$T_n^{-1} = \frac{1}{n} \sum_{m=0}^{n-1} L_{n-m} T_m^{-1} \tag{A.76}$$

where $T_0 = T_0^{-1} = 1$ because $T_0(T_0^{-1})$ corresponds to $T(T^{-1})$ at $\varepsilon = 0$. For example, to third order,

$$T_1 = -L_1 \tag{A.77}$$

$$T_2 = -\frac{1}{2}L_2 + \frac{1}{2}L_1^2 \tag{A.78}$$

$$T_3 = -\frac{1}{3}L_3 + \frac{1}{6}L_2L_1 + \frac{1}{3}L_1L_2 - \frac{1}{6}L_1^3 \tag{A.79}$$

$$T_1^{-1} = L_1 \tag{A.80}$$

$$T_2^{-1} = \frac{1}{2}L_2 + \frac{1}{2}L_1^2 \tag{A.81}$$

$$T_3^{-1} = \frac{1}{3}L_3 + \frac{1}{6}L_1L_2 + \frac{1}{3}L_2L_1 + \frac{1}{6}L_1^3 \tag{A.82}$$

(note that the T's and L's do not generally commute, e.g., $L_iL_j \neq L_jL_i$).

By inserting the series expansions of $\bar{H}$, T^{-1}, and H into $\bar{H} = T^{-1}H$ and equating like powers of ε, one can recursively solve the CPT with the Lie transforms: to second order, the new Hamiltonian $\bar{H}$ relates to the old Hamiltonian H as follows:

$$\varepsilon^0: \bar{H}_0 = H_0 \tag{A.83}$$

$$\varepsilon^1: \bar{H}_1 = T_0^{-1}H_1 + T_1^{-1}H_0 = H_1 + L_1H_0 \tag{A.84}$$

$$= H_1 + \frac{dW_1}{d\tau} \tag{A.85}$$

$$\varepsilon^2: \bar{H}_2 = T_0^{-1}H_2 + T_1^{-1}H_1 + T_2^{-1}H_0 \tag{A.86}$$

$$= H_2 + \frac{1}{2}L_1(\bar{H}_1 + H_1) + \frac{1}{2}L_2H_0 \tag{A.87}$$

$$= H_2 + \frac{1}{2}\{W_1, \bar{H}_1 + H_1\} + \frac{1}{2}\frac{dW_2}{d\tau} \tag{A.88}$$

Here,

$$L_n\bar{H}_0 = L_nH_0 = \{W_n, H_0\} = \frac{dW_n}{d\tau} \tag{A.89}$$

where τ is the time along the orbits obeying the "unperturbed" H_0. In the representations of Eqs. (A.68)–(A.89), we *intentionally* omitted the arguments, that is, which kinds of forms of canonical variables we may use. The above equations hold for all kinds of the forms because the Poisson bracket calculation is canonically invariant, that is, the arguments themselves of the functions in the Lie transforms are really dummy variables. Hereafter, we use the arguments $(\bar{\mathbf{p}}, \bar{\mathbf{q}})$ as the new canonical variables in Eqs. (A.83)–(A.88).

From Eq. (A.83) it is straightforward at $\mathcal{O}(\varepsilon^0)$ that $\bar{H}_0(\bar{\mathbf{p}}, \bar{\mathbf{q}})$ is a function that just replaces the phase-space variables $(\mathbf{p}, \mathbf{q})$ in H_0 with those $(\bar{\mathbf{p}}, \bar{\mathbf{q}})$. However this is only the exception; at each order beyond $\mathcal{O}(\varepsilon^0)$, for each condition, there successively appear two unknown quantities, for example, $\bar{H}_1$ and W_1 at $\mathcal{O}(\varepsilon^1)$, and $\bar{H}_2$ and W_2 at $\mathcal{O}(\varepsilon^2)$ after $\bar{H}_1$ and W_1 have been determined in any fashion. In other words, there is flexibility to establish the new Hamiltonian $\bar{H}(\bar{\mathbf{p}}, \bar{\mathbf{q}})$ as one wishes.

Now let us suppose that the zeroth-order Hamiltonian H_0 can be represented as a function of only the action variables of H_0, that is, an integrable form, and the perturbation terms $H_n (n \geqslant 1)$ as functions of both the action and the angle variables:

$$H = \sum_{n=0} \varepsilon^n H_n = H_0(\mathbf{J}) + \sum_{n=1} \varepsilon^n H_n(\mathbf{J}, \boldsymbol{\Theta}) \tag{A.90}$$

and determine the unknown W_n so as to make the new Hamiltonian $\bar{H}_n$ as free from the new angle variables $\bar{\boldsymbol{\Theta}}$ as possible, at each order in ε^n; $\bar{H}_1$ and W_1 are determined at $\mathcal{O}(\varepsilon^1)$ as follows:

$$\bar{H}_1 = H_1 + \frac{dW_1}{d\tau} \tag{A.91}$$

$$= \langle H_1 \rangle + \{H_1\} + \frac{dW_1}{d\tau} \tag{A.92}$$

where

$$\langle H_1 \rangle = \lim_{\tau \to \infty} \frac{1}{\tau} \int_0^\tau H_1(\bar{\mathbf{p}}(\tau'), \bar{\mathbf{q}}(\tau'))\, d\tau' \tag{A.93}$$

$$\{H_1\} = H_1 - \langle H_1 \rangle \tag{A.94}$$

Here, the time τ obeying H_0 correlates with the new angle variables $\bar{\boldsymbol{\Theta}}$

linearly:

$$\frac{d\bar{\Theta}_k}{d\tau} = \{\bar{\Theta}_k, H_0\} = \frac{\partial H_0(\bar{\mathbf{J}})}{\partial \bar{J}_k} \equiv \omega_k(\bar{\mathbf{J}}) \tag{A.95}$$

$$\bar{\Theta}_k = \omega_k(\bar{\mathbf{J}})\tau + \beta_k \quad (\beta_k\text{: initial phase factor}) \tag{A.96}$$

Therefore, $\langle f \rangle$ and $\{f\}$ representing the average and oscillating parts over τ in f correspond to the free and dependent parts in all the $\bar{\Theta}_k$, respectively. The new Hamiltonian at first order $\bar{H}_1$ can be determined to be free from all the $\bar{\Theta}_k$ by

$$\bar{H}_1 = \langle H_1 \rangle \tag{A.97}$$

$$W_1 = -\int \{H_1\}\, d\tau \tag{A.98}$$

Similarly, at the second order $\mathcal{O}(\varepsilon^2)$,

$$\bar{H}_2 = \left\langle H_2 + \frac{1}{2}\{W_1, \bar{H}_1 + H_1\} \right\rangle \tag{A.99}$$

$$W_2 = -\int \{2H_2 + \{W_1, \bar{H}_1 + H_1\}\}\, d\tau \tag{A.100}$$

If the new Hamiltonian $\bar{H}(\bar{\mathbf{J}})$ can be shown to be independent of the time τ, we immediately obtain an invariant of motion $\bar{H}_0(\bar{\mathbf{p}}, \bar{\mathbf{q}})$, since

$$0 = \frac{d\bar{H}}{d\tau} = \{\bar{H}, \bar{H}_0\} = -\{\bar{H}_0, \bar{H}\} = -\frac{d\bar{H}_0}{dt} \tag{A.101}$$

As seen in Appendix B, for any function f composed of $(\bar{\mathbf{p}}, \bar{\mathbf{q}})$, one can easily find an functional expression $\bar{f}$ in terms of the original $(\mathbf{p}, \mathbf{q})$ and ε by

$$f(\bar{\mathbf{p}}, \bar{\mathbf{q}}) = Tf(\mathbf{p}, \mathbf{q}) = \bar{f}(\mathbf{p}, \mathbf{q}; \varepsilon)$$

Hence, after W has once been established, one can find the functional expression $\bar{f}(\mathbf{p}, \mathbf{q}; \varepsilon)$ of any f at each order in ε thanks to Eq. (A.75):

$$\bar{f}(\mathbf{p}, \mathbf{q}; \varepsilon) = \sum_{n=0} \varepsilon^n \bar{f}_n(\mathbf{p}, \mathbf{q}) = \sum_{n=0} \varepsilon^n T_n f(\mathbf{p}, \mathbf{q}) \tag{A.102}$$

For example, up to $\mathcal{O}(\varepsilon^2)$,

$$\varepsilon^0: \bar{f}_0(\mathbf{p}, \mathbf{q}) = f(\mathbf{p}, \mathbf{q}) \tag{A.103}$$

$$\varepsilon^1: \bar{f}_1(\mathbf{p}, \mathbf{q}) = -L_1(\mathbf{p}, \mathbf{q}) f(\mathbf{p}, \mathbf{q}) = -\{W_1(\mathbf{p}, \mathbf{q}), f(\mathbf{p}, \mathbf{q})\} \tag{A.104}$$

$$\varepsilon^2: \bar{f}_2(\mathbf{p}, \mathbf{q}) = \frac{1}{2}(-L_2 + L_1^2) f \tag{A.105}$$

$$= \frac{1}{2}(\{W_1, \{W_1, f\}\} - \{W_2, f\}) \tag{A.106}$$

Note again that one might follow this by putting "$\mathbf{p}$" and "$\mathbf{q}$" into the "Hamiltonian" W as its arguments in the present case, while one might use "$\bar{\mathbf{p}}$" and "$\bar{\mathbf{q}}$" in an another case, for example, Eq. (A.67). A similar situation was seen in the original derivation for which the arguments of W in the transformations, for example, Eqs. (A.29) and (A.37), are either $(\mathbf{p}, \mathbf{q})$ or $(\bar{\mathbf{p}}, \bar{\mathbf{q}})$. The arguments themselves of the functions in the Lie transforms are really dummy variables and the Lie techniques involve operations on functions, rather than on variables.

An Illustrative Example. We apply LCPT to the following, simple 2D Hamiltonian, first demonstrated by Hori [51, 52],

$$H(\mathbf{p}, \mathbf{q}) = \frac{1}{2}(p_1^2 + p_2^2 + \omega_1^2 q_1^2 + \omega_2^2 q_2^2) - \varepsilon q_1 q_2^2 \tag{A.107}$$

$$= (\omega_1 J_1 + \omega_2 J_2) - \varepsilon \left(\frac{2J_1}{\omega_1}\right)^{1/2} \frac{2J_2}{\omega_2} \cos\Theta_1 \cos^2\Theta_2 \tag{A.108}$$

where the Hamiltonian is integrable at $\mathcal{O}(\varepsilon^0)$.

According to the recipe of LCPT, Eq. (A.83), the new Hamiltonian $\bar{H}_0(\bar{\mathbf{p}}, \bar{\mathbf{q}})$ at $\mathcal{O}(\varepsilon^0)$ is given by

$$\bar{H}_0(\bar{\mathbf{p}}, \bar{\mathbf{q}}) = H_0(\bar{\mathbf{p}}, \bar{\mathbf{q}}) \tag{A.109}$$

$$= \frac{1}{2}(\bar{p}_1^2 + \bar{p}_2^2 + \omega_1^2 \bar{q}_1^2 + \omega_2^2 \bar{q}_2^2) = \omega_1 \bar{J}_1 + \omega_2 \bar{J}_2 \tag{A.110}$$

By using the general solution of the equation of motion obeying a system of $\bar{H}_0(\bar{\mathbf{p}}, \bar{\mathbf{q}})$;

$$\frac{d\bar{p}_k}{d\tau} = -\frac{\partial \bar{H}_0}{\partial \bar{q}_k} \qquad \frac{d\bar{q}_k}{d\tau} = \frac{\partial \bar{H}_0}{\partial \bar{p}_k} \tag{A.111}$$

$$\bar{q}_k(\tau) = \sqrt{\frac{2\bar{J}_k}{\omega_k}} \cos \bar{\Theta}_k = \sqrt{\frac{2\bar{J}_k}{\omega_k}} \cos(\omega_k \tau + \beta_k) \tag{A.112}$$

$$\bar{p}_k(\tau) = -\sqrt{2\omega_k \bar{J}_k} \sin \bar{\Theta}_k = -\sqrt{2\omega_k \bar{J}_k} \sin(\omega_k \tau + \beta_k) \qquad (k = 1, 2) \tag{A.113}$$

Now, we have H_1 as a function of $\bar{\mathbf{J}}$ and $\bar{\mathbf{\Theta}}$,

$$H_1(\bar{\mathbf{J}}, \bar{\mathbf{\Theta}}) = -\frac{1}{4}\left(\frac{2\bar{J}_1}{\omega_1}\right)^{1/2} \frac{2\bar{J}_2}{\omega_2} (2 \cos \bar{\Theta}_1 + \cos(\bar{\Theta}_1 + 2\bar{\Theta}_2) + \cos(\bar{\Theta}_1 - 2\bar{\Theta}_2)) \tag{A.114}$$

We first decompose this to $\langle H_1 \rangle$ and $\{H_1\}$, and try to establish the new Hamiltonian as free from the angle variables $\bar{\mathbf{\Theta}}$ as possible.

1. Non-(near) Resonant Case: $n_1\omega_1 + n_2\omega_2 \neq 0$
   In the cases that ω_1 is not commensurable with ω_2; in general, $n_1\omega_1 + n_2\omega_2 \neq 0$ (n_1, n_2: arbitrary integers), from Eq. (A.114), we have

$$\bar{H}_1 = 0$$

$$W_1 = -\int \{H_1\}\, d\tau = \frac{1}{4}\left(\frac{2\bar{J}_1}{\omega_1}\right)^{1/2} \frac{2\bar{J}_2}{\omega_2} \times \left[\frac{2}{\omega_1} \sin \bar{\Theta}_1 + \frac{1}{\omega_1 + 2\omega_2} \sin(\bar{\Theta}_1 + 2\bar{\Theta}_2) + \frac{1}{\omega_1 - 2\omega_2} \sin(\bar{\Theta}_1 - 2\bar{\Theta}_2)\right] \tag{A.115}$$

   or, in terms of $(\bar{\mathbf{p}}, \bar{\mathbf{q}})$,

$$W_1 = \frac{(2\omega_2^2 - \omega_1^2)\bar{p}_1\bar{q}_2^2 + 2\omega_1^2\bar{q}_1\bar{q}_2\bar{p}_2 + 2\bar{p}_1\bar{p}_2^2}{\omega_1^2(\omega_1 + 2\omega_2)(\omega_1 - 2\omega_2)} \tag{A.116}$$

   Hence, by using $H_1(\bar{\mathbf{p}}, \bar{\mathbf{q}}) = -\bar{q}_1\bar{q}_2^2$,

$$\{W_1, H_1\} = \frac{(2\omega_2^2 - \omega_1^2)\bar{q}_2^4 + 2\bar{q}_2^2\bar{p}_2^2 + 4\omega_1^2\bar{q}_1^2\bar{q}_2^2 + 8\bar{q}_1\bar{p}_1\bar{q}_2\bar{p}_2}{\omega_1^2(\omega_1 + 2\omega_2)(\omega_1 - 2\omega_2)} \tag{A.117}$$

and, in the $(\bar{\mathbf{J}}, \bar{\boldsymbol{\Theta}})$ representation, this becomes

$$\begin{aligned}\{W_1, H_1\} = \frac{4}{\omega_1^2(\omega_1 + 2\omega_2)(\omega_1 - 2\omega_2)}\Bigg[& -\frac{1}{8}\left(\frac{\omega_1}{\omega_2}\right)^2 \\ & \times \bar{J}_2^2(\cos 4\bar{\Theta}_2 + 4\cos 2\bar{\Theta}_2 + 3) + \bar{J}_2^2(1 + \cos 2\bar{\Theta}_2) \\ & + \frac{\omega_1}{\omega_2}\bar{J}_1\bar{J}_2\Bigg(1 + \cos 2\bar{\Theta}_1 + \cos 2\bar{\Theta}_2 \\ & + \frac{1}{2}(\cos 2(\bar{\Theta}_1 + \bar{\Theta}_2) + \cos 2(\bar{\Theta}_1 - \bar{\Theta}_2))\Bigg) \\ & - \bar{J}_1\bar{J}_2(\cos 2(\bar{\Theta}_1 + \bar{\Theta}_2) - \cos 2(\bar{\Theta}_1 - \bar{\Theta}_2))\Bigg]\end{aligned}$$

Thus, up to $\mathcal{O}(\varepsilon^2)$, one can have the new Hamiltonian $\bar{H}$, given by

$$\begin{aligned}\bar{H} = \varepsilon^0(\omega_1\bar{J}_1 + \omega_2\bar{J}_2) + \varepsilon^2 & \frac{2}{\omega_1^2(\omega_1 + 2\omega_2)(\omega_1 - 2\omega_2)} \\ & \times\left[\left(1 - \frac{3}{8}\left(\frac{\omega_1}{\omega_2}\right)^2\right)\bar{J}_2^2 + \frac{\omega_1}{\omega_2}\bar{J}_1\bar{J}_2\right]\end{aligned} \tag{A.118}$$

The equation of motion obeying the new Hamiltonian $\bar{H}(\bar{\mathbf{p}}, \bar{\mathbf{q}})$ represented up to the second-order $\mathcal{O}(\varepsilon^2)$,

$$\frac{d\bar{p}_k}{dt} = -\frac{\partial\bar{H}}{\partial\bar{q}_k} \qquad \frac{d\bar{q}_k}{dt} = \frac{\partial\bar{H}}{\partial\bar{p}_k} \tag{A.119}$$

yields the general solution obeying $\bar{H}$;

$$\bar{q}_k(t) = \sqrt{\frac{2\bar{J}_k}{\omega_k}}\cos(\bar{\omega}_k(\bar{\mathbf{J}})t + \gamma_k) \tag{A.120}$$

$$\bar{p}_k(t) = -\sqrt{2\omega_k\bar{J}_k}\sin(\bar{\omega}_k(\bar{\mathbf{J}})t + \gamma_k) \tag{A.121}$$

where γ_k is the initial phase factor of mode k, and

$$\bar{\omega}_1(\bar{\mathbf{J}}) = \omega_1 + \varepsilon^2 \frac{2\bar{J}_2}{\omega_1\omega_2(\omega_1 + 2\omega_2)(\omega_1 - 2\omega_2)} \tag{A.122}$$

$$\bar{\omega}_2(\bar{\mathbf{J}}) = \omega_2 + \varepsilon^2 \frac{2}{\omega_1^2(\omega_1 + 2\omega_2)(\omega_1 - 2\omega_2)} \times \left[\left(2 - \frac{3}{4}\left(\frac{\omega_1}{\omega_2}\right)^2\right)\bar{J}_2 + \frac{\omega_1}{\omega_2}\bar{J}_1\right] \tag{A.123}$$

As described in the preceding paragraphs, one can have new functional expressions in terms of the original variables $(\mathbf{p}, \mathbf{q})$, whose functional *values* are equivalent to $f(\bar{\mathbf{p}}, \bar{\mathbf{q}})$. Here, we shall denote the new functions as $\bar{f}(\mathbf{p}, \mathbf{q})$;

$$\begin{aligned} f(\bar{\mathbf{p}}, \bar{\mathbf{q}}) &= Tf(\mathbf{p}, \mathbf{q}) \\ &= \varepsilon^0 f(\mathbf{p}, \mathbf{q}) - \varepsilon^1\{W_1, f\} + \frac{\varepsilon^2}{2}(\{W_1, \{W_1, f\}\} - \{W_2, f\}) + \cdots \\ &= \bar{f}(\mathbf{p}, \mathbf{q}) \end{aligned}$$

For example, up to $\mathcal{O}(\varepsilon^1)$,

$$\bar{q}_1(\mathbf{p}, \mathbf{q}) = q_1 - \varepsilon^1 \frac{(\omega_1^2 - 2\omega_2^2)q_2^2 - 2p_2^2}{\omega_1^2(\omega_1 + 2\omega_2)(\omega_1 - 2\omega_2)} + \mathcal{O}(\varepsilon^2) \tag{A.124}$$

$$\bar{p}_1(\mathbf{p}, \mathbf{q}) = p_1 - \varepsilon^1 \frac{2q_2p_2}{(\omega_1 + 2\omega_2)(\omega_1 - 2\omega_2)} + \mathcal{O}(\varepsilon^2) \tag{A.125}$$

$$\bar{J}_1(\mathbf{p}, \mathbf{q}) = \frac{1}{2\omega_1}(p_1^2 + \omega_1^2 q_1^2) - \varepsilon^1 \frac{(\omega_1^2 - 2\omega_2^2)q_1q_2^2 - 2q_1p_2^2 + 2p_1q_2p_2}{\omega_1(\omega_1 + 2\omega_2)(\omega_1 - 2\omega_2)} + \mathcal{O}(\varepsilon^2) \tag{A.126}$$

and, for $\bar{\omega}_1(\mathbf{p}, \mathbf{q})$ up to $\mathcal{O}(\varepsilon^3)$,

$$\bar{\omega}_1(\mathbf{p}, \mathbf{q}) = \omega_1 + \varepsilon^2 \frac{2}{\omega_1\omega_2(\omega_1 + 2\omega_2)(\omega_1 - 2\omega_2)} \times \left[\frac{1}{2\omega_2}(p_2^2 + \omega_2^2 q_2^2) + \varepsilon^1 \frac{2\omega_2^2 q_1q_2^2 - 2q_1p_2^2 + 2p_1q_2p_2}{\omega_2(\omega_1 + 2\omega_2)(\omega_1 - 2\omega_2)}\right] \tag{A.127}$$

Note here that one can straightforwardly obtain all the inverse representations, for example, $q_1(\bar{\mathbf{p}}, \bar{\mathbf{q}})$, as

$$q_1(\bar{\mathbf{p}}, \bar{\mathbf{q}}) = \bar{q}_1 + \varepsilon^1 \frac{(\omega_1^2 - 2\omega_2^2)\bar{q}_2^2 - 2\bar{p}_2^2}{\omega_1^2(\omega_1 + 2\omega_2)(\omega_1 - 2\omega_2)} + \mathcal{O}(\varepsilon^2) \qquad \text{(A.128)}$$

since

$$\begin{aligned} \bar{f}(\mathbf{p}, \mathbf{q}) &= T^{-1}\bar{f}(\bar{\mathbf{p}}, \bar{\mathbf{q}}) \\ &= \varepsilon^0 \bar{f}(\bar{\mathbf{p}}, \bar{\mathbf{q}}) + \varepsilon^1 \{W_1, \bar{f}\} + \frac{\varepsilon^2}{2}(\{W_1, \{W_1, \bar{f}\}\} + \{W_2, \bar{f}\}) + \cdots \\ &= f(\bar{\mathbf{p}}, \bar{\mathbf{q}}) \end{aligned}$$

2. (Near) Resonant Case: $n_1\omega_1 + n_2\omega_2 \simeq 0$
The expression for $W_1(\bar{\mathbf{J}}, \bar{\mathbf{\Theta}})$ becomes divergent if $\omega_1 - 2\omega_2$ vanishes or becomes as small as $\mathcal{O}(\varepsilon^1)$, that is,

$$\omega_1 - 2\omega_2 \leqslant \mathcal{O}(\varepsilon^1) \qquad \text{(A.129)}$$

One should regard the third term in the right-hand side of $H_1(\bar{\mathbf{J}}, \bar{\mathbf{\Theta}})$ [Eq. (A.114)] as free from τ and include it in $\bar{H}_1$;

$$\begin{aligned} \bar{H}_1 &= -\frac{1}{4}\left(\frac{2\bar{J}_1}{\omega_1}\right)^{1/2} \frac{2\bar{J}_2}{\omega_2} \cos(\bar{\Theta}_1 - 2\bar{\Theta}_2) \\ W_1 &= -\int (H_1 - \bar{H}_1)\, d\tau \\ &= \frac{1}{4}\left(\frac{2\bar{J}_1}{\omega_1}\right)^{1/2} \frac{2\bar{J}_2}{\omega_2}\left[\frac{2}{\omega_1}\sin\bar{\Theta}_1 + \frac{1}{\omega_1 + 2\omega_2}\sin(\bar{\Theta}_1 + 2\bar{\Theta}_2)\right] \end{aligned}$$

and so forth (see Hori [52] in detail).

Note here that in order to avoid such a small-denominator divergence, one might have to include the corresponding $\bar{\mathbf{\Theta}}$ into the new Hamiltonian, or in the case of *near*-resonance, perform the CPT to infinite order $\mathcal{O}(\varepsilon^\infty)$.

At the end, we derive a versatile recursive series, first derived by Deprit [46], hold for an arbitrary order $\mathcal{O}(\varepsilon^n)$ of autonomous Hamiltonian systems that are expandable in power series in the perturbation strength ε. The following explanation relies heavily on a tutorial article

by Cary [45, 53], which modified the original derivation by Deprit [46]:

First, we premultiply $\bar{H} = T^{-1}H$ by T and differentiate with respect to ε:

$$\frac{dT}{d\varepsilon}\bar{H} + T\frac{d\bar{H}}{d\varepsilon} = \frac{dH}{d\varepsilon} \tag{A.130}$$

By using Eq. (A.52) to eliminate $dT/d\varepsilon$ and premultiplying T^{-1}, we obtain

$$-L_W\bar{H} + \frac{d\bar{H}}{d\varepsilon} = T^{-1}\frac{dH}{d\varepsilon} \tag{A.131}$$

By inserting the series expansions and equating like powers of ε, one can have in each order of ε^n $(n > 0)$:

$$-\sum_{m=0}^{n-1} L_{n-m}\bar{H}_m + n\bar{H}_n = \sum_{m=1}^{n} mT_{n-m}^{-1}H_m \tag{A.132}$$

By writing out the first term in the first sum,

$$L_n\bar{H}_0 = L_nH_0 = \{W_n, H_0\} = \frac{dW_n}{d\tau} \tag{A.133}$$

From the last term in the last sum, and for $n > 0$, one can obtain a versatile perturbation series

$$\bar{H}_n = H_n + \frac{1}{n}\sum_{m=1}^{n-1}(L_{n-m}\bar{H}_m + mT_{n-m}^{-1}H_m) + \frac{1}{n}\frac{dW_n}{d\tau} \tag{A.134}$$

For nonautonomous systems, an additional term involving the time derivatives of $W(\mathbf{p}, \mathbf{q}; \varepsilon)$ must be included in Eq. (A.66) [45, 46, 53]. In this Appendix, we have described how Lie transforms provide us with an important breakthrough in the CPT free from any cumbersome mixed-variable generating function as one encounters in the traditional Poincaré–Von Zeipel approach. After the breakthrough in CPT by the introduction of the Lie transforms, a few modifications have been established in the late 1970s by Dewar [56] and Dragt and Finn [47]. Dewar established the general formulation of Lie canonical perturbation theories for systems in which the transformation is not

expandable in a power series. Dragt and Finn developed a technique, particularly effective for high-order calculations more than, say, $\mathcal{O}(\varepsilon^5)$: It rewrites the evolution operator T as

$$T(\varepsilon) = e^{-\varepsilon L_1} e^{-\varepsilon L_2} e^{-\varepsilon L_3} \cdots \tag{A.135}$$

[which is validated for a wide class of Hamiltonians, e.g., Eqs. (2.28)–(2.30). The higher the order $\mathcal{O}(\varepsilon^n)$ at which one may want to perform the CPT, say $n \geqslant 5$, the smaller the number of terms are needed to represent the new Hamiltonian $\bar{H}$ in Dragt and Finn's technique [45], compared with those by Hori and Deprit. Note, however, that high dimensionality of the systems, to which one may want to apply CPT based on the Lie transforms, for example, six-atom cluster with 12 internal degrees of freedom, would make the total number of terms to be elucidated increase very quickly beyond a few orders, and make the direct applications very difficult, irrespective of kinds of (at least, existent) techniques in the Lie transforms-based CPTs.

D. A Simple Illustration of Algebraic Quantization

In general, a given Hamiltonian, Eqs. (2.28)–(2.30), can be rewritten at each order $\mathcal{O}(\varepsilon^n)$ in terms of $(\mathbf{a}^*, \mathbf{a})$: for example,

$$H_0 = \sum_i a_i^* a_i$$

$$H_1 = \sum_{j,k,l} B_{jkl}(a_j^* a_k^* a_l^* - a_j a_k a_l - 3(a_j a_k^* a_l^* - a_j^* a_k a_l))$$

$$H_2 = \sum_{j,k,l,m} B_{jklm}(a_j^* a_k^* a_l^* a_m^* + a_j a_k a_l a_m + 6a_j^* a_k^* a_l a_m - 4(a_j a_k^* a_l^* a_m^* + a_j^* a_k a_l a_m))$$

where

$$B_{jkl} = \frac{C_{jkl}}{(\sqrt{2}\, i)^3 \omega_j \omega_k \omega_l} \qquad B_{jklm} = \frac{C_{jklm}}{(\sqrt{2}\, i)^4 \omega_j \omega_k \omega_l \omega_m} \tag{A.136}$$

To see how the AQ simplifies the cumbersome analytical calculations, let us apply the AQ to a 2D system far from resonance, of Eq. (A.108),

$$H(\mathbf{a}^*, \mathbf{a}) = a_1^* a_1 + a_2^* a_2 - \varepsilon \frac{i}{2\sqrt{2}} \frac{1}{\omega_1 \omega_2^2} \times (a_1^* a_2^{*2} - 2a_1^* a_2^* a_2 + a_1^* a_2^2 - a_1 a_2^{*2} + 2a_1 a_2^* a_2 - a_1 a_2^2) \tag{A.137}$$

Thanks to Eqs. (2.46)–(2.47), it is straightforward to establish that

$$\bar{H}_0(\bar{\mathbf{a}}^*, \bar{\mathbf{a}}) = H_0(\bar{\mathbf{a}}^*, \bar{\mathbf{a}}) = \bar{a}_1^* \bar{a}_1 + \bar{a}_2^* \bar{a}_2 \tag{A.138}$$

$$\bar{H}_1(\bar{\mathbf{a}}^*, \bar{\mathbf{a}}) = 0 \tag{A.139}$$

and

$$W_1(\bar{\mathbf{a}}^*, \bar{\mathbf{a}}) = -\int H_1(\bar{\mathbf{a}}^*, \bar{\mathbf{a}})\, d\tau = \frac{1}{2\sqrt{2}} \frac{1}{\omega_1 \omega_2^2} \times \left[\frac{\bar{a}_1^* \bar{a}_2^{*2} + \bar{a}_1 \bar{a}_2^2}{\omega_1 + 2\omega_2} - \frac{2}{\omega_1} (\bar{a}_1^* \bar{a}_2^* \bar{a}_2 + \bar{a}_1 \bar{a}_2 \bar{a}_2^*) + \frac{\bar{a}_1^* \bar{a}_2^2 + \bar{a}_1 \bar{a}_2^{*2}}{\omega_1 - 2\omega_2} \right] \tag{A.140}$$

$\{W_1, H_1\}$ can be solved *symbolically*, thanks to Eq. (2.50) and well-known general properties of Poisson bracket, Eqs. (A.14)–(A.17).

$$\begin{aligned} \{W_1, H_1\} = \{W_1(\bar{\mathbf{a}}^*, \bar{\mathbf{a}}),\, H_1(\bar{\mathbf{a}}^*, \bar{\mathbf{a}})\} = & \frac{1}{\omega_1^2 \omega_2^2 (\omega_1 + 2\omega_2)(\omega_1 - 2\omega_2)} \\ & \times \left[\left(4 - \frac{3}{2} \left(\frac{\omega_1}{\omega_2} \right)^2 \right) (\bar{a}_2^* \bar{a}_2)^2 + 4 \bar{a}_1^* \bar{a}_1 \bar{a}_2^* \bar{a}_2 \right. \\ & - 2(\bar{a}_1^* \bar{a}_1 (\bar{a}_2^{*2} + \bar{a}_2^2) + \bar{a}_2^* \bar{a}_2 (\bar{a}_1^{*2} + \bar{a}_1^2)) \\ & + \frac{\omega_1 - 2\omega_2}{\omega_1} ((\bar{a}_1^* \bar{a}_2^*)^2 + (\bar{a}_1 \bar{a}_2)^2) + \frac{\omega_1 + 2\omega_2}{\omega_1} ((\bar{a}_1^* \bar{a}_2)^2 + (\bar{a}_1 \bar{a}_2^*)^2) \\ & \left. + \frac{\omega_1^2 - 2\omega_2^2}{\omega_2^2} (\bar{a}_2^{*3} \bar{a}_2 + \bar{a}_2^* \bar{a}_2^3) - \frac{\omega_1^2}{4\omega_2^2} (\bar{a}_2^{*4} + \bar{a}_2^4) \right] \end{aligned} \tag{A.141}$$

By using Eqs. (2.46) and (2.47), one can immediately establish the $\bar{\mathbf{\Theta}}$-free terms in $\{W_1(\bar{\mathbf{a}}^*, \bar{\mathbf{a}}),\, H_1(\bar{\mathbf{a}}^*, \bar{\mathbf{a}})\}$, yielding

$$\bar{H}_2 = \frac{2}{\omega_1^2 \omega_2^2 (\omega_1 + 2\omega_2)(\omega_1 - 2\omega_2)} \left[\left(1 - \frac{3}{8} \left(\frac{\omega_1}{\omega_2} \right)^2 \right) (\bar{a}_2^* \bar{a}_2)^2 + \bar{a}_1^* \bar{a}_1 \bar{a}_2^* \bar{a}_2 \right] \tag{A.142}$$

Here, one can see this being equal to $\bar{H}_2$, since $\bar{a}_k^* \bar{a}_k = \omega_k \bar{J}_k$ [see Eq. (A.118)].

All the functions ξ appearing through the LCPT–AQ procedure as Eq. (2.41),

$$\xi(\bar{\mathbf{a}}^*, \bar{\mathbf{a}}) = \sum_s d_s \bar{\mathbf{a}}^{*\mathbf{v}_s} \bar{\mathbf{a}}^{\mathbf{u}_s} \tag{A.143}$$

can be characterized by a set of parameters, $\{d_s, \mathbf{v}^s, \mathbf{u}^s\}_\xi$ for all the s in $\xi(\bar{\mathbf{a}}^*, \bar{\mathbf{a}})$, where coefficient d_s for the s-term can be real or imaginary, for systems involving imaginary frequency mode(s); $\mathbf{v}^s$ and $\mathbf{u}^s$ denote the vectors $\{v_1^s, v_2^s, \ldots\}$ and $\{u_1^s, u_2^s, \ldots\}$ (v_k^s, u_k^s: integers $\geqslant 0$). The integrations of ξ over τ, for example, Eq. (A.140), can symbolically be carried out using the mathematical properties of exponential functions, for example,

$$\{d_s, \mathbf{v}^s, \mathbf{u}^s\}_{W_1} \leftarrow \left\{ \frac{id_s}{(\mathbf{v}^s - \mathbf{u}^s)\cdot\boldsymbol{\omega}}, \mathbf{v}^s, \mathbf{u}^s \right\}_{H_1} \tag{A.144}$$

The Poisson bracket calculations, for example, $\{\xi(\bar{\mathbf{a}}^*, \bar{\mathbf{a}}), \eta(\bar{\mathbf{a}}^*, \bar{\mathbf{a}})\}$ where $\eta(\bar{\mathbf{a}}^*, \bar{\mathbf{a}})$ is an arbitrary function of $\bar{\mathbf{a}}^*$ and $\bar{\mathbf{a}}$ as represented by Eq. (A.143), can also be established symbolically through Eq. (2.50), which replaces the cumbersome analytical derivations to searching the combinations $\{\cdots(\bar{a}_k^*)^n \cdots, \cdots(\bar{a}_k)^m \cdots\}$ and $\{\cdots(\bar{a}_k)^{n'} \cdots, \cdots(\bar{a}_k^*)^{m'} \cdots\}$ (n, m, n', m': arbitrary positive integers): for example,

$$\begin{aligned}
\{\xi, \eta\} &= \sum_{s,t} d_{s(\xi)}\, d_{t(\eta)} \{\xi_s, \eta_t\} \\
&= \sum_{s,t}{}' d_{s(\xi)}\, d_{t(\eta)} \{\xi_{s'}(\bar{a}_k^*)^n \xi_{s''}, \eta_{t'}(\bar{a}_k)^m \eta_{t''}\} \\
&\quad + \sum_{s,t}{}'' d_{s(\xi)}\, d_{t(\eta)} \{\xi_{s'}(\bar{a}_k)^{n'} \xi_{s''}, \eta_{t'}(\bar{a}_k^*)^{m'} \eta_{t''}\} \\
&= \sum_{s,t}{}' d_{s(\xi)}\, d_{t(\eta)} (\cdots + inm\omega_k \xi_{s'}(\bar{a}_k^*)^{n-1} \xi_{s''} \eta_{t'}(\bar{a}_k)^{m-1} \eta_{t''} + \cdots) \\
&\quad + \sum_{s,t}{}'' d_{s(\xi)}\, d_{t(\eta)} (\cdots - in'm'\omega_k \xi_{s'}(\bar{a}_k)^{n'-1} \xi_{s''} \eta_{t'}(\bar{a}_k^*)^{m'-1} \eta_{t''} + \cdots)
\end{aligned}$$

where $\xi_{s'}(\xi_{s''})$ and $\eta_{t'}(\eta_{t''})$ denote arbitrary multiplications over $\bar{a}_j^*$ and $\bar{a}_j$ involved in $\xi_s(\bar{\mathbf{a}}^*, \bar{\mathbf{a}})$ and $\eta_t(\bar{\mathbf{a}}^*, \bar{\mathbf{a}})$, respectively; Σ' and Σ'' mean that the summations are taken over all the terms which have the combinations $\{\cdots(\bar{a}_k^*)^n \cdots, \cdots(\bar{a}_k)^m \cdots\}$ and $\{\cdots(\bar{a}_k)^{n'} \cdots, \cdots(\bar{a}_k^*)^{m'} \cdots\}$ [all the other terms simply vanish because of Eq. (2.50)].

E. LCPT with One Imaginary Frequency Mode

In general, we may write the Hamiltonian in terms of N-dimensional actions $\mathbf{J}$ and angles Θ of H_0:

$$\begin{aligned} H(\mathbf{J}, \boldsymbol{\Theta}) &= H_0(\mathbf{J}) + \sum_n \varepsilon^n H_n(\mathbf{J}, \boldsymbol{\Theta}) \\ &= H_0(\mathbf{J}) \\ &\quad + \varepsilon \sum_{\mathbf{m}}^{\infty} H_{1\mathbf{m}}(\mathbf{J}) e^{i\mathbf{m}\cdot\boldsymbol{\Theta}} + \varepsilon^2 \sum_{\mathbf{m}}^{\infty} H_{2\mathbf{m}}(\mathbf{J}) e^{i\mathbf{m}\cdot\boldsymbol{\Theta}} + \cdots \end{aligned}$$

for example,

$$H_{1\mathbf{m}}(\mathbf{J}) e^{i\mathbf{m}\cdot\boldsymbol{\Theta}} \equiv \prod_{k=1}^{N} H_{1m_k}(J_k) e^{im_k\Theta_k} \tag{A.145}$$

where m_k and $H_{1m_k}(J_k)$ are integers and Fourier coefficients depending on the action of mode k, J_k. The frequencies of the unperturbed $H_0(\mathbf{J})$ are given by

$$\boldsymbol{\omega}(\mathbf{J}) = \frac{\partial H_0(\mathbf{J})}{\partial \mathbf{J}} \tag{A.146}$$

Here, we assume that ω_k may vary depending on the point $(\mathbf{p}, \mathbf{q})$ in the phase space as a function of the action J_k, for example, N-dimensional Morse oscillators,

$$H_0(\mathbf{p}, \mathbf{q}) = \sum_{k=1}^{N} \left[\frac{p_k^2}{2m_k} + D_k(e^{-2a_k(q_k - q_k^{eq})} - 2e^{-a_k(q_k - q_k^{eq})}) \right] \tag{A.147}$$

$$\rightarrow H_0(\mathbf{J}) = -\sum_{k=1}^{N} D_k \left(1 - \frac{a_k J_k}{\sqrt{2m_k D_k}} \right)^2 \tag{A.148}$$

where

$$\omega_k = \frac{\partial H_0(\mathbf{J})}{\partial J_k} = a_k \sqrt{\frac{2D_k}{m_k}} \left(1 - \frac{a_k J_k}{\sqrt{2m_k D_k}} \right) \tag{A.149}$$

According to the recipe of LCPT, we have at zeroth order,

$$\bar{H}_0(\bar{\mathbf{J}}) = H_0(\bar{\mathbf{J}}) \tag{A.150}$$

and at first order,

$$\bar{H}_1 = H_1(\bar{\mathbf{J}}, \bar{\boldsymbol{\Theta}}) + \frac{dW_1(\bar{\mathbf{J}}, \bar{\boldsymbol{\Theta}})}{d\tau} \tag{A.151}$$

Extracting the $\bar{\boldsymbol{\Theta}}$-free part from H_1 by averaging it over τ yields

$$\bar{H}_1(\bar{\mathbf{J}}) = \langle H_1(\bar{\mathbf{J}}, \bar{\boldsymbol{\Theta}}) \rangle \tag{A.152}$$

and

$$W_1 = -\int^{\tau} d\tau' \{H_1(\bar{\mathbf{J}}, \bar{\boldsymbol{\Theta}}(\tau'))\} \tag{A.153}$$

Thus, one can solve W_1 by integrating the Fourier series for the oscillating part of H_1,

$$W_1(\bar{\mathbf{J}}, \bar{\boldsymbol{\Theta}}) = i \sum_{\mathbf{m} \neq \mathbf{0}} \frac{H_{1\mathbf{m}}(\bar{\mathbf{J}})}{\mathbf{m} \cdot \boldsymbol{\omega}(\bar{\mathbf{J}})} e^{i\mathbf{m} \cdot \bar{\boldsymbol{\Theta}}} \tag{A.154}$$

Suppose that in the vicinity of a first-rank saddle, the system is composed of one unstable mode F associated with an imaginary frequency $\omega_F(\bar{\mathbf{J}})(\in \tilde{\mathfrak{F}})$ and the other stable modes B with real frequencies $\boldsymbol{\omega}_B(\bar{\mathbf{J}})(\in \mathfrak{R})$. Then, one can see that all the terms involving $\omega_F(\bar{\mathbf{J}})$ in Eq. (A.154) are prevented from diverging regardless of where the system dwells in the phase space, even though all the other terms excluding that mode may be ill-behaved. This is because, so long as the summation includes $\omega_F(\bar{\mathbf{J}})$, any arbitrary combination of a single imaginary, and the other real frequencies cannot be arbitrarily close to zero, that is, $|\mathbf{m} \cdot \boldsymbol{\omega}(\bar{\mathbf{J}})| \geqslant |\omega_F(\bar{\mathbf{J}})| > \mathcal{O}(\varepsilon^n)$. However, for all the other terms involved in the Eq. (A.154), that is, those excluding $\omega_F(\bar{\mathbf{J}})$, one may find any $\bar{\mathbf{J}}$ and $\mathbf{m}$ that assures that $\mathbf{m} \cdot \boldsymbol{\omega}(\bar{\mathbf{J}})$ is arbitrarily close to zero, threatening to cause a divergence of the parts of the summation.

How does the new Hamiltonian $\bar{H}(\bar{\mathbf{J}})$ become ruined or not, in the event of such a resonance? Suppose, for example, that $\bar{H}_2$ can be obtained by

$$\bar{H}_2 = \left\langle H_2 + \frac{1}{2}\{W_1, H_1 + \bar{H}_1\} \right\rangle \tag{A.155}$$

with

$$\begin{aligned}\langle\{W_1, H_1 + \bar{H}_1\}\rangle &= \langle\{W_1, H_1\}\rangle \\ &= \sum_{\mathbf{m}\neq\mathbf{0}} \sum_{\mathbf{m}'=\mathbf{0}} \left\langle \left\{ i \frac{H_{1\mathbf{m}}(\bar{\mathbf{J}})}{\mathbf{m}\cdot\boldsymbol{\omega}(\bar{\mathbf{J}})} e^{i\mathbf{m}\cdot\bar{\boldsymbol{\Theta}}},\ H_{1\mathbf{m}'}(\bar{\mathbf{J}}) e^{i\mathbf{m}'\cdot\bar{\boldsymbol{\Theta}}} \right\} \right\rangle \\ &= -\sum_{\mathbf{m}\neq\mathbf{0}} \sum_{\mathbf{m}'\neq\mathbf{0}} \left\langle \frac{e^{i(\mathbf{m}+\mathbf{m}')\cdot\bar{\boldsymbol{\Theta}}}}{\mathbf{m}\cdot\boldsymbol{\omega}(\bar{\mathbf{J}})} \right. \\ &\quad \times \sum_k \left[m_k \frac{\partial(H_{1\mathbf{m}} H_{1\mathbf{m}'})}{\partial \bar{J}_k} - (m_k + m_k') H_{1\mathbf{m}'} \frac{\partial H_{1\mathbf{m}}}{\partial \bar{J}_k} \right. \\ &\quad \left. \left. + m_k' \frac{H_{1\mathbf{m}} H_{1\mathbf{m}'}}{\mathbf{m}\cdot\boldsymbol{\omega}(\bar{\mathbf{J}})} \frac{\mathbf{m}\cdot\partial\boldsymbol{\omega}(\bar{\mathbf{J}})}{\partial \bar{J}_k} \right] \right\rangle \end{aligned} \tag{A.156}$$

Here, $\{W_1, \bar{H}_1\}$ has no average part free from τ because W_1 is oscillatory and $\bar{H}_1$ is averaged. Likewise, the second summation has no average part to emerge from a condition that $\mathbf{m}' = \mathbf{0}$. The average part of $\{W_1, H_1\}$ consists of all the terms such that

$$\begin{aligned}(\mathbf{m} + \mathbf{m}')\cdot\boldsymbol{\omega}(\bar{\mathbf{J}}) &= (m_F + m_F')\omega_F(\bar{\mathbf{J}}) + (\mathbf{m}_B + \mathbf{m}_B')\cdot\boldsymbol{\omega}_B(\bar{\mathbf{J}}) \\ &= -(m_F + m_F')|\omega_F(\bar{\mathbf{J}})|i + \sum_{k\in B}^{N} (m_k + m_k')\omega_k(\bar{\mathbf{J}}) \leqslant \mathcal{O}(\varepsilon^2)\end{aligned}$$

that is,

$$m_F = -m_F' \qquad \text{and} \qquad \sum_{k\in B}^{N} (m_k + m_k')\omega_k(\bar{\mathbf{J}}) \simeq 0 \tag{A.157}$$

Then, Eq. (A.156) becomes

$$\begin{aligned}\langle\{W_1, H_1\}\rangle = \sum_{\mathbf{m}\neq\mathbf{0}} \sum_{\mathbf{m}'\neq\mathbf{0}}{}' & \frac{1}{m_F\omega_F(\bar{\mathbf{J}}) + \mathbf{m}_B\cdot\boldsymbol{\omega}_B(\bar{\mathbf{J}})} \\ & \times \left[\sum_k \left(m_k \frac{\partial}{\partial \bar{J}_k} (G_{m_F, -m_F}(\bar{J}_F) G_{\mathbf{m}_B, \mathbf{m}_B'}(\bar{\mathbf{J}}_B)) \right. \right. \\ & + m_k' \frac{G_{m_F, -m_F}(\bar{J}_F) G_{\mathbf{m}_B, \mathbf{m}_B'}(\bar{\mathbf{J}}_B)}{m_F\omega_F(\bar{\mathbf{J}}) + \mathbf{m}_B\cdot\boldsymbol{\omega}_B(\bar{\mathbf{J}})} \frac{\mathbf{m}\cdot\partial\boldsymbol{\omega}(\bar{\mathbf{J}})}{\partial \bar{J}_k} \Big) \\ & \left. \left. - \sum_{k\in B} \left(G_{m_F, -m_F}(\bar{J}_F) H_{1\mathbf{m}_B'}(\bar{\mathbf{J}}_B)(m_k + m_k') \frac{\partial H_{1\mathbf{m}_B}(\bar{\mathbf{J}}_B)}{\partial \bar{J}_k} \right) \right] \end{aligned} \tag{A.158}$$

where

$$G_{m_k, m_k'} = H_{1m_k} H_{1m_k'} \qquad \text{and} \qquad G_{\mathbf{m},\mathbf{m}'} = \prod_k G_{m_k m_k'} \tag{A.159}$$

and the symbol Σ' denotes that the summation is taken under the condition of Eq. (A.157).

Note that all the terms in $\langle\{W_1, H_1\}\rangle$ involving the contribution of mode F, that is, $m_F = -m'_F \neq 0$, provide us with the *nondivergent* part of $\bar{H}_2(\bar{\mathbf{J}})$ (irrespective of where the system dwells in the phase space) as a function of $\bar{J}_F$ and $\bar{\mathbf{J}}_B$ because $\mathbf{m}\cdot\boldsymbol{\omega}(\bar{\mathbf{J}})$ involving one imaginary frequency $\omega_F(\bar{\mathbf{J}})$ always removes the small-denominator problem. The other terms in $\langle\{W_1, H_1\}\rangle$ excluding the F's, for which we have $m_F = m'_F = 0$ and $G_{m_F, -m_F}(\bar{J}_F) = 1$ in Eq. (A.158), that is, functions of $\bar{\mathbf{J}}_B$, may bring about divergence in such phase space regions that $\mathbf{m}\cdot\boldsymbol{\omega}_B(\bar{\mathbf{J}})$ becomes close to zero. This might require that we include the corresponding angle variables in the new Hamiltonian to avoid the divergence [48–50, 55]. Thus, one can deduce a generic feature inherent in the region of (first-rank) saddles, irrespective of the systems, that a negatively curved, reactive mode F tends *more* to preserve its invariant of action, than all the other stable, nonreactive modes B.

In turn, How does such a resonance occurring in the vicinity of first-rank saddles affect the associated local frequencies $\bar{\omega}_k(\bar{\mathbf{J}})$? One might anticipate naively that, if the system is not in the quasiregular regime where all or almost of all the actions are "good" approximate invariants, the invariants of all $\bar{\omega}_k(\bar{\mathbf{J}})$ are spoiled, including that of the reactive mode F, since $\bar{\omega}_F(\bar{\mathbf{J}})$ depends not only on the invariant $\bar{J}_F$ but also on the other $\bar{\mathbf{J}}_B$. Now, let us look into $\bar{\omega}_k(\bar{\mathbf{J}})$ at second order:

$$\bar{\omega}_k(\bar{\mathbf{J}}) = \frac{\partial \bar{H}}{\partial \bar{J}_k} = \omega_k(\bar{\mathbf{J}}) + \varepsilon \frac{\partial \langle H_1\rangle}{\partial \bar{J}_k} + \varepsilon^2 \left(\frac{\partial \langle H_2\rangle}{\partial \bar{J}_k} + \frac{1}{2} \frac{\partial \langle\{W_1, H_1\}\rangle}{\partial \bar{J}_k} \right) + \mathcal{O}(\varepsilon^3) \tag{A.160}$$

From Eq. (A.158),

$$\frac{\partial \langle\{W_1, H_1\}\rangle}{\partial \bar{J}_k} \sim \frac{\partial}{\partial \bar{J}_k} \left(\frac{h(\bar{J}_F, \bar{\mathbf{J}}_B)}{(m_F \omega_F(\bar{\mathbf{J}}) + \mathbf{m}_B \cdot \boldsymbol{\omega}_B(\bar{\mathbf{J}}))^n} + \frac{h'(\bar{\mathbf{J}}_B)}{(\mathbf{m}_B \cdot \boldsymbol{\omega}_B(\bar{\mathbf{J}}))^n} \right) \tag{A.161}$$

where exponent n is 1 or 2, and h and h' are, respectively, functions of $\bar{J}_F$ and $\bar{\mathbf{J}}_B$, and of $\bar{\mathbf{J}}_B$ only. If one takes the partial derivative of $\langle\{W_1, H_1\}\rangle$ with respect to $\bar{J}_F$, one can see that $\bar{\omega}_F(\bar{\mathbf{J}})$ is not affected by the second term of the right-hand side, where any $\bar{\mathbf{J}}_B$ and $\mathbf{m}_B$ can be found such that $\mathbf{m}_B \cdot \boldsymbol{\omega}_B(\bar{\mathbf{J}})$ is arbitrarily close to zero. Even if the implicit contributions from some fluctuating $\bar{\mathbf{J}}_B$ exist in the $\bar{\omega}_F(\bar{\mathbf{J}})$ at second order, they will be suppressed by the nonvanishing denominators that are always larger than $|\omega_F(\bar{\mathbf{J}})|$. On the contrary, if one takes the partial derivatives with respect to $\bar{\mathbf{J}}_B$, they are affected by both the first and second terms. Especially the

second term may enhance the contributions from the fluctuating $\bar{\mathbf{J}}_B$ to the $\bar{\boldsymbol{\omega}}_B(\bar{\mathbf{J}})$ through the small denominators occurring in some phase-space regions. Thus, one can deduce a generic consequence that the local frequency $\bar{\omega}_F(\bar{\mathbf{J}})$ is less influenced by the fluctuations of $\bar{\mathbf{J}}_B$ and more persistent as an approximate invariant than $\bar{\boldsymbol{\omega}}_B(\bar{\mathbf{J}})$. [In fact, as shown in our recent numerical analysis using a bundle of well–saddle–well trajectories [44], even at a moderately high energy where almost all $\bar{\mathbf{J}}$ do not preserve their invariance — the exception being that $\bar{J}_F - \bar{\omega}_F^{2\text{nd}}(\bar{\mathbf{J}})$ tends to exhibit near-constancy with a much smaller fluctuation than those of $\bar{\boldsymbol{\omega}}_B^{2\text{nd}}(\bar{\mathbf{J}})$].

It can easily be shown that the equation of motion of mode F obeying a Hamiltonian $\bar{H}(\bar{J}_F, \bar{\boldsymbol{\xi}}_B)$ ($\bar{\boldsymbol{\xi}}_B \equiv (\bar{\mathbf{J}}_B, \bar{\boldsymbol{\Theta}}_B)$) is given by

$$\ddot{\bar{q}}_F(\mathbf{p},\mathbf{q}) - \frac{\dot{\bar{\omega}}_F}{\bar{\omega}_F}\dot{\bar{q}}_F(\mathbf{p},\mathbf{q}) + \bar{\omega}_F^2 \bar{q}_F(\mathbf{p},\mathbf{q}) = 0 \tag{A.162}$$

$$\bar{p}_F(\mathbf{p},\mathbf{q}) = \frac{\omega_F}{\bar{\omega}_F}\dot{\bar{q}}_F(\mathbf{p},\mathbf{q}) \tag{A.163}$$

where

$$\bar{\omega}_F = \bar{\omega}_F(\bar{J}_F, \bar{\boldsymbol{\xi}}_B) = \frac{\partial \bar{H}(\bar{J}_F, \bar{\boldsymbol{\xi}}_B)}{\partial \bar{J}_F} \tag{A.164}$$

Here, $\dot{x}$ and $\ddot{x}$ represent the first and second derivatives of x with respect to time t. $\bar{\omega}_F(\bar{J}_F, \bar{\boldsymbol{\xi}}_B)$ depends on time only through nonreactive modes $\bar{\boldsymbol{\xi}}_B$ because $\bar{J}_F$ is free from t; the $\bar{\boldsymbol{\xi}}_B$ contributions to $\bar{\omega}_F$ usually arise from higher orders in ε; for example, it is second order in the vicinity of first-rank saddles, yielding [the second term of the left hand side of Eq. (A.162)] $\simeq \mathcal{O}(\varepsilon^2)\dot{\bar{\mathrm{q}}}_F$, and, furthermore, these are suppressed due to nondivergent denominators involving one imaginary frequency ω_F.

Eq. (A.162) corresponds to a one-dimensional pendulum whose length will slowly change, being a well-used example to present the robust persistence of invariance of action under a small perturbation, referred to as "adiabatic invariance" (for example, see [53, 81]). By introducing the time dependencies of α, β, and $\bar{\omega}_F$ into the general solution of the "auxiliary equation" of Eq. (A.162) imposing $\dot{\bar{\omega}}_F = 0$, that is,

$$\bar{q}_F(t) = \alpha(t) l^{i\bar{\omega}_F(t)t} + \beta(t) e^{-i\bar{\omega}_F(t)t} \tag{A.165}$$

and setting the supplementary condition

$$\dot{\alpha} e^{i\bar{\omega}_F t} + \dot{\beta} e^{-i\bar{\omega}_F t} + i\dot{\bar{\omega}}_F t(\alpha e^{i\bar{\omega}_F t} - \beta e^{-i\bar{\omega}_F t}) = 0 \tag{A.166}$$

one can obtain [82] the solution of Eq. (A.162) with a slowly varying frequency by using the method of variation of constants:

$$\bar{q}_F(t) = \alpha(0) e^{i\int^t \bar{\omega}_F(t')dt'} + \beta(0) e^{-i\int^t \bar{\omega}_F(t')dt'} \tag{A.167}$$

and

$$\bar{p}_F(t) = i\alpha(0)\omega_F e^{i\int^t \bar{\omega}_F(t')dt'} - i\beta(0)\omega_F e^{-i\int^t \bar{\omega}_F(t')dt'} \tag{A.168}$$

(One can easily verify that Eqs. (A.167) and (A.168) satisfy Eq. (A.6)). To pass through the dividing surface from the one side to the other, the crossing trajectories typically require, at most, only a half period of the reactive hyperbolic orbit $\sim \pi/|\bar{\omega}_F|$. Furthermore, in the regions of first-rank saddles, such passage time intervals are expected to be much shorter than a typical time of the systems to find the variation or modulation of the frequency $\bar{\omega}_F$ with respect to the curvature, that is, $\pi/|\bar{\omega}_F| (= \mathcal{O}(\varepsilon^0)) \ll |\bar{\omega}_F/\dot{\bar{\omega}}_F| (= \mathcal{O}(\varepsilon^{-2}))$. Thus, if $\bar{J}_F$ is conserved (i.e., the Hamiltonian is free from $\bar{\Theta}_F$), independent of the constancy or nonconstancy of $\bar{\omega}_F(\mathbf{p}, \mathbf{q})$, we can expect any nonconstancy of $\bar{\omega}_F$ to leave the separability of $\bar{q}_F$ as unaffected as $\bar{J}_F$ in the region of first-rank saddles. That is,

$$\bar{q}_F(t) \simeq \alpha(0)e^{|\bar{\omega}_F|t} + \beta(0)e^{-|\bar{\omega}_F|t} \tag{A.169}$$

and

$$\bar{p}_F(t) \simeq \alpha(0)|\omega_F|e^{|\bar{\omega}_F|t} - \beta(0)|\omega_F|e^{-|\bar{\omega}_F|t} \tag{A.170}$$

Note here that, even though the fluctuation of $\bar{\omega}_F(t)$ in a short passage time would be large enough to spoil the separability of $\bar{q}_F$ of Eqs. (A.169) and (A.170), one may still predict the final state of reactions *a priori* as far as the *sign* of $i\int^t \bar{\omega}_F(t')dt'$ will not change during the passage through the saddle. That is, for example, if the system leaving $S(q_F = 0)$ at time $t = 0$ have $\alpha(0) > 0$, the final state can be predicted at that time to be a stable state directed by $\bar{q}_F > 0$.

References

1. B. J. Berne, M. Borkovec, and J. E. Straub, *J. Phys. Chem.* **92**, 3711 (1988).
2. D. G. Truhlar, B. C. Garrett, and S. J. Klippenstein, *J. Phys. Chem.* **100**, 12771 (1996).
3. H. Eyring, *J. Chem. Phys.* **3**, 107 (1935).
4. M. G. Evans and M. Polanyi, *Trans. Faraday Soc.* **31**, 875 (1935).
5. E. Wigner, *J. Chem. Phys.* **5**, 720 (1938).
6. L. S. Kassel, *J. Phys. Chem.* **32**, 1065 (1928).
7. O. K. Rice and H. C. Ramsperger, *Am. Chem. Soc. Jpn.* **50**, 617 (1928).
8. R. A. Marcus, *J. Chem. Phys.* **20**, 359 (1952).
9. J. C. Keck, *Adv. Chem. Phys.* **13**, 85 (1967).
10. D. G. Truhlar and B. C. Garrett, *Acc. Chem. Res.* **13**, 440 (1980).
11. J. Villa and D. G. Truhlar, *Theor. Chem. Acc.* **97**, 317 (1997).
12. W. H. Miller, *Faraday Discuss. Chem. Soc.* **62**, 40 (1977).
13. T. Seideman and W. H. Miller, *J. Chem. Phys.* **95**, 1768 (1991).

14. H. A. Kramers, *Physica* **7**, 284 (1940).
15. J. T. Hynes, in *Theory of Chemical Reaction Dynamics*, edited by B. Baer (CRC Press, Boca Raton, FL, 1985), pp. 171–234.
16. C. Amitrano and R. S. Berry, *Phys. Rev. Lett.* **68**, 729 (1992); *Phys. Rev. E* **47**, 3158 (1993).
17. T. L. Beck, D. M. Leitner, and R. S. Berry, *J. Chem. Phys.* **89**, 1681 (1988).
18. R. S. Berry, *Chem. Rev.* **93**, 237 (1993).
19. R. S. Berry, *Int. J. Quantum Chem.* **58**, 657 (1996).
20. R. J. Hinde, R. S. Berry, and D. J. Wales, *J. Chem. Phys.* **96**, 1376 (1992).
21. R. J. Hinde and R. S. Berry, *J. Chem. Phys.* **99**, 2942 (1993).
22. D. J. Wales and R. S. Berry, *J. Phys. B: At. Mol. Opt. Phys.* **24**, L351 (1991).
23. S. K. Nayak, P. Jena, K. D. Ball, and R. S. Berry, *J. Chem. Phys.* **108**, 234 (1998).
24. M. J. Davis and S. K. Gray, *J. Chem. Phys.* **84**, 5389 (1986).
25. S. K. Gray and S. A. Rice, *J. Chem. Phys.* **87**, 2020 (1987).
26. M. Zhao and S. A. Rice, *J. Chem. Phys.* **96**, 6654 (1992).
27. R. E. Gillilan and G. S. Ezra, *J. Chem. Phys.* **94**, 2648 (1991).
28. N. De Leon, *J. Chem. Phys.* **96**, 285 (1992).
29. J. R. Fair, K. R. Wright, and J. S. Hutchinson, *J. Phys. Chem.* **99**, 14707 (1995).
30. E. R. Lovejoy, S. K. Kim, and C. B. Moore, *Science* **256**, 1541 (1992).
31. E. R. Lovejoy and C. B. Moore, *J. Chem. Phys.* **98**, 7846 (1993).
32. D. C. Chatfield, R. S. Friedman, D. G. Truhlar, B. C. Garrett, and D. W. Schwenke, *J. Am. Chem. Soc.* **113**, 486 (1991).
33. R. A. Marcus, *Science* **256**, 1523 (1992).
34. M. Toda, *Phys. Rev. Lett.* **74**, 2670 (1995).
35. M. Toda, *Phys. Lett. A* **227**, 232 (1997).
36. S. Wiggins, *Normally Hyperbolic Invariant Manifolds in Dynamical Systems* (Springer-Verlag, New York, 1991).
37. (a) P. Pechukas and E. Pollak, *J. Chem. Phys.* **67**, 5976 (1977); (b) E. Pollak and P. Pechukas, ibid. **69**, 1218 (1978); (c) ibid. **70**, 325 (1979); (d) E. Pollak, M. S. Child, and P. Pechukas, (e) ibid. **72**, 1669 (1980); (f) M. S. Child and E. Pollak, ibid. **73**, 4365 (1980).
38. T. Komatsuzaki and M. Nagaoka, *J. Chem. Phys.* **105**, 10838 (1996).
39. T. Komatsuzaki and M. Nagaoka, *Chem. Phys. Lett.* **265**, 91 (1997).
40. T. Komatsuzaki and R. S. Berry, *J. Chem. Phys.* **110**, 9160 (1999).
41. T. Komatsuzaki and R. S. Berry, *Phys. Chem. Chem. Phys.* **1**, 1387 (1999).
42. T. Komatsuzaki and R. S. Berry, *J. Mol. Struct.*(*THEOCHEM*) **506**, 55 (2000).
43. T. Komatsuzaki and R. S. Berry, *Proc. Natl. Acad. Sci. USA* **78**, 7666 (2001).
44. T. Komatsuzaki and R. S. Berry, *J. Chem. Phys.* **115**, 4105 (2001).
45. J. R. Cary, *Phys. Rep.* **79**, 130 (1981).
46. A. Deprit, *Celest. Mech.* **1**, 12 (1969).
47. A. J. Dragt and J. M. Finn, *J. Math. Phys.* **17**, 2215 (1976); **20**, 2649 (1979).
48. L. E. Fried and G. S. Ezra, *J. Chem. Phys.* **86**, 6270 (1987).
49. L. E. Fried and G. S. Ezra, *Comput. Phys. Commun.* **51**, 103 (1988).
50. L. E. Fried and G. S. Ezra, *J. Phys. Chem.* **92**, 3144 (1988).
51. G. Hori, *Pub. Astro. Soc. Jpn.* **18**, 287 (1966).

52. G. Hori, *Pub. Astro. Soc. Jpn.* **19**, 229 (1967).
53. A. J. Lichtenberg and M. A. Lieberman, *Regular and Chaotic Dynamics*, 2nd ed. (Springer, New York, 1992).
54. G. D. Birkhoff, *Dynamical Systems* (American Mathematical Society, New York, 1927).
55. F. Gustavson, *Astron. J.* **21**, 670 (1966).
56. R. L. Dewar, *J. Phys. A: Gen. Phys.* **9**, 2043 (1976).
57. M. Page and J. W. McIver, Jr., *J. Chem. Phys.* **88**, 922 (1988).
58. At a nonstationary point there exist only three zero-frequency modes corresponding to the total translational motions and the normal coordinates of the infinitesimal rotational motions appear in all the terms including H_0. The canonical perturbation theory can be applied to some non-zero total angular momentum systems by Dragt and Finn's two-step transformation [47].
59. This analysis has neglected any explicit treatment of the complex issue of systems that develop internal, vibrational angular momentum and, consequently, a counter-rotating "rigid body" angular momentum that just balances the vibrational angular momentum, leaving the total at its original, constant value. Such phenomena will require a higher level of analysis than is presented here.
60. R. Hernandez and W. H. Miller, *Chem. Phys. Lett.* **214**, 129 (1993).
61. W. H. Press, S. A. Teukolsky, W. T. Vetterling, and B. P. Flannery, *Numerical Recipes*, 2nd ed. (Cambridge University, New York, 1992).
62. T. Komatsuzaki and R. S. Berry, *J. Phys. Chem.* (submitted for publication).
63. G. van der Zwan and J. T. Hynes, *J. Chem. Phys.* **78**, 4174 (1983).
64. T. Komatsuzaki, Y. Matsunaga, M. Toda, S. A. Rice, and R. S. Berry (unpublished).
65. S. Keshavamurthy and W. H. Miller, *Chem. Phys. Lett.* **205**, 96 (1993); see His thesis at the University of California, Berkeley, CA, 1994, Chapt. 2, pp. 9–36.
66. G. V. Mil'nikov and A. J. C. Varandas, *Phys. Chem. Chem. Phys.* **1**, 1071 (1999).
67. S. Takada and H. Nakamura, *J. Chem. Phys.* **100**, 98 (1994).
68. C. C. Martens, M. J. Davis, and G. S. Ezra, *Chem. Phys. Lett.* **142**, 519 (1987).
69. M. J. Davis, *J. Chem. Phys.* **83**, 1016 (1985).
70. K. Fukui, *J. Phys. Chem.* **74**, 4161 (1970).
71. K. Fukui, S. Kato, and H. Fujimoto, *J. Am. Chem. Soc.* **97**, 1 (1975).
72. J. Laskar, *Icarus* **88**, 266 (1990).
73. J. C. Losada, J. M. Estebaranz, R. N. Benito, and F. Borondo, *J. Chem. Phys.* **108**, 63 (1998).
74. S. Wiggins, L. Wiesenfeld, C. Jaffé, and T. Uzer, *Phys. Rev. Lett.* **86**, 5478 (2001).
75. A. E. García and G. Hummer, *Proteins* **36**, 175 (1999).
76. A. E. García, R. Blumenfeld, G. Hummer, and J. A. Krumhansl, *Physica D*, **107**, 225 (1997).
77. B. Vekhter, K. D. Ball, J. Rose, and R. S. Berry, *J. Chem. Phys.* **106**, 4644 (1997).
78. Y. Matsunaga, K. S. Kostov, and T. Komatsuzaki, *J. Phys. Chem.* (submitted for publication).
79. S. S. Plotkin and P. G. Wolynes, *Phys. Rev. Lett.* **80**, 5015 (1998).
80. M. Toda, T. Komatsuzaki, R. S. Berry, and S. A. Rice (unpublished).
81. V. I. Arnold, *Mathematical Methods of Classical Mechanics*, 2nd Ed. (Springer, New York, 1978).
82. M. Toda, *Theory of Oscillations* (Japanese) (Baifukan, Tokyo, 1968).